# NAVAL POSTGRADUATE SCHOOL
## Monterey, California

# THESIS

AN INVESTIGATION OF THE CORROSION
SUSCEPTIBILITY OF FLAME-SPRAYED AND
ELECTRIC-ARC SPRAYED ANODIC METAL COATINGS
OF ALUMINUM, ZINC, AND
AN ALUMINUM-ZINC ALLOY

by

Gregory Gower Mead

March 1983

Thesis Advisor: A.J. Perkins

Approved for public release, distribution unlimited.

## REPORT DOCUMENTATION PAGE

READ INSTRUCTIONS BEFORE COMPLETING FORM

1. REPORT NUMBER

2. GOVT ACCESSION NO.

3. RECIPIENT'S CATALOG NUMBER

4. TITLE (and Subtitle) An Investigation of the Corrosion Susceptibility of Flame-Sprayed and Electric-Arc Sprayed Anodic Metal Coatings of Aluminum, Zinc, and an Aluminum-Zinc Alloy

5. TYPE OF REPORT & PERIOD COVERED
Master's Thesis;
March 1983

6. PERFORMING ORG. REPORT NUMBER

7. AUTHOR(s)

Gregory Gower Mead

8. CONTRACT OR GRANT NUMBER(s)

9. PERFORMING ORGANIZATION NAME AND ADDRESS

Naval Postgraduate School
Monterey, California 93940

10. PROGRAM ELEMENT, PROJECT, TASK AREA & WORK UNIT NUMBERS

11. CONTROLLING OFFICE NAME AND ADDRESS

Naval Postgraduate School
Monterey, California 93940

12. REPORT DATE
March 1983

13. NUMBER OF PAGES
120

14. MONITORING AGENCY NAME & ADDRESS(if different from Controlling Office)

15. SECURITY CLASS. (of this report)
Unclassified

15a. DECLASSIFICATION/DOWNGRADING SCHEDULE

16. DISTRIBUTION STATEMENT (of this Report)

Approved for public release, distribution unlimited.

17. DISTRIBUTION STATEMENT (of the abstract entered in Block 20, if different from Report)

18. SUPPLEMENTARY NOTES

19. KEY WORDS (Continue on reverse side if necessary and identify by block number)

Corrosion
Flame Spray
Electric Arc Spray
Zinc Coatings
Aluminum Coatings
Aluminum/Zinc Coatings

20. ABSTRACT (Continue on reverse side if necessary and identify by block number)

Anodic coatings of aluminum, zinc, and an alloy consisting of 99% aluminum and 1% zinc, applied to a mild steel substrate by either the oxygen-acetelyne wire flame spray method or the electric-arc spray method, were evaluated for their corrosion protection abilities. The coatings tested were prepared by the Puget Sound Naval Shipyard using standard production methods. The corrosion testing utilized in the present research included

planned interval immersion/emersion, continuous spray, and electrochemical techniques in a solution of 3.5% NaCl. The response of the different coatings to the various tests were studied microscopically. The corrosion products were also studied by x-ray spectroscopy and x-ray diffraction.

Results of the investigation indicate that coatings of aluminum are the most resistant to corrosion in a simulated, aggressive marine environment, that alloying aluminum with 1% zinc in the coating material has no beneficial corrosion preventive effect, and that a pure zinc coating is unsuited for service in a severe marine environment.

Approved for public release, distribution unlimited.

# An Investigation of the Corrosion Susceptibility of Flame-Sprayed and Electric-Arc Sprayed Anodic Metal Coatings of Aluminum, Zinc, and an Aluminum-Zinc Alloy

by

Gregory Gower Mead
Lieutenant Commander, United States Navy
B.S., U.S. Naval Academy, 1972

Submitted in partial fulfillment of the
requirements for the degree of

MASTER OF SCIENCE IN MECHANICAL ENGINEERING

from the

NAVAL POSTGRADUATE SCHOOL
March 1983

## ABSTRACT

Anodic coatings of aluminum, zinc, and an alloy consisting of 99% aluminum and 1% zinc, applied to a mild steel substrate by either the oxygen-acetelyne wire flame spray method or the electric-arc spray method, were evaluated for their corrosion protection abilities. The coatings tested were prepared by the Puget Sound Naval Shipyard using standard production methods. The corrosion testing utilized in the present research included planned interval immersion/emersion, continuous spray, and electrochemical techniques in a solution of 3.5% NaCl. The response of the different coatings to the various tests were studied microscopically. The corrosion products were also studied by x-ray spectroscopy and x-ray diffraction.

Results of the investigation indicate that coatings of aluminum are the most resistant to corrosion in a simulated, aggressive marine environment, that alloying aluminum with 1% zinc in the coating material has no beneficial corrosion preventive effect, and that a pure zinc coating is unsuited for service in a severe marine environment.

TABLE OF CONTENTS


I. INTRODUCTION ---------- 16

A. BACKGROUND ---------- 16

B. THIS WORK ---------- 17

II. EXPERIMENTAL PROCEDURE ---------- 19

A. THE ELECTROLYTE ---------- 19

B. TEST COUPONS ---------- 20

1. Cleaning and Weighing the Coupon ---------- 21

C. CHAMBER TESTING ---------- 22

1. The Chamber ---------- 22

2. Planned Interval Immersion Mass Loss Test (PIML) ---------- 23

3. Continuous Spray Testing (CSP) ---------- 24

D. ELECTROCHEMICAL TESTING ---------- 25

1. The Corrosion Cell and Test Coupons ------- 25

2. Corrosion Measurement System ---------- 25

3. Potentiodynamic Polarization Measurement (PDP) ---------- 26

4. Anodic Polarization Test (PSP) ---------- 27

E. POST TESTING EVALUATION ---------- 28

III. RESULTS AND DISCUSSION ---------- 30

A. PRE-TESTING COATING EXAMINATION ---------- 30

B. MACROSCOPIC OBSERVATIONS OF COATING BEHAVIOR DURING PIML/CSP ---------- 31

1. Aluminum Coatings ---------- 31

2. Zinc Coatings ---------- 33
3. Alloy Coatings ---------- 37
C. CORROSION RATES ---------- 39
1. PIML ---------- 39
2. PDP ---------- 40
D. SEM MICROSCOPY ---------- 40
1. Al Coatings ---------- 40
2. Zn Coatings ---------- 43
3. Alloy Coatings ---------- 44
E. CORROSION PRODUCT ANALYSIS ---------- 46
1. PGT Analysis ---------- 46
2. X-ray Diffraction ---------- 47
F. COMPARISONS OF COATINGS ---------- 48
1. Zn versus Al ---------- 48
2. Al versus Alloy ---------- 48
IV. CONCLUSIONS AND RECOMMENDATIONS ---------- 50
A. CONCLUSIONS ---------- 50
B. RECOMMENDATIONS ---------- 51
APPENDIX A: REPRESENTATIVE CALCULATIONS USED IN DETERMINING CORROSION RATES ---------- 52
APPENDIX B: TEST DATA ---------- 55
A. POTENTIODYNAMIC POLARIZATION (PDP) TEST DATA -- 55
B. PLANNED INTERVAL IMMERSION MASS LOSS (PIML) TEST DATA ---------- 56
C. CONTINUOUS SPRAY (CSP) TEST DATA ---------- 58
LIST OF REFERENCES ---------- 117
INITIAL DISTRIBUTION LIST ---------- 120

LIST OF TABLES

I. Comparison of Average Corrosion Rates ---------- 41

II. PDP Test Data ---------- 55

III. PIML Test Data, Weight Gain ---------- 56

IV. PIML Test Data, Corrosion Rate ---------- 57

V. CSP Test Data ---------- 58

LIST OF FIGURES


B.1 Schematic of Typical Flame Spray Device ---------- 59

B.2 Schematic of Typical Electric-Arc Spray Device --- 59

B.3 Spectrographic Analysis Data for Alloy Wire ------ 60

B.4 1100 Al F.S. Application Parameters -------------- 61

B.5 1100 Al A.S. Application Parameters -------------- 62

B.6 Zn F.S. Application Parameters ------------------- 63

B.7 Zn A.S. Application Parameters ------------------- 64

B.8 Alloy F.S. Application Parameters ---------------- 65

B.9 Alloy A.S. Application Parameters ---------------- 66

B.10 Spray Chamber ---------- 67

B.11 Corrosion Cell, PARC Model 9700, atop magnetic stirrer ---------- 67

B.12 Schematic of Flat Specimen Holder ---------- 68

B.13 Corrosion Measurement System, PARC Model 331 ----- 69

B.14 Scanning Electron Microscope, Cambridge Model S4-10 ---------- 69

B.15 X-ray Fluorescence Analyzer, PGT Model 1000 ------ 70

B.16 Al A.S. Coated Coupon, new ---------- 71

B.17 Al F.S. Coated Coupon, new ---------- 71

B.18 Zn A.S. Coated Coupon, new ---------- 72

B.19 Zn F.S. Coated Coupon, new ---------- 72

B.20 Alloy A.S. Coated Coupon, new ---------- 73

B.21 Alloy F.S. Coated Coupon, new ---------- 73

B.22 (X425), Al A.S. coating viewed in cross section, LM ---------- 74

B.23 (X250), Zn A.S. coating viewed in cross section, LM ---------- 74

B.24 Al F.S. coating, 14 days PIML ---------- 75

B.25 Al A.S. coating, 14 days PIML ---------- 75

B.26 Al A.S. coating, 28 days PIML ---------- 76

B.27 Al A.S. coating, 42 days PIML ---------- 76

B.28 Al A.S. coating, 56 days PIML ---------- 77

B.29 Al A.S. coating, 70 days PIML ---------- 77

B.30 Al F.S. coating, 28 days PIML ---------- 78

B.31 Al F.S. coating, 42 days PIML ---------- 78

B.32 Al F.S. coating, 56 days PIML ---------- 79

B.33 Al F.S. coating, 70 days PIML ---------- 79

B.34 Al A.S. coating, 21 days CSP ---------- 80

B.35 Al A.S. coating, 42 days CSP ---------- 80

B.36 Al F.S. coating, 21 days CSP ---------- 81

B.37 Al F.S. coating, 42 days CSP ---------- 81

B.38 Zn A.S. coating, 21 days CSP ---------- 82

B.39 Zn A.S. coating, 42 days CSP ---------- 82

B.40 Zn F.S. coating, 21 days CSP ---------- 83

B.41 Zn F.S. coating, 42 days CSP ---------- 83

B.42 Zn A.S. coating, 14 days PIML ---------- 84

B.43 Zn F.S. coating, 14 days PIML ---------- 84

B.44 Zn A.S. coating, 42 days PIML ---------- 85

B.45 Zn F.S. coating, 56 days PIML ---------- 85

B.46 Zn A.S. coating, 28 days PIML ---------- 86

B.47 Zn A.S. coating, 56 days PIML ---------- 86
B.48 Zn A.S. coating, 70 days PIML ---------- 87
B.49 Alloy F.S. coating, 14 days PIML ---------- 88
B.50 Alloy F.S. coating, 28 days PIML ---------- 88
B.51 Alloy F.S. coating, 42 days PIML ---------- 89
B.52 Alloy F.S. coating, 70 days PIML ---------- 89
B.53 Alloy A.S. coating, 14 days PIML ---------- 90
B.54 Alloy A.S. coating, 28 days PIML ---------- 90
B.55 Alloy A.S. coating, 42 days PIML ---------- 91
B.56 Alloy A.S. coating, 56 days PIML ---------- 91
B.57 Alloy A.S. coating, 70 days PIML ---------- 92
B.58 Alloy F.S. coating, 21 days CSP ---------- 93
B.59 Alloy F.S. coating, 42 days CSP ---------- 93
B.60 Alloy A.S. coating, 21 days CSP ---------- 94
B.61 Alloy A.S. coating, 42 days CSP ---------- 94
B.62 Plot of Zn A.S. Corrosion Rate ---------- 95
B.63 Plot of Zn F.S. Corrosion Rate ---------- 96
B.64 Plot of Alloy F.S. Corrosion Rate ---------- 97
B.65 Plot of Alloy A.S. Daily Weight Gain ---------- 98
B.66 Plot of Al A.S. Daily Weight Gain ---------- 99
B.67 Plot of Al F.S. Daily Weight Gain ----------100
B.68 (X135) Al A.S. coating, 14 days PIML, SEM --------101
B.69 (X155) Al A.S. coating, new, SEM ----------101
B.70 (X660) Al A.S. coating, 14 days PIML, SEM --------102
B.71 (X130) Al A.S. coating, 28 days PIML, SEM --------102
B.72 (X110) Al A.S. coating, 42 days PIML, SEM --------103

B.73 (X110) Al A.S. coating, 42 days PIML, SEM ---------- 103

B.74 (X110) Al A.S. coating, 56 days PIML, SEM ---------- 104

B.75 (X110) Al A.S. coating, 70 days PIML, SEM ---------- 104

B.76 (X120), Zn F.S. coating, new, SEM ---------- 105

B.77 (X140), Zn F.S. coating, new, cross section, SEM - 105

B.78 (X130), Zn F.S. coating, 14 days PIML, SEM ---------- 106

B.79 (X140), Zn F.S. coating, 14 days PIML, cross section, LM ---------- 106

B.80 (X650), Zn F.S. coating, cross section, 28 days PIML, SEM ---------- 107

B.81 (X140), Zn F.S. coating, 28 days PIML, SEM ---------- 107

B.82 (X110), Zn F.S. coating, 42 days PIML, SEM ---------- 108

B.83 (X110), Zn F.S. coating, 56 days PIML, SEM ---------- 108

B.84 (X110), Zn F.S. coating, 70 days PIML, SEM ---------- 109

B.85 (X130), Alloy F.S. coating, new, SEM ---------- 110

B.86 (X110), Alloy F.S. coating, 14 days PIML, SEM ---- 110

B.87 (X110), Alloy F.S. coating, 28 days PIML, SEM ---- 111

B.88 (X110), Alloy F.S. coating, 42 days PIML, SEM ---- 111

B.89 (X110), Alloy F.S. coating, 56 days PIML, SEM ---- 112

B.90 (X110), Alloy F.S. coating, 70 days PIML, SEM ---- 112

B.91 X-ray spectrum of Alloy A.S. corrosion products, 42 days ---------- 113

B.92 X-ray spectrum of Alloy A.S. corrosion products, 12 hours ---------- 113

B.93 X-ray spectrum of Zn F.S. corrosion products, 6 hours ---------- 114

B.94 X-ray spectrum of Zn F.S. corrosion products, 42 days ---------- 114

B.95 Pourbaix Diagram for Aluminum ---------- 115

B.96 Pourbaix Diagram for Zinc ---------- 115

B.97 Schematic Representation of a PDP Curve ---------- 116

## TABLE OF SYMBOLS

| | |
|---|---|
| Al | aluminum |
| Alloy | 99% aluminum, 1% zinc |
| uA | microamp |
| A.S. | arc spray |
| cm | centimeter |
| cm#2 | square centimeter |
| cm#3 | cubic centimeter |
| CSP | continuous spray |
| da | day |
| dm | decimeter |
| dm#2 | square decimeter |
| E(corr) | corrosion potential |
| F.S. | flame spray |
| gm | gram |
| hr | hour |
| I(corr) | corrosion current |
| l | liter |
| LM | light microscope |
| ml | milliliter |
| PDP | potentiodynamic polarization |
| PGT | Princeton Gamma Tech, Model 1000, x-ray fluorescence analyzer |
| PIML | planned interval immersion mass loss |

| | |
|---|---|
| PSP | potentiostatic polarization |
| min | minute |
| R(mdd) | corrosion rate (milligrams per decimeter per day) |
| R(mpy) | corrosion rate (mils per year) |
| SCE | standard calomel electrode |
| sec | second |
| SEM | scanning electron microscope |
| SHE | standard hydrogen electrode |
| V | volt |
| mV | millivolt |
| *W | weight gain |
| Zn | zinc |
| $\underline{\sigma}$ | standard deviation |

ACKNOWLEDGEMENT

I would like to express my appreciation to my advisor, Professor Jeff Perkins, for his guidance and timely advice during this undertaking; to Tom Kellogg who answered all my "little" questions and unselfishly gave his time to teach me the techniques I would use during this investigation; and finally, above all, to my wife who persevered through "one more deployment."

# I. INTRODUCTION

## A. BACKGROUND

The prevention of corrosion is an extremely important issue to the U.S. Navy. The National Bureau of Standards in their annual report to Congress in fiscal year 1975, stated that thirty percent of the Navy's maintenance budget some $392,000,000, was attributed to corrosion. During 1979, a panel of flag officers in their review of the work load imposed upon shipboard personnel to find means of reducing unnecessary expenditure of labor, found marine corrosion to be the major, continuing source of wasted manpower, [Ref. 1]. One of the most promising techniques available to slow the unending destructive attack of marine corrosion and thus reduce this inefficient drain of our labor resources has been found to be the application of molten anodic metal coatings over the corrosion-prone substrate. Currently there are two deposition processes widely in use by the Navy to accomplish this: oxygen-acetelyne flame wire spray and electric arc wire spray. Of the two, the oxygen-acetelyne is used most frequently in the Naval repair activities and will be discussed first.

In the oxygen-acetelyne flame wire spray process, the oxygen-gas mixture is ignited to produce a high temperature flame, approximately 3000 degrees Kelvin, through which a wire of the coating metal/alloy is passed. The feed metal

wire becomes molten as its tip passes through the flame. The liquified metal particles are then projected to the surface that is to be protected by a jet of compressed air, directed through an annulus surrounding the flame. Figure B.1 shows a typical flame spray gun. The coating particles solidify almost immediately upon striking the surface and solidification rates as high as 100,000 degrees Kelvin per second have been reported [Ref. 2].

Electric arc spraying is a similar process to flame spraying. Here an electric arc is used to supply the heat required to melt the feed wire. Again, compressed air is used to propel the molten metal droplets to the substrate surface. This process generates much greater temperatures that are attainable with the flame spray technique, 6300 degrees Kelvin. [Ref. 3]. Figure B.2 depicts a commonly used electric arc spray device.

## B. THIS WORK

Considerable investigation has been done with regard to the suitability for use of thermally applied coatings for anti-corrosion protection on large fixed structures [Ref. 4], [Ref. 5], and on marine vehicles [Ref. 6]. This technique has in fact been widely accepted for the protection of steel in both industrial and marine environments for some time. It is thus surprising that the U.S. Navy first adopted the thermal spray technique only 6 years ago [Ref. 7]. The

capability to routinely apply thermal coatings now exists throughout the Navy. At this point there has been a commitment made to the use of Wire Sprayed Aluminum for corrosion prevention, [Ref. 8], while shipboard evaluation of the results is continuing [Ref. 9 and 10].

Testing conducted on an 85% Zinc- 15% Aluminum alloy conducted in Europe during the mid 1970's indicated the possibility of a hybrid coating incorporating the most favorable qualities of the constituent materials in a number of corrosive environments [Ref. 11]. No structured testing and evaluation is currently in progress in this country to determine the suitability of these Al/Zn alloys for naval use [Ref. 12].

The intention of this research is to compare a thermally applied alloy coating composed of 99% Al and 1% Zn to coatings of pure Al and pure Zn applied by the same techniques for its ability to protect against the corrosion of a mild steel substrate; to develop corrosion rate information; to provide a relative ranking of suitability of this alloy coating with respect to Al and Zn for marine application, and to investigate the mode of corrosive attack and the composition of the corrosion products for each of these coatings.

## II. EXPERIMENTAL PROCEDURE

### A. THE ELECTROLYTE

A 3.5% NaCl solution was used as the electrolyte for all phases of testing during this investigation. The solution was prepared by adding the proper proportion of reagent grade NaCl to distilled water. The concentration of the original solution was verified utilizing the titration of the NaCl solution in the presence of sodium chromate ($Na_2CrO_4$) by a silver nitrite ($AgNO_3$) solution. In addition to its use in confirming the concentration of the original NaCl solution, this technique was utilized to verify the NaCl concentration daily, prior to the use of the solution in electrochemical testing, and every five days throughout the length of the PIML test. The NaCl concentration increased during the PIML test, requiring that distilled water be added to the electrolyte in order to maintain the desired concentration limit. An increase of 0.1% NaCl concentration could be expected in a 5 day period. The pH of the solution was measured at the beginning of the PIML test with litmus paper and upon the completion of testing with a Beckman 4500 pH meter. The initial indication was of a pH of 7.0, as was expected; the reading at the end of the PIML test was pH 6.8.

B. TEST COUPONS

Three coatings and two application methods were considered in this study. An alloy coating, a coating of 1100 aluminum and a zinc coating were used in this test. Figure B.3 provides the results of a spectrographic analysis conducted on the alloy wire. Figures B.4 to B.9 contain the flame/thermal spray data sheets which fully describe each coating and the techniques of application used for each sample type.

The coatings studied represent not only those currently in use, but also, in the case of the alloy, one of an untested composition. The samples were provided by the Puget Sound Naval Shipyard in Bremerton, Washington, and are representative of flame sprayed and arc sprayed coatings routinely produced by this activity for "Fleet" use. The samples used in this test, consisted of 2" X 6" X 1/8" (3.08 cm X 9.24 cm X 0.3175 cm) plates of mild steel coated on all surfaces with thermally applied coatings of about 10 mils, (25 um) thickness. It is necessary to apply the coating to this thickness, because otherwise the high degree of porosity would allow access of a corrosive medium to the substrate [Ref. 13]. The large coupon size was decided upon in an attempt to minimize unwanted edge effects. The six combinations of coating and deposition technique were:

i) Aluminum Arc Spray

ii) Aluminum Flame Spray

iii) Zinc Arc Spray

iv) Zinc Flame Spray

v) Alloy Arc Spray

vi) Alloy Flame Spray

1. Cleaning and Weighing the Coupon

The coupons were cleaned before and after each test. Upon initial receipt of the specimens, they were rinsed with warm running tap water to remove any packing material that might loosely adhere to the surface and then immediately placed in an ultrasonically agitated acetone bath for two minutes of degreasing. After being completely dried with warm air, the coupons were weighed using a Mettler Model H15 analytical balance, sealed in marked plastic bags for identification, and placed in a desiccator until required for use.

The mechanical cleaning process utilized to remove corrosion products after testing consisted of:

i) 5 minutes of vigorous scrubbing with a hard-bristle brush under a warm stream of tap water

ii) 5 minutes total immersion in an ultrasonic bath containing acetone

iii) 10 minutes, drying in warm air, (5 minutes per coupon side)

Reweighing of samples occurred immediately after the completion of the cleaning process, with the same analytical balance used. Prior to every use of the analytical balance, its consistency was verified utilizing a set of standard weights.

C. CHAMBER TESTING

1. The Chamber

The test chamber, depicted in Figure B.10 was constructed of marine grade plywood and painted with water sealing paint. The tank dimensions are 50 inches X 30 inches X 12.5 inches, (127 cm X 76.2 cm X 31.75 cm). During the testing, the tank contained approximately 25 gallons, (94.6 l) of electrolyte at room temperature. The sample holder rack. visible at the rear of the tank in Figure B.10, was constructed of Plexiglas and Lexan. A silicon adhesive caulking was used to isolate all metal screws used in the construction of the rack from the environment. The test rack was attached to a pneumatic actuator fixed to the rear of the tank. A timing device provided the control to allow the alternate raising and lowering of the sample holder at 30 minute intervals. The samples, when placed in the rack, rested at an angle of 45 degrees with respect to the horizontal. Contact between the sample and the holder was minimized by allowing only line contact by the holder at two positions on opposite ends of the specimen. This double fulcrum arrangement permitted the electrolyte to contact the vast majority of the coupon's surface.

The forward portion of the tank consisted of a spray chamber containing a mist of the solution being held in the tank. The spray chamber was completely isolated from the immersion section of the tank by Plexiglas baffle plates.

A Plexiglas sheet on the roof of the chamber served as the access point to the interior of the device. Two exhaust ports constructed of 2 inch (5.08 cm) diameter PVC piping were located at the rear of the spray chamber to act as an atmospheric vent for excess moisture. Within the chamber a 20 inch (50.8 cm), diameter steel rim rotated at 1/3 rpm in a horizontal plane. The rim was coated with a marine type, water sealing paint. The mist was provided by a glass nozzle that had a single stream of electrolyte pumped into its center by a roto-flex pump. The fluid was atomized by a jet of air that was injected about the periphery of the nozzle. A Teflon sheet was placed directly in front of the nozzle discharge, between the nozzle and the rotating rim, to insure that the electrolyte could not directly impinge upon the test coupons and to physically reduce the size of the mist droplets. The spray chamber fully complied with ASTM requirements for spray testing [Ref. 14].

2. Planned Interval Immersion Mass Loss Test (PIML)

Each type of coating was subjected to a 70 day PIML test. The test began with a total of 30 standard coupons, 5 coupons representing each coating type. The samples were placed in the holding rack attached to the rear of the test chamber. The test began when the rack was lowered into the electrolyte and the test coupons were completely immersed. After an immersion of 30 minutes, the samples were lifted clear of the electrolyte. They remained in this position for the succeeding 30 minutes. This lowering and raising of the

specimens comprised the complete immersion/emersion cycle which was used throughout the test. The total cycle time was one hour.

At the end of the first 14 days of the test, and each 14 days thereafter, one sample of each coating type was removed from the holder. This regimen was followed for 70 days. As the coupons were removed from the test, they were allowed to dry for one day, then were photographed, cleaned as previously noted, reweighed, and sectioned for further examination. Utilizing the information gained from the re-weight, the corrosion rate was calculated, if applicable, utilizing the methods described in Appendix B.

3. Continuous Spray Testing (CSP)

Two standard coupons of each coating type were flat mounted on a Lexan holder with a plastic screw. The coupons were mounted in such a manner that the entire back face of the coupon rested flush against the Lexan, effectively insulating it from its environment. The Lexan holder with coupon attached was placed upon the rotating rim, so that the coupon's length was perpendicular to the plane of the rim's rotation. Once fixed to the rim, the coupon was subjected to the 3.5% NaCl atmosphere in the spray portion of the test chamber. The mist was provided by the atomizer which was being supplied with the electrolyte at the rate of 25 ml/min and compressed air at 5 psig. One test coupon of each coating type was removed at 21 and 42 days after the start of the test.

D. ELECTROCHEMICAL TESTING

1. The Corrosion Cell and Test Coupons

The corrosion cell used in the electrochemical phase of testing was the Model 9700 manufactured by Princeton Applied Research, (PARC), shown in Figure B.11. This cell, which consists of a 1000 cubic ml round bottom flask with five necks, was recommended by the ASTM standard for electrochemical testing [Ref. 15]. For the experiments, two necks of the flask held high density graphite auxilary electrodes, the third neck a gas sparger, the fourth a Luggin probe-salt bridge, and the center a flat specimen holder. Figure B.12 schematically displays the flat specimen holder.

The test specimens were machined from the large coated coupons provide by the Puget Sound Naval Shipyard into disks 5/8 inches (1.59 cm) in diameter to fit in the flat specimen holder. Special effort was made to insure that the coated surfaces of the disks were not disturbed during the cutting. The Luggin probe-salt bridge; used as the reference electrode, was of the saturated Calomel variety.

2. Corrosion Measurement System

The corrosion measurement system, pictured in Figure B.13, used for the electrochemical portion of the testing consisted of:

A. Potentiostat/Galvanostat, Princeton Applied Research Model 173

B. Programmer, Princeton Applied Research Model 175

C. X-Y Recorder, Hewlett-Packard Model 7040A (PDP test only)

D. Strip Chart Plotter, Gould Brush 110 (PSP test only)

3. Potentiodynamic Polarization Measurement (PDP)

Approximately 800 ml of the 3.5% NaCl electrolyte were poured into the corrosion cell. The electrolyte was stirred with a magnetic stirring device while air was bubbled through it for ten minutes. The flat specimen holder containing a specimen was inserted into the aerated electrolyte. Any air bubbles that might attach themselves to the specimen or holder were gently shaken off before the testing commenced. The coupon remained in the electrolyte for one hour to insure that it was corroding freely [Ref. 16] before the linear potential variation was initiated. When the period of aging was completed, the temperature was recorded and the Model 175 Programmer adjusted to traverse the voltage range from 200 mV less positive than E(corr) to 200 mV more positive than E(corr). This potential range was scanned at a rate of 2 mV/sec. The resulting plot of log current versus potential comprises a complete potentiodynamic curve for the particular test specimen and and solution. Three runs per coating and deposition method, a total of eighteen in all, were conducted. The plots produced were analyzed using standard methods to determine E(corr) and I(corr), the corrosion rates in both milligrams per square

decimeter per day (MDD) and in mils penetration per year (MPY) and standard deviation for each group of specimens so tested were calculated [Ref. 17].

4. Anodic Polarization Test (PSP)

The standard test coupon for electrochemical testing was used, as was the specified corrosion cell and corrosion measurement system. The specimen and holder were immersed in the electrolyte and allowed to age for one hour. At this time, the E(corr) was read directly from the Model 173 Potentiostat/ Galvanostat. A potential 50 mv more positive than this value of E(corr) was applied for a predetermined interval. This applied potential induced the coupon to act as the anode and thus to stimulate oxidation. Run times were 30, 60, 360, and 720 minutes in duration. Current was recorded as a function of time with a strip chart recorder connected to current-to-voltage module of the potentiostat. The amount of coating oxidized during each run was then calculated using the HP 9875A digitizer to generate X,Y pairs corresponding to the current versus time plot. An HP 9845A was used to fit an equation to the digitized points. The equations for the I(t) curves thus generated were substituted into Faraday's law:

$$\text{mass lost} = (e/F) \int I dt$$

Where e is the equivalent weight of the metal in grams per equivalent, $\int$ Idt is the current-time integral in coulombs,

and F is the Faraday constant in coulumbs/equivalent. The result of this equation is mass loss in grams, assuming the reaction products are soluble.

## E. POST TESTING EVALUATION

Specimens from the PIML test, the CSP test, and the PSP test were examined after the completion of each test or test period. The samples resulting from the immersion test and the spray test were examined with the intention of discovering information concerning the mode of corrosion and the distribution of corrosion products. The PSP samples were examined to determine if a film similar in chemical composition to that formed on the coatings during the PIML test and CSP test could be electrochemically produced.

Following each cycle of PIML testing and CSP testing, the samples that had been removed from the test were allowed to air dry. Observations were made as to the color and distribution of the corrosion product prior to photographing the samples the following day. The specimens were then mechanically cleaned in a attempt to remove all corrosion products. When this cleaning was completed, the distribution and type of corrosive attack upon the coating was noted. Sectioning of the coupon into a small square that could and was mounted on an SEM stub followed.

These specimens were than examined utilizing a Cambridge S4-10 Steroscan, scanning electron microscope, SEM, shown in Figure B.14. This microscopic examination technique proved to

to be extremely fruitful because of the SEM's ability to focus at high magnifications on the irregular coating surface.

While the sample was in the SEM, X-ray fluorescence analysis also was performed on the adhering corrosion products using a Princeton Gamma Tech, PGT Model 1000, X-ray fluorescence analyzer, displayed in Figure B.15. The spectrum emitted when the corrosion product was subjected to an X-ray beam was analyzed to quickly identify the substance's basic chemical composition. It should be noted that the analysis performed by the PGT 1000 does not include the presence of lighter elements (e.g.: hydrogen and oxygen), leaving one at the mercy of one's "educated" intuition to determine the complete composition of the corrosion products present.

The PSP samples' corrosion product were so little in quantity that they were merely rinsed in distilled water to remove any electrolyte that might remain after the electrochemical test and prior to X-ray fluorescence analysis.

In addition, the corrosion products scraped from several samples were examined by powder X-ray diffraction techniques. The powdered sample of corrosion product was subjected to a monochromated beam generated from a copper tube at 30Kv/40ma. The output intensity versus 2$\theta$ angle was plotted on a strip chart and analyzed using standard methods [Ref. 18].

# III. RESULTS AND DISCUSSION

## A. PRE-TESTING COATING EXAMINATION

The coatings could immediately be separated by their visual dissimilarities. The coatings that had been applied by the F.S. method were much duller than the A.S. coatings. The A.S. coatings had a slight metallic shimmer, while the F.S. coupons were a dull, flat gray. The Zn coated coupons were noticeably darker than their Al and Alloy counterparts, with the texture of the F.S. samples much finer (similar to 200 grit sandpaper) than the surface of the A.S. sample. Figures B.16 to B.21 show the coupons in their as received condition.

Light microscope examination of the coatings displayed their extreme porosity. Figure B.22 shows the cross section of an Al A.S. coating, typical of all Al and Alloy coatings applied by either the A.S. or F.S. process. Figure B.23 shows a Zn A.S. coating in cross section. This structure is typical of Zn coatings applied using either process. Notice that the Zn coating has a much more compact, less porous structure than the others. This more fluid structure results because the lower solidification temperature of Zn allows it to flow for a longer time before freezing in its final configuration when compared to the structures formed by Al, which solidifies at a much higher temperature, [Ref. 19].

## B. MACROSCOPIC OBSERVATIONS OF COATING BEHAVIOR DURING PIML/CSP

### 1. Aluminum Coatings

Light brown patches began to appear on the 1100 Aluminum coatings after only five hours of the PIML test. The brown spots grew larger over the next two days, at which point the entire visible portion of the coupon had been transformed from its original silver-gray color to a faded brown. During the next five days, dots of a white corrosion product became clearly visible. Close examination of the coupons as they neared the end of their interval of immersion, showed that the coupon surface had become covered with a very light, white haze and that the prominent white spots were nodules of corrosion product accumulation. The Al coupons removed after the first 14 days of the test displayed a definite white haze over a dark brown background with the intense white spots randomly dotting the surface. This accumulation was much more apparent in the case of the Al F.S., Figure B.24, than for the Al A.S., Figure B.25. The accumulation of nodules on the F.S. coating grouped together more rapidly making larger globules than on the A.S. sample even though the total number of nodules was approximately equal. During the remainder of the PIML test, the white corrosion product seemed to uniformly thicken over both types of aluminum coating surfaces. The sites of original rapid corrosion product build-up appeared not to have increased in size after their initial burst of growth. Figures B.25 to B.29 detail the response

of the Al A.S. coatings and Figure B.24 and Figures B.28 to B.33 that of the Al F.S. coating to the prolonged testing. It appears that the white film of corrosion product that eventually formed a thick blanket on the coupon's surface intentionally grew around the nodules.

Those coupons that participated in the CSP test displayed the same general film formation tendency as the coupons in the PIML test; however, the rate of formation was decidedly longer. After six weeks in the atomized 3.5% NaCl environment samples of both coatings had been covered with a white hazy film and nodule growth was slight but still perceptable. The brown discoloration that was immediately prominent in the samples that had been immersed in the electrolyte was barely visible on these coupons. Careful examination of Figures B.34 to B.37, allows one to detect a very slight dark shadow on the lower third of the coupons.

During the mechanical cleaning process, the white film became slippery immediately when wetted and was easily removed from the specimen. After the cleaning was finished, all aluminum coated coupons that had participated in the PIML had taken on a dark brownish appearance splotched with patches of dull gray. These dull gray patches, initially visible on the first group of samples removed from the test, became the sites for pitting attack of the coating to occur as the test progressed. The surface of the coating was visibly pierced in six weeks time.

As the test continued, these pits could be seen to increase in both depth and width. The coupons from the CSP test showed only slight dulling of their original finish and minimal discoloration.

2. Zinc Coatings

During the initial five hours of the PIML test, the Zn coated coupons began turning a green-gray color and tracks appeared where the electrolyte had flowed off the coupon when it was emersed. The tracks, which resembled the path left by a water drop as it slides down a pane of glass, were highlighted by the accumulation of a corrosion product in the space between them. These strips of corrosion product grew very rapidly, and during the third day of the test were continuous over the sample's length. Simultaneously, the once green-gray tracks were filling in with the corrosion product. By the end of the second week of immersion testing the entire sample was completely covered with the corrosion product and, as a result, took on a snowy white appearance. This voluminous corrosion product is often referred to as "white rust". During the primary stages of growth, the thickness and intensity of this product layer seemed to increase rapidly. As the test continued, the thickening of the film seemed to subside. The once apparent river pattern quickly evolved into a grotesque series of tongues and fissures on the white corrosion product surface. The form of corrosion product growth seemed to be similar for both types of Zn coatings.

The Zn coatings involved in the CSP test, as in the case of the Al coated coupons, appeared to undergo the identical film forming sequence that the PIML coupons experienced but over a significantly longer period of time. Figure B.38 shows the "water tracks" on the Zn A.S. Figure B.39 shows the Zn A.S. coupon after six weeks of exposure to the continuous electrolyte mist. A comparison of the effect of the CSP test on coupons of Zn F.S. after three weeks, Figure B.40, and after six weeks, Figure B.41, with the Zn A.S. coupons, Figures B.38 and B.39, shows that initial corrosion product occurs more rapidly for the Zn A.S. coatings.

The appearance of iron oxide, red rust, occurred for the Zn A.S. 39 days after the start of the test, and for the Zn F.S. 45 days after the test beginning. The presence of red rust indicated that the coating had been penetrated. As the test continued, the white corrosion product took on a reddish tint as the red rust bled into it. Initial points of coating failure can be seen in Figure B.44 for the Zn A.S. and in Figure B.45 for the Zn F.S. coating. Figures B.42, B.46, B.44, B.47, and B.48 show the progression of the corrosion product's advance on Zn A.S. coupons. Note that the coating breakdown seems to initially occur at the center of the coupon and then concentrates at the lower edges as the test length increased. Coating failure was most apparent on the underside of the test coupons where drops of the electrolyte collected during the emersion portion of the test cycle. It has been suggested

that an acidic environment retards the reformation of the passivating film of zinc, thus speeding its consumption [Ref. 20]. Once coating break-through had occurred, further deterioration of the substrate followed.

Mechanical cleaning of these samples caused some of the film turn to a soft, white mush which was easily rinsed off. During the latter phases of the test, cleaning the samples resulted in a significant amount of the white corrosion deposit coming off in large, irregularly shaped flakes; additionally, a small proportion of the product, perhaps that covering 5% of the surface area, adhered tightly to the coating. The areas of adhering white film seemed to closely correspond to the spaces between the "water tracks" that formed early in the test. Mechanical cleaning of the coupons with red rust present resulted in portions of the coating being removed with the large white flakes. The substrate thus revealed appeared to be suffering from general corrosion. This phenomenon leads to the notion that once the coating fails, the corrosive attack takes place not only at the coating surface, but also at the interface of coating and substrate. Here it spreads quickly to undermine the coating.

The cleared coupons of both Zn coatings that were removed from the test at the end of the eighth and tenth weeks, showed in addition to their rusty appearance, that attack of the substrate had occurred predominantly on the lower portion of the coupon. The white patches of adherent corrosion product

found on these specimens could be removed by scraping them with a fingernail. Removal of these last vestiges of the corrosion product revealed more general corrosion.

The coating breakthrough apparently began in areas where the corrosion product film had repeatedly ruptured, eventually exposing the steel substrate to the corrosive action of the electrolyte. The significance of the first failure near the sample center can be explained by realizing that tensile stresses are produced in the film as it dries upon emersion from the bath. These stresses cause the film to split, exposing fresh coating to the corrosive medium. It has been suggested that the formation of the oxide film on Zn is retarded or stopped completely by the presence of an acidic electrolyte. The absence of this film evidently allows the corrosive attack on the coating. The protective film of Zn slowly reforms upon immersion, but the Zn exposed is subjected to direct attack. The many recurrences of this sequence of events during the test resulted in coating failure. Failure of the coating on edge surfaces in all probability occurred because the thickness of the coating at these points was less than on the surface of the coupons. This lesser thickness can be rationalized if one realizes the difficulty involved in coating the very thin edges of coupons of this geometry. It should be noted, that none of the coupons participating in the CSP's less corrosive environment experienced any visible deterioration.

3. Alloy Coatings

The alloy coatings began turning a dark brown during the second day of the test. A light, hazy white film was seen to form on the Alloy F.S. samples during the fourth day. By the end of the first week, localized thickening of the film was clearly visible. As these patches of film thickened, they began reaching upward, above the coating surface and eventually formed distinct nodules as is shown in Figure B.49. Between the second and sixth weeks, the film at the base of these nodules grew thicker and the nodules increased in size. Comparing Figures B.49, B.50, and B.51; the high initial growth rate of the film and nodules is apparent. Examination of the coupon removed at the four week point resulted in the observation that the nodules were clustering along the longitudinal edges of the coupon. Figure B.52, showing the coupon removed upon completion of the test, demonstrates the extent to which this clustering occurred.

The A.S. Alloy coatings appeared to develop the continuous white film at a much slower rate than was observed with the F.S. Examination of Figure B.55 shows an A.S. coupon after six weeks; this was the first A.S. coupon which clearly had a complete film. The coupon removed at the end of the first two weeks of testing, Figure B.53 showed the typical dark brown background, intermittently splotched with the white corrosion product. The nodules began appearing during the third week, and are visible in Figure B.54. Through the tenth week the

nodules continued to grow and the film increased in thickness. This can be seen in Figures B.56 and B.57. It is notable that the Alloy F.S. coating corrosion product growth rate seemed to start off high and end at a much lower level, while the growth rate of the A.S. coating seemed to remain relatively constant throughout the test.

When coupons were cleaned, the surfaces of the samples were generally a brownish-gray, except where the corrosion product deposits were thick or nodules had grown. In these areas the samples were a dull metallic gray. On the F.S. samples removed at the eighth and tenth week, the coating directly beneath the nodules was cracked and in some cases pitting had started.

Those F.S. coupons that were in the spray chamber showed very slight discoloration in the form of indistinct brown water tracks running the length of the sample. This can be seen in Figure B.58. Figure B.59 shows the tracks being blotted out by a white film. It can be seen that the first film forms on the lower portion of the sample. This results from the accumulated condensed mist traveling down the sample face, back to the electrolyte bath under the force of gravity. The A.S. coated samples showed no response to the corrosive mist for the majority of the test, as can be seen in Figure B.60. The duller appearance of the sample of Figure B.61 is the first indication that film formation has occurred on this type of coating.

## C. CORROSION RATES

### 1. PIML

The immersion/emersion corrosion rates were calculated as described in Appendix A upon the bi-weekly removal of one coupon of each coating of Zn and Alloy A.S.; the results of these calculations appear in Table IV. Graphs depicting the change in corrosion rate during test interval for the coupons showing a weight loss are displayed in Figures B.62, B.63, and B.64. It can be said that the corrosion rates for both Zn coatings generally decreased as time progressed. As was predicted by the results of the PDP test, the Zn F.S. was less susceptible to corrosion than the Zn A.S. The Alloy F.S. fell victim to the corrosive attack of the electrolyte, yet the Alloy A.S. showed a weight gain, albeit one decreasing with time. This is depicted in Figure B.65. Both Al coatings showed weight gains consistently during the test. The bi-weekly weight gains are displayed in Table III, Appendix B, and presented graphically in Figures B.66 and B.67. This weight gain is caused by the products of corrosion filling the pores of the coating and forming an additional protective barrier for the substrate, [Ref. 21].

The effectiveness of a coating subjected to a corrosive environment must be considered adequate if it gains weight and no visible deterioration occurs. In this case, Al coatings of both types and the Alloy F.S. coating were found to be suitable anti-corrosion protection.

A disturbing aspect of the PDP testing was the discovery that the Al and possibly the Alloy coupons had picked up some Zn in the course of the test. This contamination undoubtedly resulted from conducting the test in a common electrolyte bath. Future experimenters should take care to insure that samples of various coating materials are physically segregated from one another.

2. PDP

The results of the PDP test, tabulated in Table II, show that for Al and Zn coatings, the flame spray deposition method is superior to the arc spray method. The reverse situation was predicted for the Alloy coatings. The calculated corrosion rates were arrived at using the procedures found in Appendix A. Variations in the predicted corrosion rates may have resulted from the different value of equilibrium reached prior to each run. In one case a 35 mV discrepancy existed between the equilibrium E(corr) of specimens of the same coating type at the beginning of test runs.

D. SEM MICROSCOPY

1. Al Coatings

The coupons removed after two weeks of testing showed small, isolated areas of corrosive attack. These remote patches were characterized by jagged, uniformly low projections, as seen in Figure B.68. The original surface structure of the coating was much more rounded, less uniform in height, and

TABLE I

Comparison of Average Corrosion Rates

| Coating | Rate (MDD) | | Rate (MPY) | |
|---|---|---|---|---|
| | PDP | PIML | PDP | PIML |
| Al A.S. | 11.4±2.1 | * | 4.2±.8 | * |
| Al F.S. | 6.8±1.9 | * | 2.5±.7 | * |
| Zn A.S. | 376±35 | 236±82 | 52.7±4.9 | 47.1±17 |
| Zn F.S. | 170±41 | 229±53 | 24±5.6 | 46±10.6 |
| Alloy A.S. | 26.3±4.7 | * | 9.4±1.7 | * |
| Alloy F.S. | 28.5±7.8 | 8.9±10.4 | 10.2±2.8 | 4.6±5.3 |

* indicates no corrosion rate calculated because of continuous weight gain by coating

generally less cluttered, Figure B.69. Closer investigation of the corroding surface, Figure B.70, shows a snowy white, irregularly shaped corrosion product to be enveloping the coating surface. After four weeks, "mud-cracking" was visible, indicating that an oxide film had formed and was possibly aiding in corrosion prevention. These mud-cracks can be seen in Figure B.71. Aluminum and its alloys typically form a durable oxide film as a means of impeding corrosive attack [Ref. 22]. Six weeks after the start of the test the first significant signs of coating deterioration were observed. Figure B.72, shows one large surface excavation surrounded by several smaller indentations of lesser depth. PGT analysis of the large hole showed that this pit did not extend through the coating to the substrate. In another area of the sample, Figure B.73, shows the several forms that the attack was taking. At the extreme top of the micrograph can be seen a region that has suffered little from the corrosive attack; the destruction that has occurred is similar to that seen in Figure B.68. The center of this photo shows an area where the large puffy protruberances have been reduced to little stubs; finally, cracks in the protective film are visible at the lower right. During the seventh and eighth weeks the coating surface appears to have become more uniform. The corrosion seems satisfied to level any projecting remnants of the original surface. Figure B.74 shows the level landscape. By the tenth week the corrosion has turned

to burrowing in the direction of the substrate. It can be seen in Figure B.75 that pitting attack of the coating has begun to reestablish itself.

While this series of observations applied directly to Al A.S. coatings, the response of the Al F.S. coatings was very similar. The A.S. coating was chosen as the example here because it was predicted to be more susceptible to corrosion than the F.S. coating by the PDP tests.

2. Zn Coatings

The SEM of the Zn A.S. and F.S. coatings showed that both had responded almost identically during this test. Unless specifically stated, all comments hereafter refer to the Zn A.S. coating. The surface structure of the coating in the as received condition is shown in Figure B.76. Notice the large puffy projections. In cross section, it was observed that very little oxide had formed on the exposed coating, Figure B.77. By the end of the second week, the surface of the coating was beginning to appear gnawed upon, and indications of pit initiation were visible as can be seen in Figure B.78. Looking at the coating cross section again in Figure B.79, it is observed that the products of corrosion have begun to form within the coating itself. This accumulation of corrosion products, while only of interest in this case, becomes important when it is considered that some specimens gained weight during the PIML test, undoubtably by this mechanism. The coupons removed from the test at the four week point showed much larger areas of

general deterioration than had been previously observed. Figure B.81, and much more concentrated pit formation. The coating thickness was seen to uniformly decrease in general, and decrease markedly around areas of pitting. Figure B.80 reveals a pit in the substrate beneath an intact segment of Zn coating. It is generally agreed upon that Zn protects a substrate by means of sacrificially corroding. The pit beneath the coating would indicate that the mode of corrosive attack on the coating is intergranular [Ref. 23]. Figure B.82 shows an area racked by pitting in just six weeks. The examination of the samples removed after eight weeks showed the first large areas of coating dissolution. The boundary at the center of Figure B.83 shows the separation of coating and substrate. By the end of the test, areas where no coating remained were prevalent. The patches of coating that did remain were extremely thin and flaked off easily. Figure B.84 shows a thin ring of coating surrounding an exposed portion of substrate.

3. Alloy Coatings

SEM examination of the as-sprayed Alloy specimens showed their surface structures to be remarkably similar. Figure B.85 shows a typical Alloy F.S. surface prior to exposure to a corrosive environment. The response of both coating types to the PIML was very similar; however, the reaction of the Zn A.S. lagged behind that of the Zn A.S. coating. At the end of the PIML test, the Alloy A.S. coupon appearance was identical to that of the Zn F.S. after only six weeks of exposure.

The initial stages of corrosive attack were visible on the F.S. sample removed after the second week. Figure B.86 shows the boundary between a region of heavy oxide formation, and a more vigorously corroded area. Notice the seemingly intact original structures surrounding a pit site. The areas of obvious attack comprised a small percentage of the total surface area. By the end of the fourth week, the patches of corrosive attack had become much more numerous and larger. The rate of corrosive attack became accelerated as the oxide layer was broken through. Figure B.87 reveals the indentation in the coating surface resulting from the varied rates of attack. Between the fourth and sixth weeks significant pitting transpired. One of the many pits is shown in Figure B.88. The white oxide deposit about the edge of the pit reaffirms the observation that the surfaces surrounding a pit are passivated as a result of the pitting mechanism. In the center of Figure B.89, visible amidst a field of cracked oxide, pits, and remnants of the attack, stands a lone reminder of the original coating structure. The attack of the corrosive electrolyte had enveloped the overwhelming majority of the surface area by the end of the eighth week. The area of heavy pitting and protruding oxide correspond to a location of a nodule prior to cleaning. Figure B.90 shows a portion of the coupon located beneath a clustering of nodules at test's end. It is apparent that the nodule's presence stimulates an increased attack of the Alloy coatings.

## E. CORROSION PRODUCT ANALYSIS

### 1. PGT Analysis

The Princeton Gamma Tech spectral analysis occurred concurrently with the SEM examination of the PIML, PSP, and CSP samples. The analysis of all the Al coatings that had participated in the PIML test showed that they had accumulated a large amount of Zn in their corrosion product. Additionally, the Alloy coated coupons contained what was considered to be a higher proportion of Zn than could reasonably be expected. The amount of Zn in the corrosion products increased as the test proceeded, indicating that the concentration of the Zn ions in the common electrolyte steadily increased during the ten week period and migrated to the Al and predominantly aluminum, Alloy. This same effect was observed to a lesser extent in the Al and Alloy coated coupons that participated in the CSP test. Figure B.91 shows the PGT analysis of the corrosion product scraped from an Alloy A.S. coated specimen that had undergone six weeks of PIML testing. Comparing it to Figure B.92, which shows the spectrum derived from the analysis of a PSP Alloy A.S. sample, (this spectrum is normalized with respect to the PIML specimen), one sees that the energy levels of the first large peak, Al, and the following peak, Cl, correspond exactly. These figures vary in the degree that the Cl ion is present in the corrosion products and in the previously mentioned Zn peak visible in the PIML corrosion product. The different Cl ion concentration can be understood

by realizing that the PIML test allowed the coupons to be physically immersed in an electrolyte containing a plethora of the Cl ion, as opposed to the coupons exposed in the CSP test that were in contact with significantly fewer of these ions. The results of the analysis of the PSP Zn samples, Figure B.93, and the Zn CSP coupons, Figure B.94, show a correlation between the Zn; first, third, and fourth peak in Figure B.94 and the first, eighth, and ninth peaks in Figure B.93. The Cl peaks, the second peak in Figure B.94, is much more intense than in Figure B.93. This results from the much greater period of contact the coupon in the CSP accumulated in contact with the Cl ion as compared with the PSP specimen. The specimen of Figure B.94, shows the presence of Al, again indicating that some concentration of the metal ions occurred in the immersion bath. The analysis of the corrosion products produced by the Alloy coatings was generally identical to that of the Al coating.

2. X-ray Diffraction

The analysis of the corrosion products by x-ray diffraction proved to produce ambiguous results because of the complexity of the plots produced. In many cases the diffraction pattern peaks were not distinct, but composed of several underlying peaks; thus effectively masking the identities of the compounds involved.

F. COMPARISONS OF COATINGS

1. Zn versus Al

The tests obviously highlighted the fact that Al coatings are a better means of corrosion protection than Zn coatings. By examining the Pourbaix diagrams, [Ref. 24], for both Al, Figure B.95 and Zn, Figure B.96, we see that Zn is in a region of corrosion when the electrolyte is even slightly acidic and the potential is above -.8 mV (SCE) or -.559 mV (SHE). The test environment met these conditions. In the case of the Al coatings, the reduction potential of approximately -.478 mV (SHE) or -.719 mV (SCE) and the slightly acidic condition of the electrolyte placed it in an area where the formation of a passive film of $Al_2O_3$ is possible.

2. Al versus Alloy

While nothing as straightforward as the Pourbaix diagram comparison exists for the Al and Alloy coating comparison, the results gained from the tests conducted do shed some light on the subject. The results of the PIML test showed that both Al coatings were able to withstand this environment, while one Alloy coating type failed. The PDP test predicted that the Al coatings would corrode less than their Alloy counterparts. Finally the CSP can be considered a draw, in that both coatings gained weight. Those wishing to be more critical of this test may observe that the Zn coatings also gained weight in this test; no, considering this test proof of equivalence between

the performance of two coating types is suspect. That said, the Al coatings were clearly superior in one test, somewhat better in another, and roughly equivalent in the third to the Alloy coating. These results, combined with the lower density of Al, 2.72 q/cm 3, as compared with 2.80 g/cm 3 for the Alloy coating, and the greater ease of manufacturing the Al wire, make Al coatings the better choice for these conditions in particular, and generally for use in harsh marine environments.

# IV. CONCLUSIONS AND RECOMMENDATIONS

## A. CONCLUSIONS

1. In the case of the 1100 Al and the Zn coatings, electric-arc sprayed anodic metal coatings are not as effective in preventing corrosion as coatings of similar materials applied by flame-spraying.

2. The corrosion rates predicted by the PDP test, while showing little resemblance to the average rates resulting from the PIML test, can be used to predict the relative corrosive prevention effectiveness of a given coating in an aggressive marine environment.

3. The 99% Al/1% Zn coating shows no significant advantage over the Al coating.

4. Zinc coatings are not suited for use in a harsh marine environment.

5. Oxide films similar to those naturally occurring on the coatings can be produced electrochemically.

6. Relative rankings of the coatings tested for use in a harsh marine environment are:

Al F.S.

Al A.S.

Alloy A.S.

Alloy F.S.

Zn F.S.

Zn A.S.

B. RECOMMENDATIONS

Further investigation should be carried out to evaluate individual coatings to:

i) Determine the effect of different types of attack on thermally applied coatings, (e.g.; bimetallic corrosion, crevice corrosion, impingement attack, cavitation)

ii) Determine the effect of cooling rate on microstructure, and how microstructure relates to the mechanical properties of a coating job,

iii) Determine the mechanical properties of the coating, particularly as they relate to bond strength,

iv) Develop a technique to accurately, easily, and reproducibly evaluate the mechanical properties of a coating job.

## APPENDIX A

## REPRESENTATIVE CALCULATIONS USED IN DETERMINING CORROSION RATES

Corrosion rates were calculated from experimentally derived data and presented in terms of a penetration rate (mils per year, MPY) and as a mass loss rate (milligrams per square decimeter per day, MDD).

$$\text{RATE (penetration)} = \frac{AI_{corr}}{zF\rho} \qquad \text{(B-1)}$$

$$\text{RATE (mass loss)} = \frac{AI_{corr}}{zF\rho} \qquad \text{(B-2)}$$

F = Faraday's Constant ($9.64848 \times 10^4$ coulombs/equivalent)

$\rho$ = coating density (grams/$cm^3$)

$I_{corr}$ = current density (amps/$cm^2$)

A = atomic weight (grams/mole)

z = valence (equivalents/mole)

Calculations for PIML Tests

$$\text{RATE (mass loss, MDD)} = \frac{\text{(measured weight loss in mg)}}{\text{(area in } dm^2\text{)(time of test in days)}} \qquad \text{(B-3)}$$

$$\text{RATE (penetration, MPY)} = \frac{R(mdd) \times 1.437}{} = R(mpy) \qquad \text{(B-4)}$$

Calculations for the PDP Test

$I_{corr}$ is extracted from the polarization curves as shown in Figure B.97. This value is converted to current density by dividing it with the exposed surface area of the test coupon, 1 $cm^2$ in this case, and then using equations (B-1) and (B-2) to determine the corrosion rates.

Calculations for the PSP Tests

The area under the current versus time curve produced during the experiment is used to establish the mass loss during the test using Faraday's Law:

$$\text{Mass Loss} = A/zF \int Idt$$

where $Idt$ is the area under the curve. This area was determined by first digitizing the experimentally produced curve, fitting a curve to the digitized points, and then integrating the equation of I(t) thus determined. The calculated mass loss was then converted to a corrosion rate by using equations (B-3) and (B-4).

The following values were used in the calculation of corrosion rates:

| Coating | Atomic Weight (A) | Valence (Z) | Density (@) |
|---|---|---|---|
| Al. | 26.98 | 3 | 2.72 |
| Zn. | 65.37 | 2 | 7.13 |
| Alloy | 27.14 | 3 | 2.80 |

Statistical analysis of the data derived from all test runs and calculated values were conducted utilizing standard techniques, [Ref. 25]. Error bars appear an all graphs, except in the instances that the scale of the graph made them impossible to distinguish.

# APPENDIX B

## TEST DATA

### A. POTENTIODYNAMIC POLARIZATION (PDP) TEST DATA

TABLE II

PDP Test Data

| Coating | I(corr) (uA) | E(corr) (Volts) | Corr. Rate MDD | MPY |
|---|---|---|---|---|
| Al A.S. | 7.88 | -.713 | 9.12 | 3.4 |
| Al A.S. | 10.2 | -.722 | 11.8 | 4.3 |
| Al A.S. | 11.5 | -.725 | 13.3 | 4.9 |
| Al F.S. | 4.6 | -.765 | 5.3 | 2.0 |
| Al F.S. | 5.3 | -.740 | 6.1 | 2.3 |
| Al F.S. | 7.7 | -.721 | 8.9 | 3.3 |
| Zn A.S. | 93.0 | -1.033 | 391 | 55 |
| Zn A.S. | 79.9 | -1.068 | 336 | 47 |
| Zn A.S. | 95.0 | -1.083 | 400 | 56 |
| Zn F.S. | 42.0 | -1.089 | 177 | 25 |
| Zn F.S. | 49.5 | -1.076 | 208 | 29 |
| Zn F.S. | 30.0 | -1.140 | 126 | 18 |
| Alloy A.S. | 20.0 | -.751 | 23.3 | 8.3 |
| Alloy A.S. | 20.5 | -.760 | 23.9 | 8.5 |
| Alloy A.S. | 27.2 | -.754 | 31.7 | 11.3 |
| Alloy F.S. | 26.5 | -.869 | 30.8 | 11.0 |
| Alloy F.S. | 30.0 | -.832 | 34.9 | 12.5 |
| Alloy F.S. | 17.0 | -.838 | 19.8 | 7.1 |

B. PLANNED INTERVAL IMMERSION MASS LOSS (PIML) TEST DATA

TABLE III

PIML Test Data, Weight Gain

| Composition | Length of Test (da) | *Wt. (mg/dm2) | Avg. *Wt. (mg/dm2-da) |
|---|---|---|---|
| Al A.S. | 14 | 169.3 | 12.10± .30 |
| Al A.S. | 28 | 138.3 | 4.90± .13 |
| Al A.S. | 42 | 73.7 | 1.75± .04 |
| Al A.S. | 56 | 126.6 | 2.26± .04 |
| Al A.S. | 70 | 225.1 | 3.22± .08 |
| Al F.S. | 14 | 101.4 | 7.24± .19 |
| Al F.S. | 28 | 1.201 | 4.20± .11 |
| Al F.S. | 42 | 1.113 | 2.70± .07 |
| Al F.S. | 56 | 1.005 | 1.80± .05 |
| Al F.S. | 70 | 1.214 | 1.70± .05 |
| Alloy A.S. | 14 | 89.5 | 6.40± .17 |
| Alloy A.S. | 28 | 227.5 | 8.12± .22 |
| Alloy A.S. | 42 | 258.8 | 6.16± .16 |
| Alloy A.S. | 56 | 247.5 | 4.420±.12 |
| Alloy A.S. | 70 | 62.4 | .89 ± .02 |

TABLE IV

PIML Test Data, Corrosion Rate

| Composition | Length of Test (da) | *Wt. (mg) | Corrosion Rate (MDD) | (MPY) |
|---|---|---|---|---|
| Zn A.S. | 14 | 4929.7 | 312 | 62.9 |
| Zn A.S. | 28 | 10244.0 | 324 | 65.3 |
| Zn A.S. | 42 | 10580.4 | 233 | 45.0 |
| Zn A.S. | 56 | 9617.0 | 152 | 30.7 |
| Zn A.S. | 70 | 12399.8 | 157 | 31.6 |
| | | | | |
| Zn F.S. | 14 | 3641.4 | 230 | 46.4 |
| Zn F.S. | 28 | 9165.9 | 290 | 58.4 |
| Zn F.S. | 42 | 12007.9 | 253 | 51.0 |
| Zn F.S. | 56 | 14133.8 | 224 | 45.1 |
| Zn F.S. | 70 | 11553.0 | 146 | 29.5 |
| | | | | |
| Alloy F.S. | 14 | 430.0 | 27.2 | 14.0 |
| Alloy F.S. | 28 | 241.9 | 7.7 | 3.9 |
| Alloy F.S. | 42 | 199.4 | 4.2 | 2.2 |
| Alloy F.S. | 56 | 176.8 | 2.8 | 1.4 |
| Alloy F.S. | 70 | 234.0 | 2.9 | 1.5 |

C. CONTINUOUS SPRAY (CSP) TEST DATA

TABLE V

CSP Test Data

| Composition | Length of Test (da) | *Wt. (mg/dm2) | Avg. *Wt. (mg/dm2-da) |
|---|---|---|---|
| Al A.S. | 21 | 250.3 | 11.8 ± .6 |
| Al A.S. | 42 | 357.5 | 8.5 ± .4 |
| Al F.S. | 21 | 183.9 | 8.8 ± .4 |
| Al F.S. | 42 | 179.2 | 4.3 ± .2 |
| Zn A.S. | 21 | 927.1 | 44.2 ± 2.2 |
| Zn A.S. | 42 | 1169.2 | 27.8 ± 1.4 |
| Zn F.S. | 21 | 554.1 | 26.4 ± 1.3 |
| Zn F.S. | 42 | 676.9 | 16.1 ± .8 |
| Alloy A.S. | 21 | 257.1 | 12.2 ± .6 |
| Alloy A.S. | 42 | 252.6 | 6.0 ± .3 |
| Alloy F.S. | 21 | 108.3 | 5.2 ± .3 |
| Alloy F.S. | 42 | 83.9 | 2.0 ± .1 |

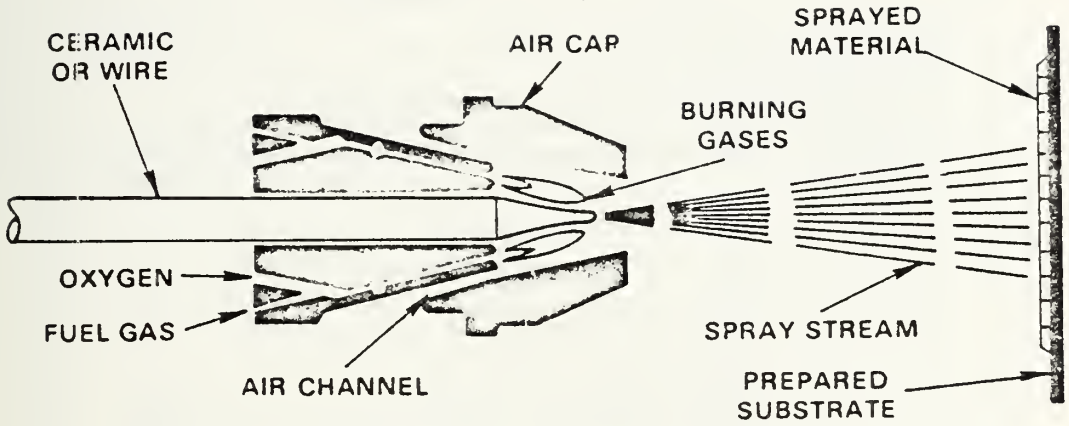


Figure B.1 Schematic of Typical Flame Spray Device

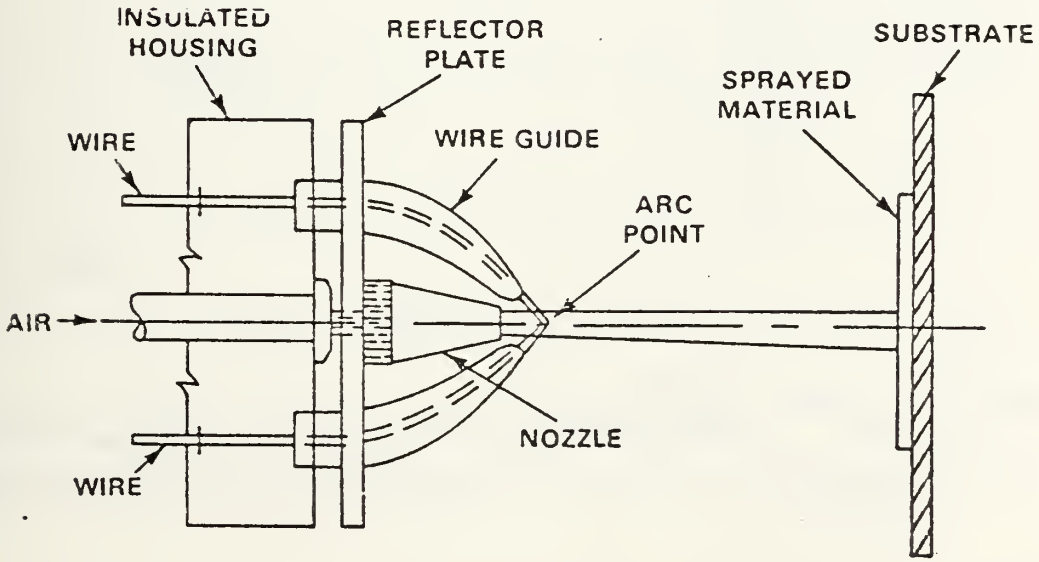


Figure B.2 Schematic of Typical Electric-Arc Spray Device

PUGET SOUND NAVAL SHIPYARD
QUALITY ASSURANCE OFFICE
LABORATORY DIVISION

| FROM | TO | MIC NO. | LABORATORY/HEAT NO. |
|---|---|---|---|
| 1341 | 1346 | | 4148 |

MATERIAL: ALUM.-ZINC WIRE ?

NO. OF SAMPLES AND IDENTIFICATION: 1 CHEM AAD

JOB ORDER: 9138-030330-000

SPECIFICATION:

DATE RECEIVED:

| ELEMENT | NUMBER | | | SPECIFICATION REQUIREMENTS |
|---|---|---|---|---|
| ALUMINUM | REMAINDER | | | |
| CADMIUM | | | | |
| CARBON | | | | |
| CHROMIUM | | | | |
| COBALT | | | | |
| COLUMBIUM | | | | |
| COPPER | .02 | 1A-7072 | | |
| IRON | .16 | | | |
| LEAD | .01 | | | |
| MAGNESIUM | .02 | | | |
| MANGANESE | .004 | | | |
| MOLYBDENUM | | | | |
| NICKEL | | | | |
| PHOSPHOROUS | | | | |
| SILICON | .10 | | | |
| SILVER | | | | |
| SULFUR | | | | |
| TIN | .03 | | | |
| TITANIUM | .005 | | | |
| TUNGSTEN | | | | |
| VANADIUM | | | | |
| ZINC | .15 | | | |

REMARKS: GREG,
THIS IS THE CHEMICAL BREAKDOWN OF THE WIRE WE USED TO SPRAY THE ALUM.-ZINC TEST PLATES.

Jim Boyd C/139

| DATA BOOK PAGE NO. | SPECTRO | X-RAY | WET | CHEMIST (SIGNATURE) | CODE |
|---|---|---|---|---|---|
| | X | | | | |

LABORATORY DIVISION RECORD 13ND PSNS 10300/3 (REV. 4-73)

DATE REPORTED: 10/25/82

Figure B.3 Spectrographic Analysis Data for Alloy Wire

FLAME SPRAY PARAMETERS

| TEST | CORROSION EVALUATION |
|---|---|
| BASE MATERIAL (TYPE & THICKNESS) | CARBON STEEL 1/8 11 EA |
| PREPARATION METHOD | GRIT BLAST |
| GRIT TYPE AND SIZE | AL OXIDE 24 |
| BLAST NOZZLE TO WORK DISTANCE | 4 TO 6 INCHES |
| BLAST NOZZLE TO WORK ANGLE | 90° |
| GUN TYPE/MODEL | METCO 10E/12E |
| NOZZLE SIZE | 1/8 INCH |
| FUEL GAS | ACETYLENE |
| AIR CAP TYPE | EC |
| FUEL GAS REGULATOR P.S.I. (LIGHTING) | 15 |
| OXYGEN REGULATOR P.S.I. (LIGHTING) | 40 |
| AIR REGULATOR P.S.I. | 100 |
| FUEL GAS FLOWMETER C.F.H. | 40 |
| OXYGEN FLOWMETER C.F.H. | 44 |
| ...R FLOWMETER C.F.H. | 53 |
| WIRE TIP LENGTH-INCHES | 1/2 |
| WIRE TYPE | 1100 ALUMINUM 1/8 |
| GUN TO WORK DISTANCE | 6 TO 8 INCHES |
| GUN ANGLE | 90° |
| PREHEAT TEMPERATURE °F | NO PREHEAT |
| MAX. TEMPERATURE OF PART °F | 400 |
| THICKNESS OF SPRAY COAT | 0.007 TO 0.010 |
| DATE SPRAYED | 11-9-82 |

SEALING AND PAINTING DATA

| | TYPE | THICKNESS |
|---|---|---|
| AL COAT | NA | NA |
| PRIMER COAT | NA | NA |

Figure B.4 1100 Al F.S. Application Parameters

THERMAL SPRAY DATA

| | |
|---|---|
| TEST | RESISTENCE TO CORROSION |
| NUMBER OF SPECIMENS | 11 |
| PROCESS | ARC SPRAY |
| WIRE TYPE | 1100 GRADE ALUMINUM |
| WIRE SIZE | 3/32 |
| GUN TYPE | 30° ANGLE |
| POWER SUPPLY/POLARITY | 600 AMP CONSTANT VOLTAGE |
| ARC CONTROL UNIT | YES |
| VOLTS | 35-37 |
| AMPERAGE | 335-350 |
| ATOMIZING AIR PRESSURE (PSI) | 100 P.S.I. |
| SPRAYING DISTANCE | 6" - 7" |
| CONTACT TIP SIZE | 5/32 |
| AIR NOZZLE TYPE | 5 HOLE |
| AIR NOZZLE SIZE | 7/16 |
| STICK OUT LENGTH | EVEN |
| BASE MATERIAL TYPE | CARBON STEEL |
| BASE MATERIAL THICKNESS | 1/8 |
| TYPE OF PREPARATION | ABRASIVE BLAST #24 ALUM OXIDE |
| THICKNESS OF SPRAY COAT | .008"- .012" |
| DATE SPRAYED | 11-10-82 |

SEALING AND PAINTING DATA

| | TYPE | THICKNESS |
|---|---|---|
| SEAL COAT | NA | NA |
| PRIMER COAT | NA | NA |

Figure B.5 1100 Al A.S. Application Parameters

FLAME SPRAY PARAMETERS

| TEST | CORROSION EVALUATION |
|---|---|
| BASE MATERIAL (TYPE & THICKNESS) | CARBON STEEL 1/8 [illegible] EA |
| PREPARATION METHOD | GRIT BLAST |
| GRIT TYPE AND SIZE | AL OXIDE #4 |
| BLAST NOZZLE TO WORK DISTANCE | 4 TO 6 INCHES |
| BLAST NOZZLE TO WORK ANGLE | 90° |
| GUN TYPE/MODEL | METCO 10E/12E |
| NOZZLE SIZE | 1/8 INCH |
| FUEL GAS | ACETYLENE |
| AIR CAP TYPE | EC |
| FUEL GAS REGULATOR P.S.I. (LIGHTING) | 15 |
| OXYGEN REGULATOR P.S.I. (LIGHTING) | 40 |
| AIR REGULATOR P.S.I. | 100 |
| FUEL GAS FLOWMETER C.F.H. | 42 |
| OXYGEN FLOWMETER C.F.H. | 45 |
| [illegible] FLOWMETER C.F.H. | 53 |
| WIRE TIP LENGTH-INCHES | 1/2 |
| WIRE TYPE | ZINC 1/8 |
| GUN TO WORK DISTANCE | 6 TO 8 INCHES |
| GUN ANGLE | 90° |
| PREHEAT TEMPERATURE °F | NO PREHEAT - |
| MAX. TEMPERATURE OF PART °F | 400 |
| THICKNESS OF SPRAY COAT | 0.007 TO 0.010 |
| DATE SPRAYED | 11-9-82 |

SEALING AND PAINTING DATA

| | TYPE | THICKNESS |
|---|---|---|
| [illegible]L COAT | NA | NA |
| PRIMER COAT | NA | NA |

Figure B.6 Zn F.S. Application Parameters

THERMAL SPRAY DATA

| | |
|---|---|
| TEST | CORROSION |
| NUMBER OF SPECIMENS | 11 |
| PROCESS | ARC SPRAY |
| WIRE TYPE | ZINC |
| WIRE SIZE | 1/8 |
| GUN TYPE | 30° ANGLE |
| POWER SUPPLY/POLARITY | 600 AMP CONSTANT VOLTAGE |
| ARC CONTROL UNIT | YES |
| VOLTS | 28 |
| AMPERAGE | 150 |
| ATOMIZING AIR PRESSURE (PSI) | 100 P.S.I. |
| SPRAYING DISTANCE | 6" - 7" |
| CONTACT TIP SIZE | 5/32" |
| AIR NOZZLE TYPE | 5 HOLE |
| AIR NOZZLE SIZE | 7/16" |
| STICK OUT LENGTH | EVEN |
| BASE MATERIAL TYPE | CARBON STEEL |
| BASE MATERIAL THICKNESS | 1/8" |
| TYPE OF PREPARATION | ABRASIVE BLAST #24 ALUM OXIDE |
| THICKNESS OF SPRAY COAT | .008" - .012" |
| DATE SPRAYED | 11-10-82 |

SEALING AND PAINTING DATA

| | TYPE | THICKNESS |
|---|---|---|
| SEAL COAT | NA | NA |
| PRIMER COAT | NA | NA |

Figure B.7 Zn A.S. Application Parameters

FLAME SPRAY PARAMETERS

| TEST | CORROSION EVALUATION |
|---|---|
| BASE MATERIAL (TYPE & THICKNESS) | CARBON STEEL 1/8 11 EA |
| PREPARATION METHOD | GRIT BLAST |
| GRIT TYPE AND SIZE | AL OXIDE 24 |
| BLAST NOZZLE TO WORK DISTANCE | 4 TO 6 INCHES |
| BLAST NOZZLE TO WORK ANGLE | 90° |
| GUN TYPE/MODEL | METCO 10E/12E |
| NOZZLE SIZE | 3/32 ~~1/8~~ INCH |
| FUEL GAS | ACETYLENE |
| AIR CAP TYPE | EC |
| FUEL GAS REGULATOR P.S.I. (LIGHTING) | 15 |
| OXYGEN REGULATOR P.S.I. (LIGHTING) | 40 |
| AIR REGULATOR P.S.I. | 100 |
| FUEL GAS FLOWMETER C.F.H. | 30 |
| OXYGEN FLOWMETER C.F.H. | 33 |
| AIR FLOWMETER C.F.H. | 48 |
| WIRE TIP LENGTH-INCHES | 1/2 |
| WIRE TYPE | 1% ZINC REMAINDER ALUMINUM 3/32 |
| GUN TO WORK DISTANCE | 6 TO 8 INCHES |
| GUN ANGLE | 90° |
| PREHEAT TEMPERATURE °F | NO PREHEAT - |
| MAX. TEMPERATURE OF PART °F | 400 |
| THICKNESS OF SPRAY COAT | 0.007 TO 0.010 |
| DATE SPRAYED | 11-18--82 |

SEALING AND PAINTING DATA

| | TYPE | THICKNESS |
|---|---|---|
| COAT | NA | NA |
| PRIMER COAT | NA | NA |

Figure B.8 Alloy F.S. Application Parameters

THERMAL SPRAY DATA

| | |
|---|---|
| TEST | CORROSION |
| NUMBER OF SPECIMENS | 13 |
| PROCESS | ARC SPRAY |
| WIRE TYPE | 1% ZINC REMAINDER ALUMINUM |
| WIRE SIZE | ~~1/8~~ 3/32" |
| GUN TYPE | 30° ANGLE |
| POWER SUPPLY/POLARITY | 600 AMP CONSTANT VOLTAGE |
| ARC CONTROL UNIT | YES |
| VOLTS | 28 |
| AMPERAGE | 150 |
| ATOMIZING AIR PRESSURE (PSI) | 100 P.S.I. |
| SPRAYING DISTANCE | 6" - 7" |
| CONTACT TIP SIZE | ~~5/32"~~ 1/8" |
| AIR NOZZLE TYPE | 5 HOLE |
| AIR NOZZLE SIZE | 7/16" |
| STICK OUT LENGTH | EVEN |
| BASE MATERIAL TYPE | CARBON STEEL |
| BASE MATERIAL THICKNESS | 1/8" |
| TYPE OF PREPARATION | ABRASIVE BLAST #24 ALUM OXIDE |
| THICKNESS OF SPRAY COAT | .008" - .012" |
| DATE SPRAYED | 11-18-82 |

SEALING AND PAINTING DATA

| | TYPE | THICKNESS |
|---|---|---|
| SEAL COAT | NA | NA |
| PRIMER COAT | NA | NA |
| | | |

Figure B.9 Alloy A.S. Application Parameters

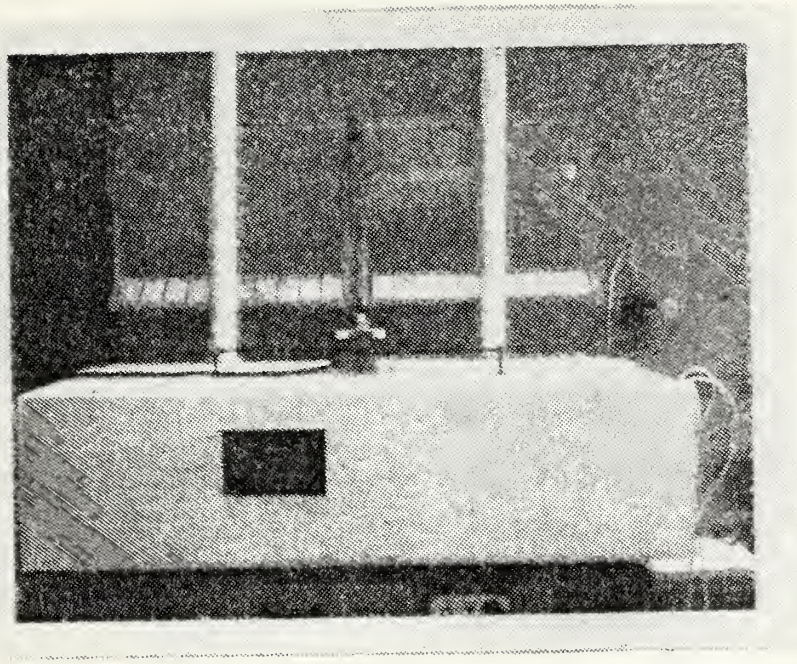

Figure B.10 Spray Chamber

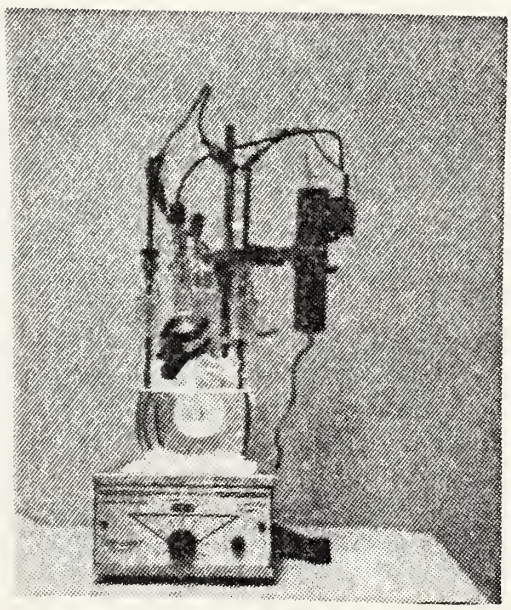

Figure B.11 Corrosion Cell, PARC Model 9700, atop magnetic stirrer

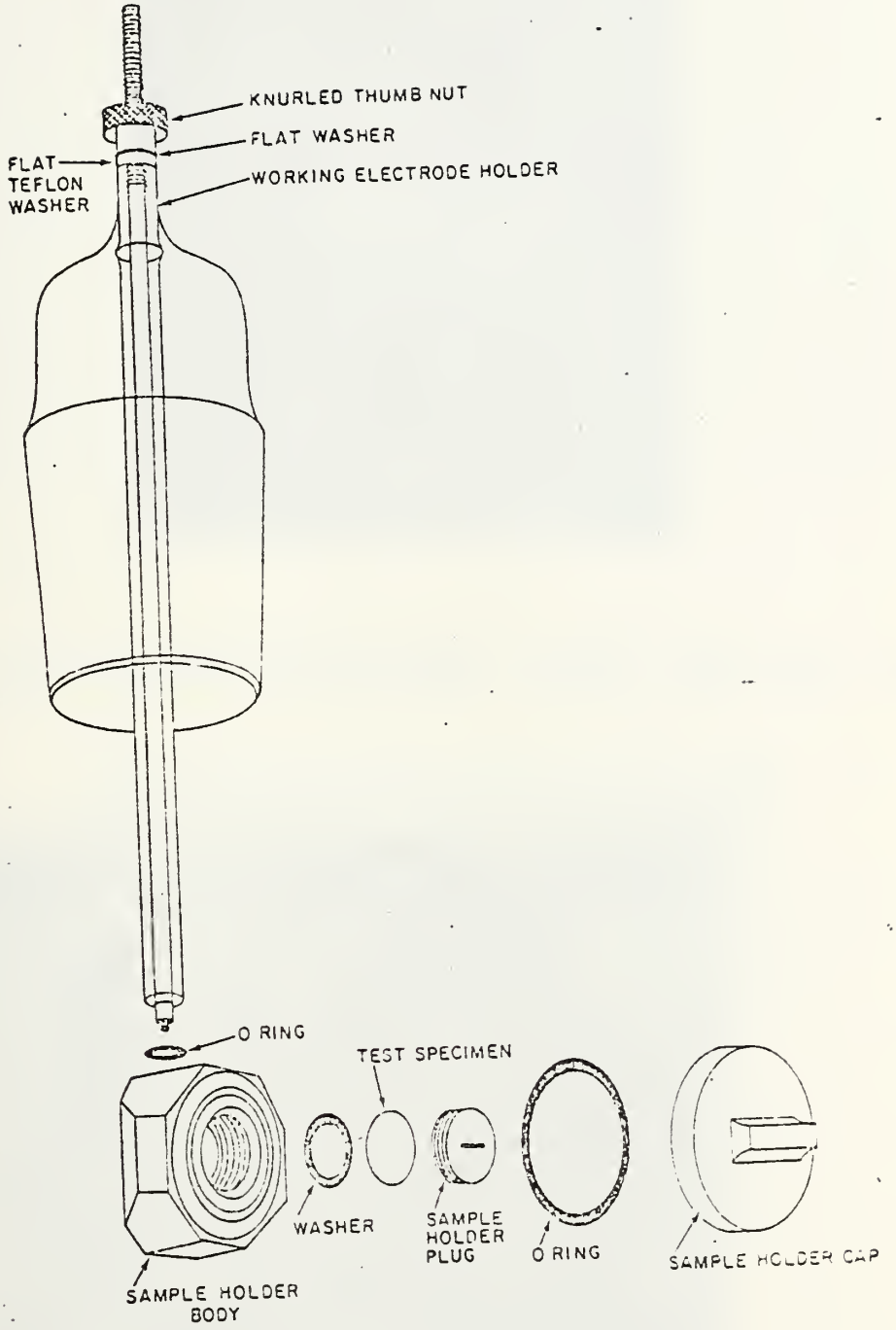


Figure B.12 Schematic of Flat Specimen Holder

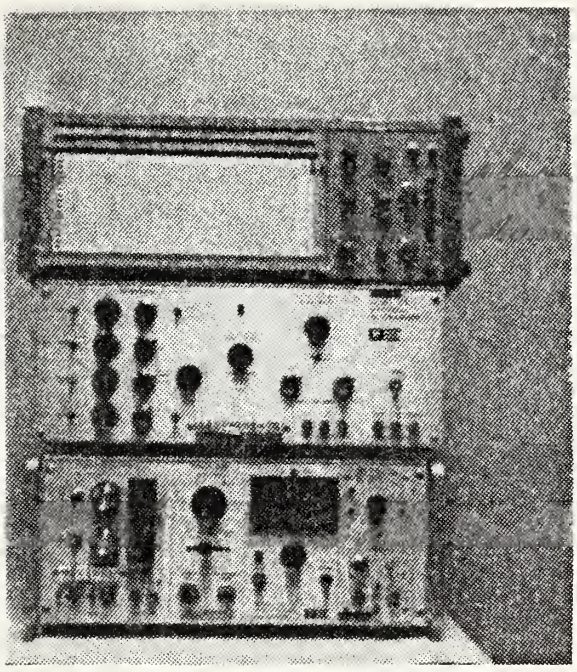

Figure B.13 Corrosion Measurement System, PARC Model 331

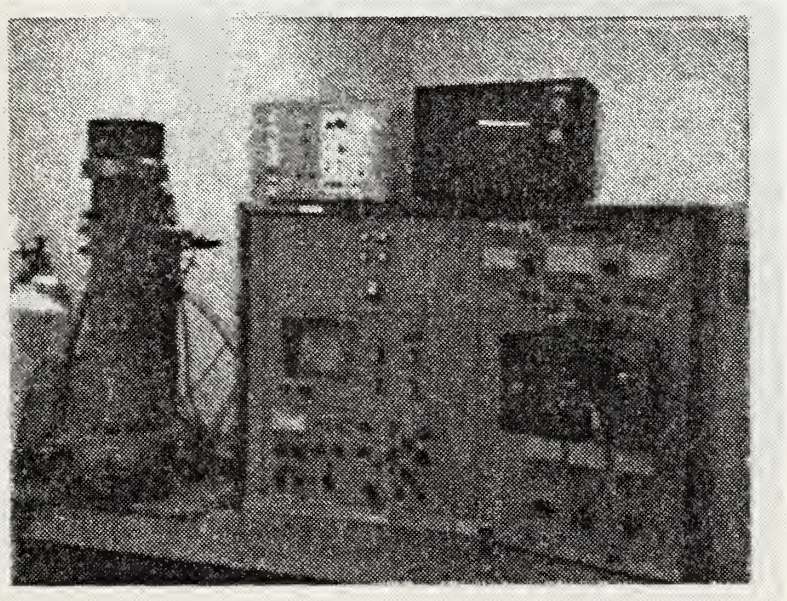

Figure B.14 Scanning Electron Microscope, Cambridge Model S4-10

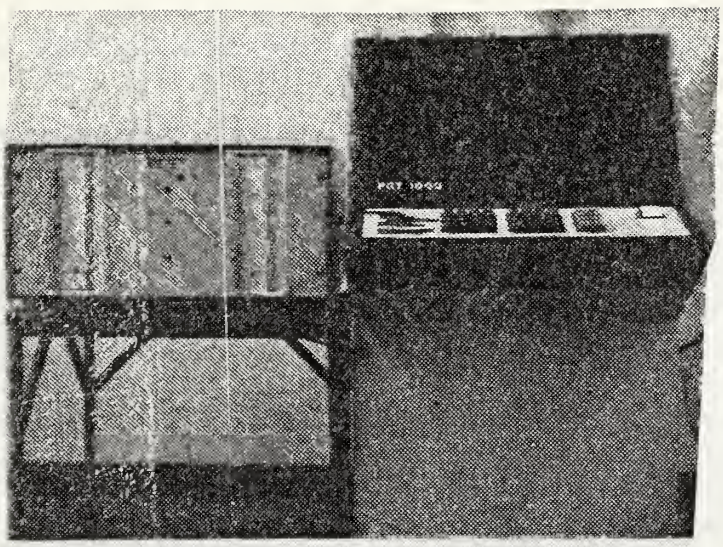

Figure B.15 X-ray Fluorescence Analyzer, PGT Model 1000

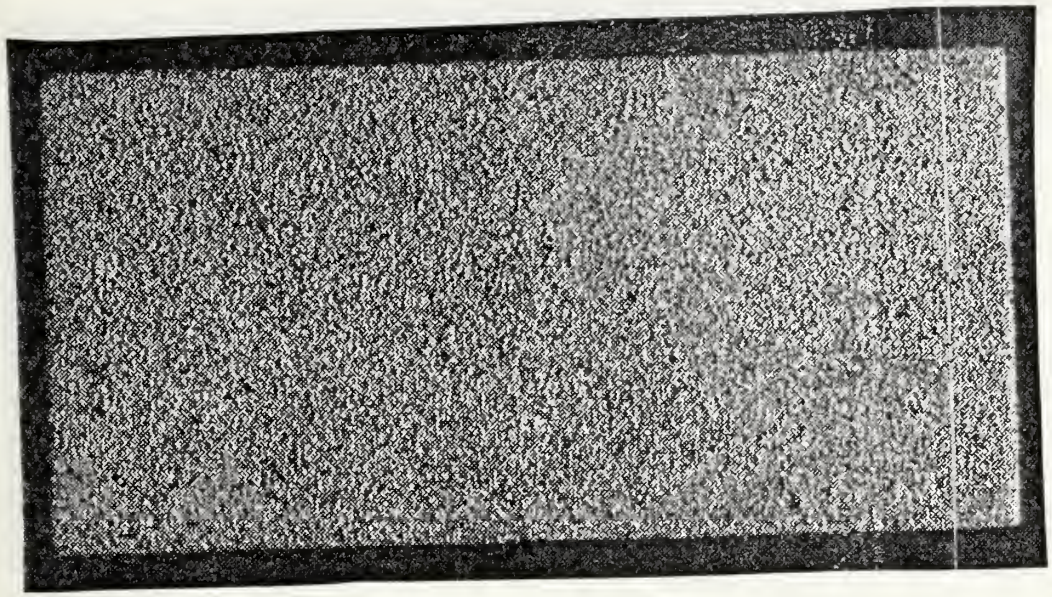

Figure B.16 Al A.S. Coated Coupon, new

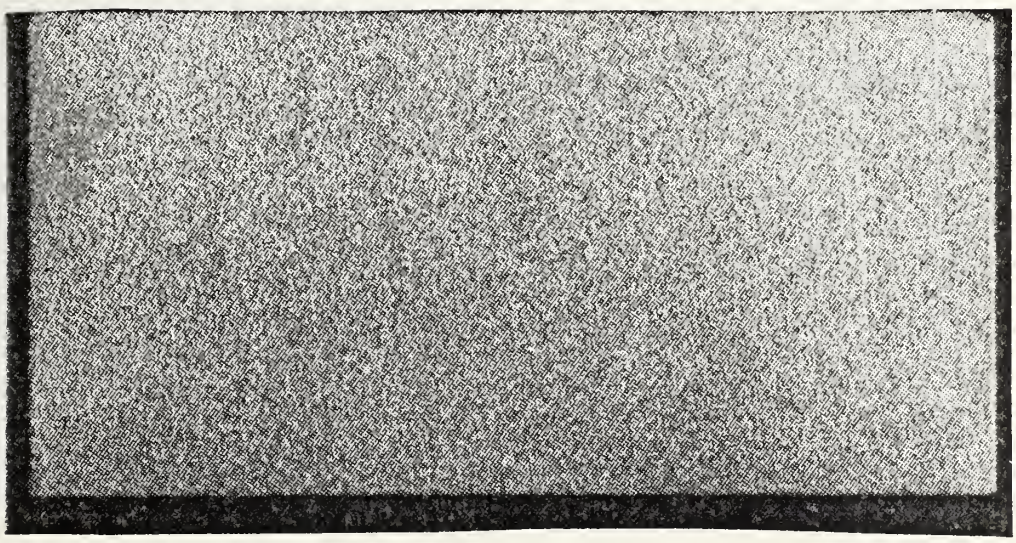

Figure B.17 Al F.S. Coated Coupon, new

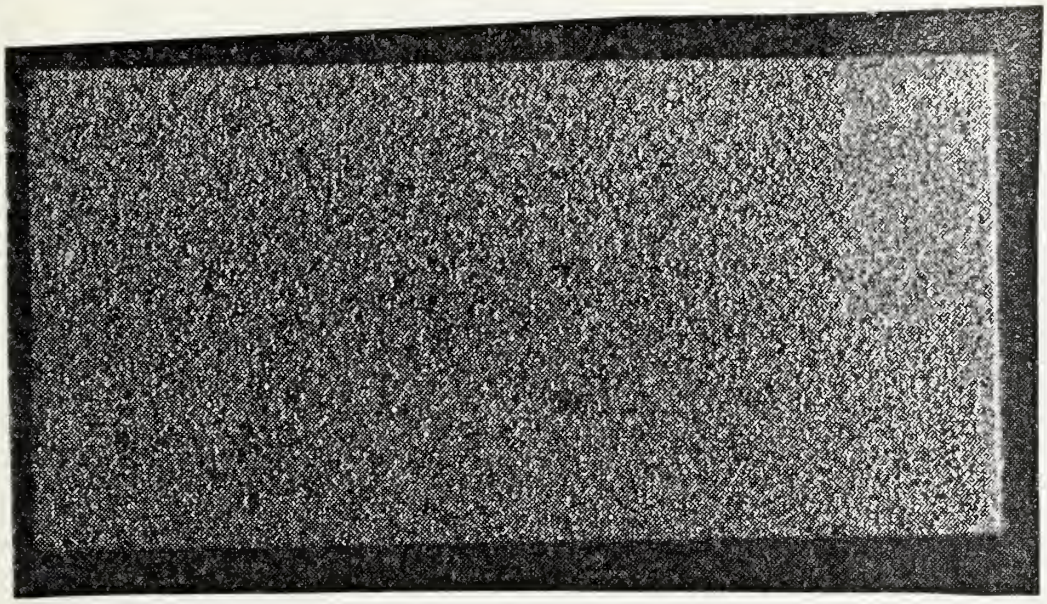

Figure B.18 Zn A.S. Coated Coupon, new

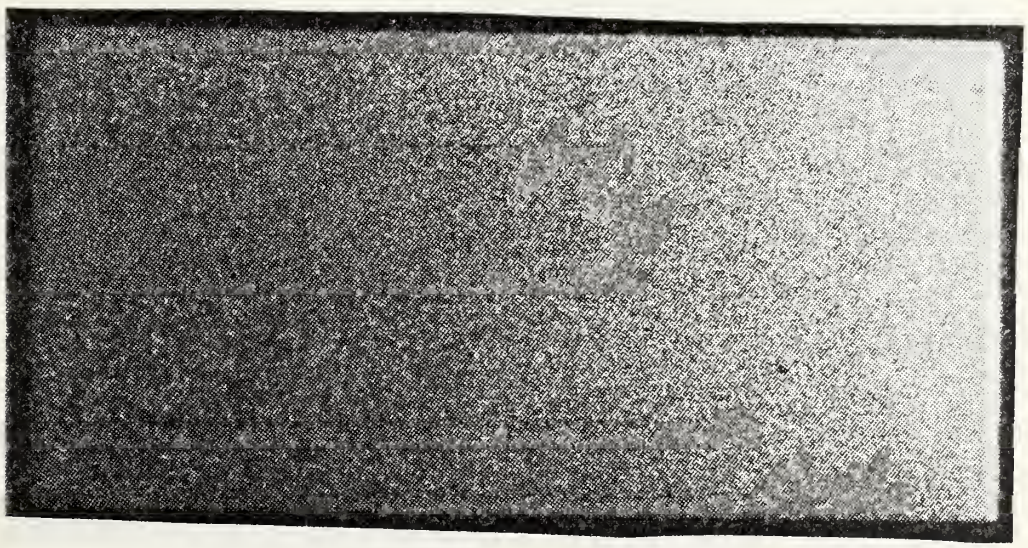

Figure B.19 Zn F.S. Coated Coupon, new

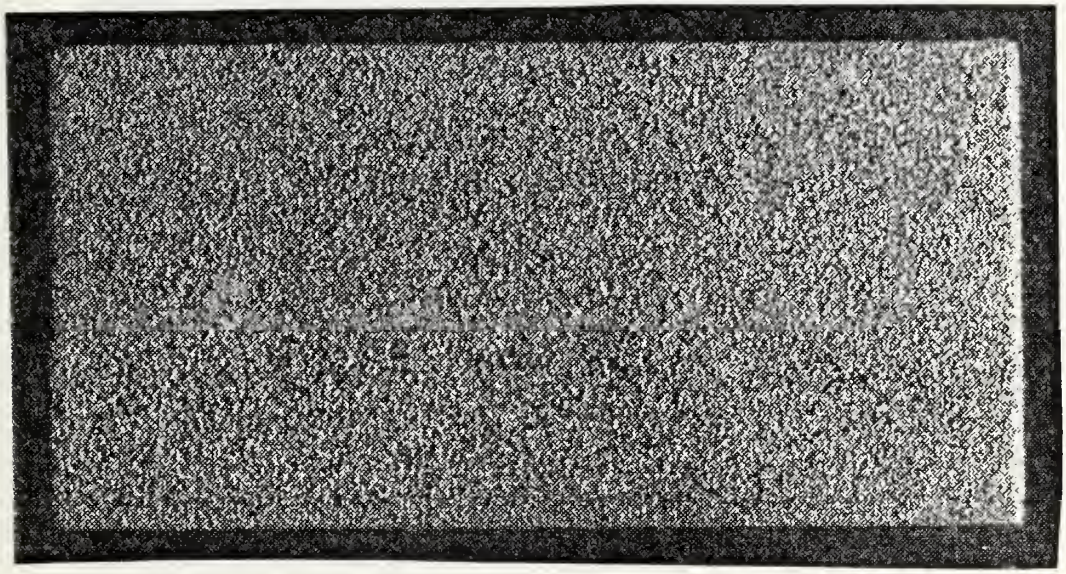

Figure B.20 Alloy A.S. Coated Coupon, new

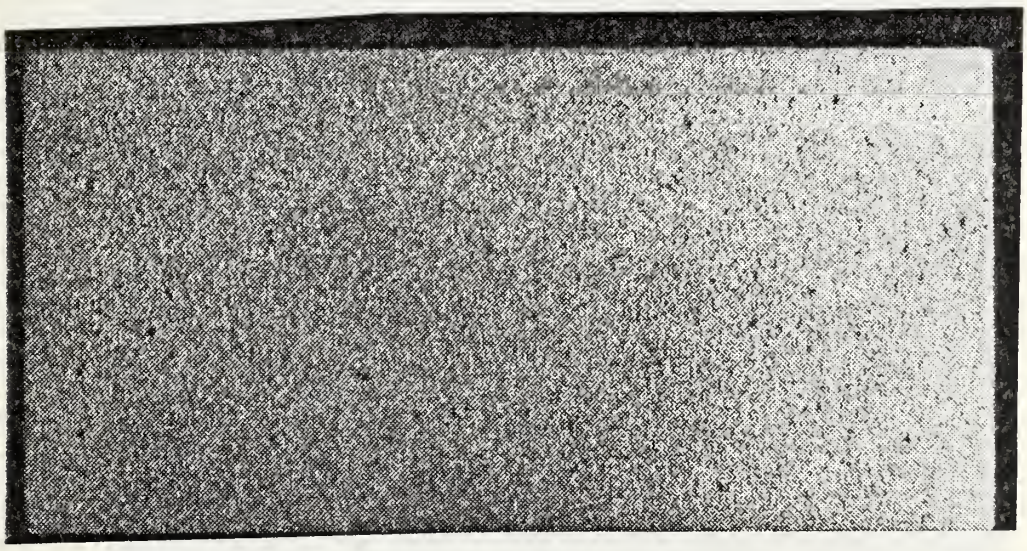

Figure B.21 Alloy F.S. Coated Coupon, new

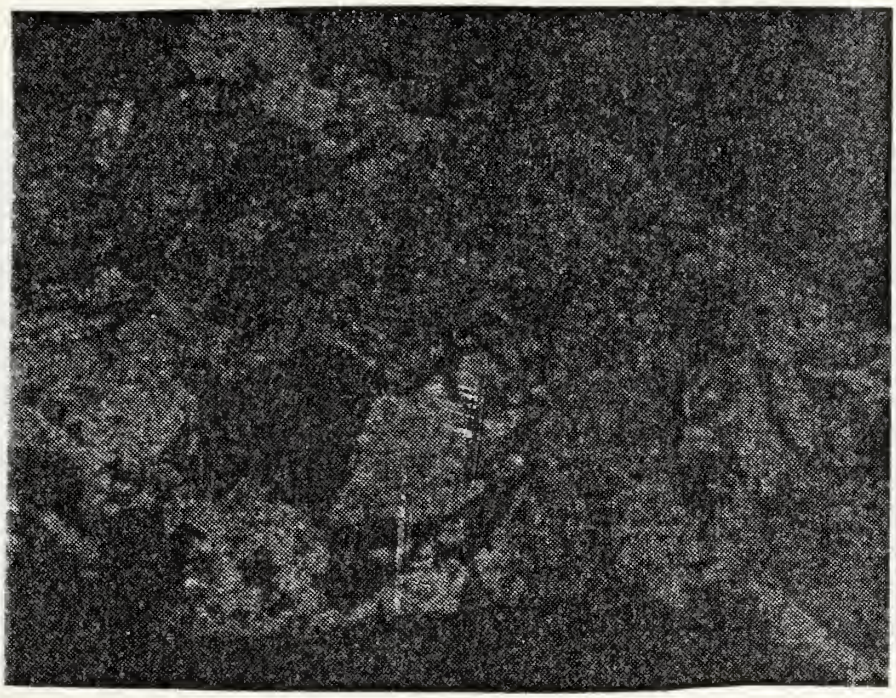

Figure B.22 (X425), Al A.S. coating viewed in cross section LM

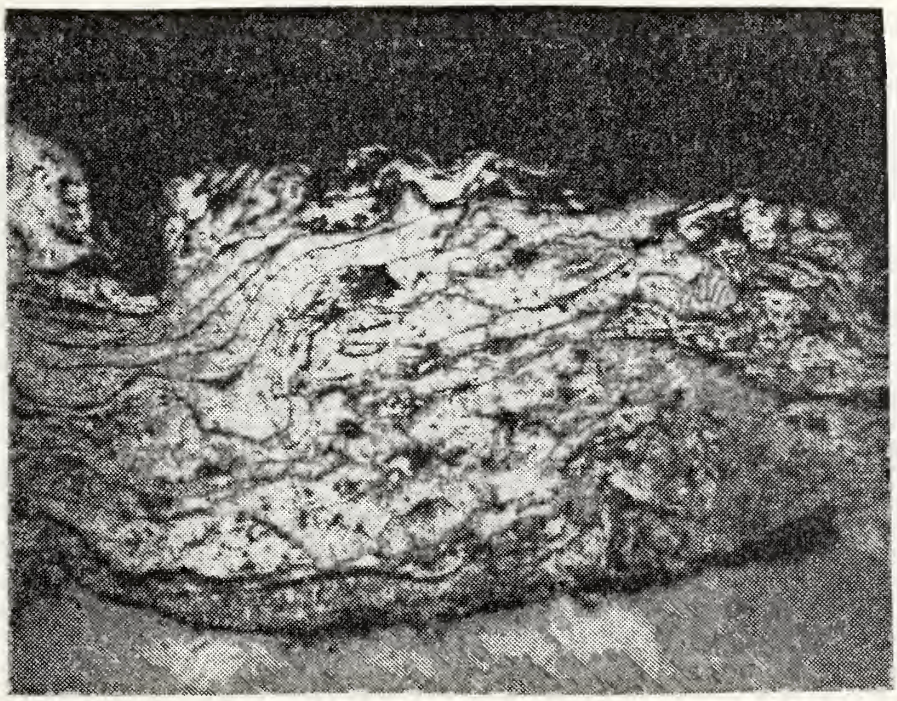

Figure B.23 (X250), Zn A.S. coating viewed in cross section LM

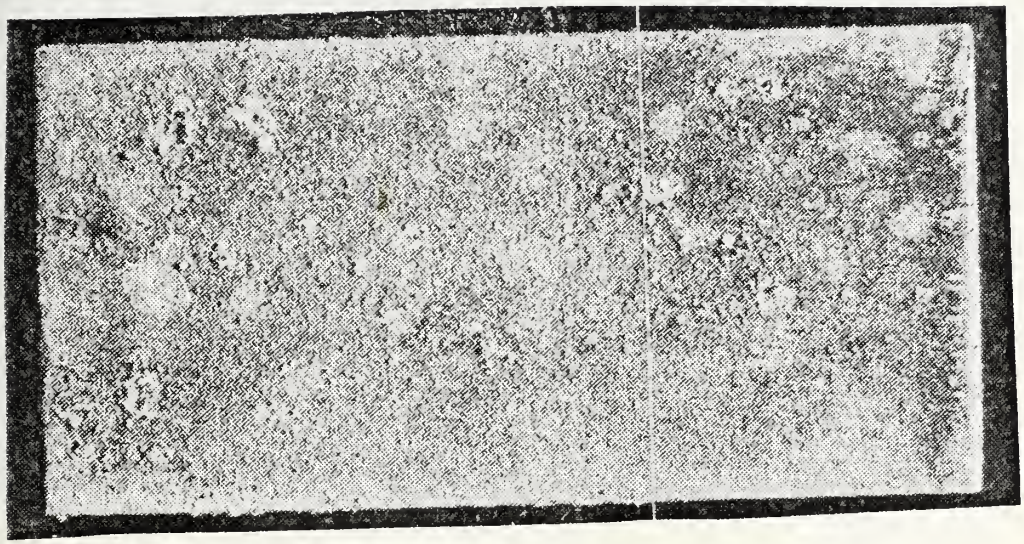

Figure B.24 Al F.S. coating, 14 days PIML

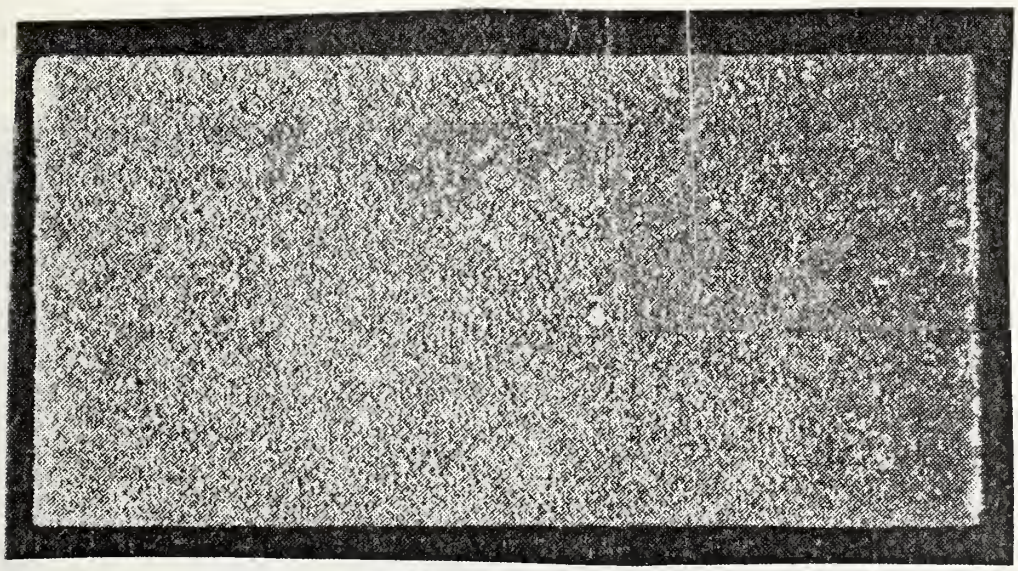

Figure B.25 Al A.S. coating, 14 days PIML

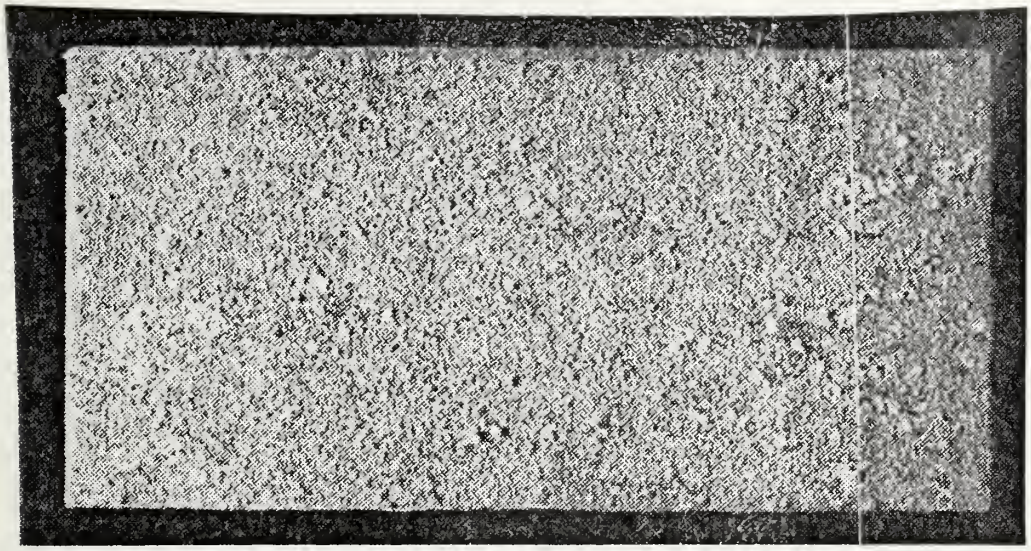

Figure B.26 Al A.S. coating, 28 days PIML

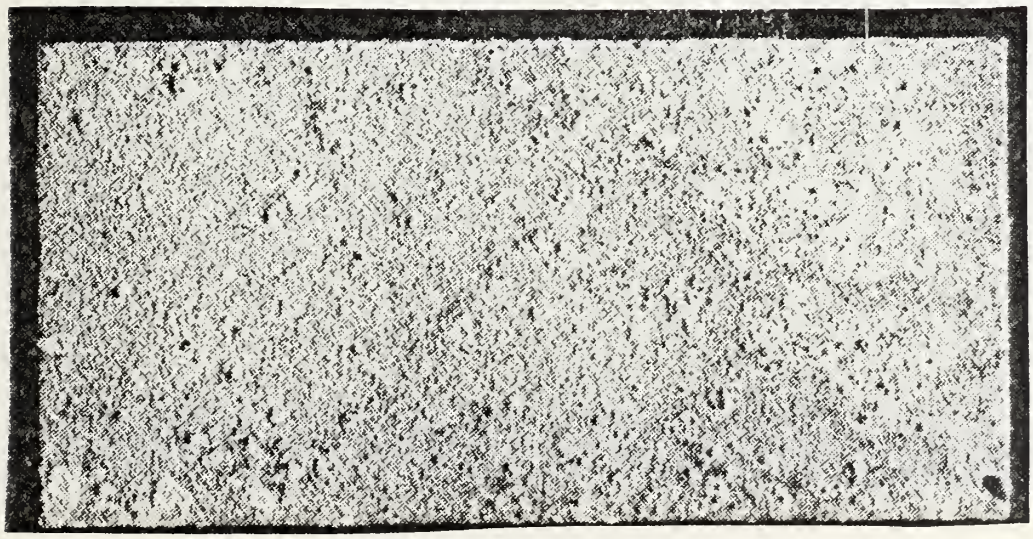

Figure B.27 Al A.S. coating, 42 days PIML

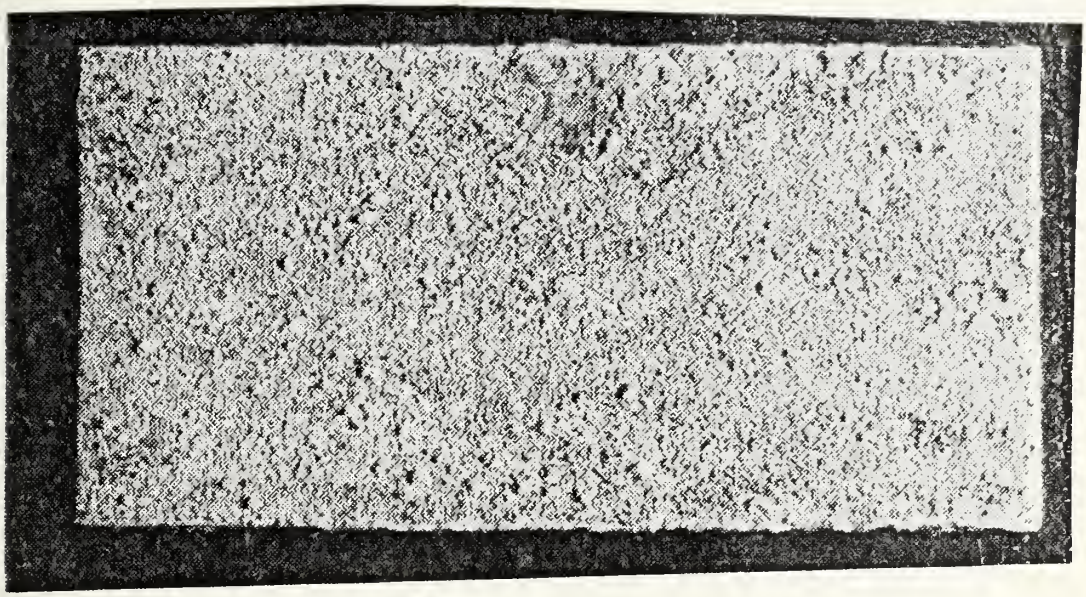

Figure B.28 Al A.S. coating, 56 days PIML

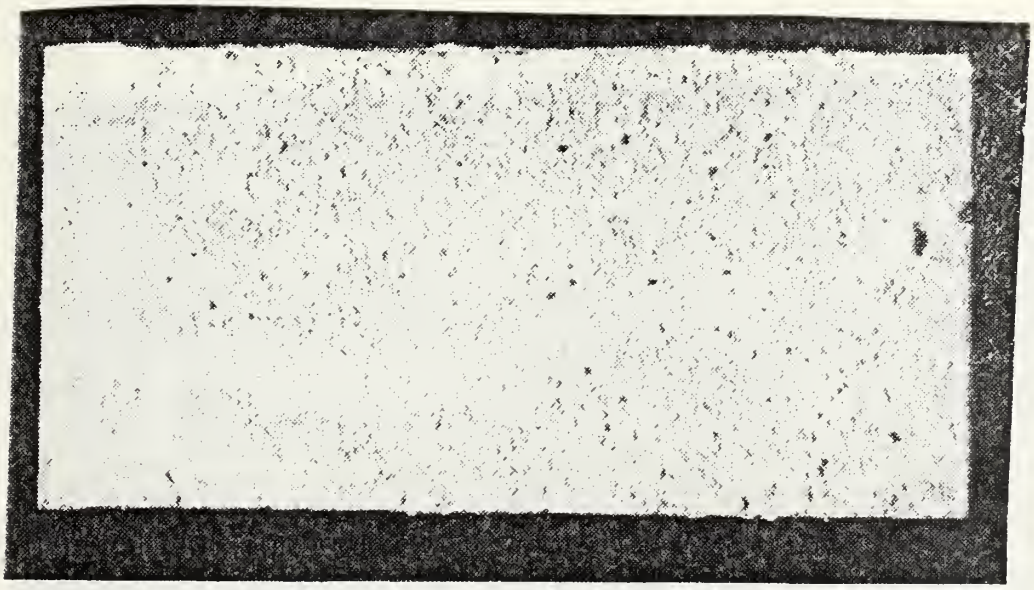

Figure B.29 Al A.S. coating, 70 days PIML

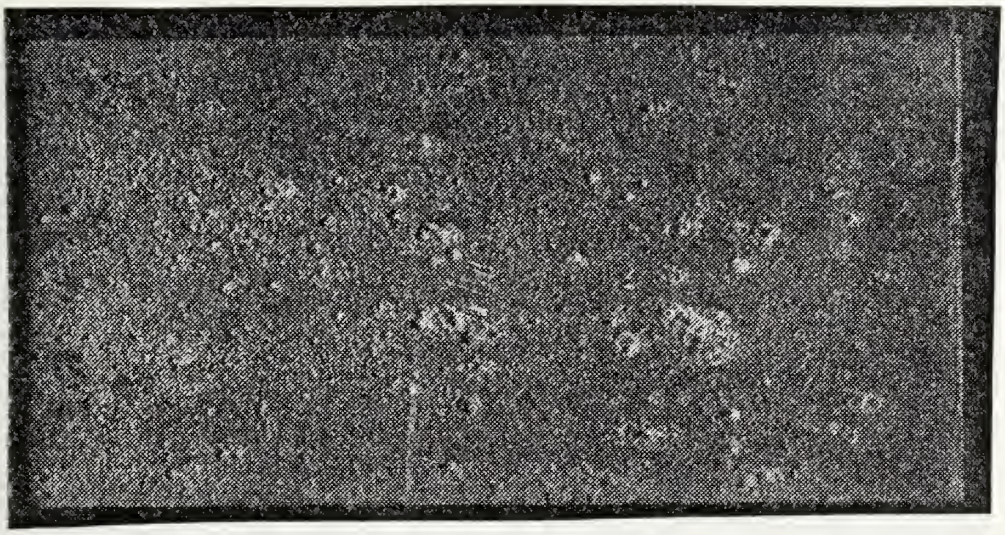

Figure B.30 Al F.S. coating, 28 days PIML

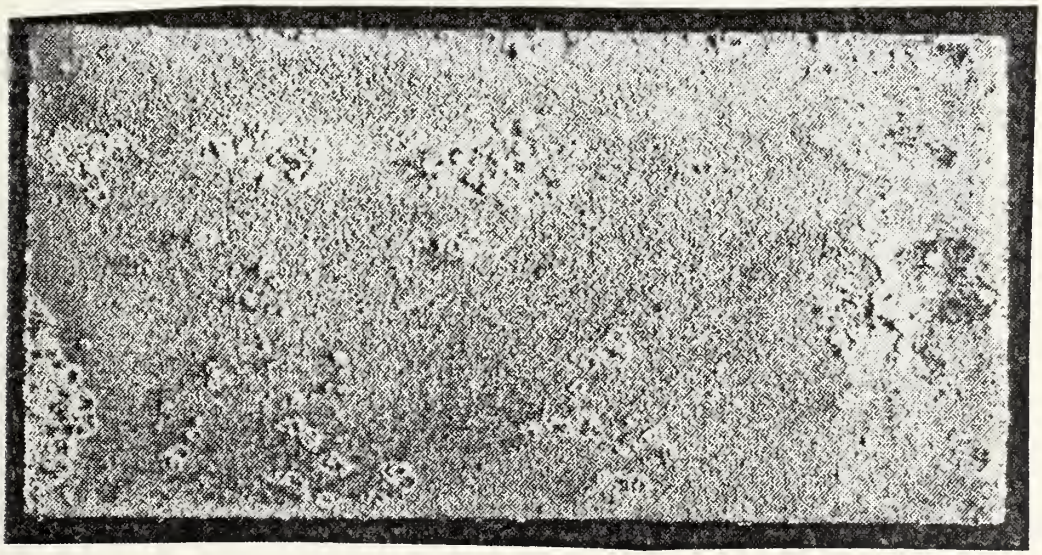

Figure B.31 Al F.S. coating, 42 days PIML

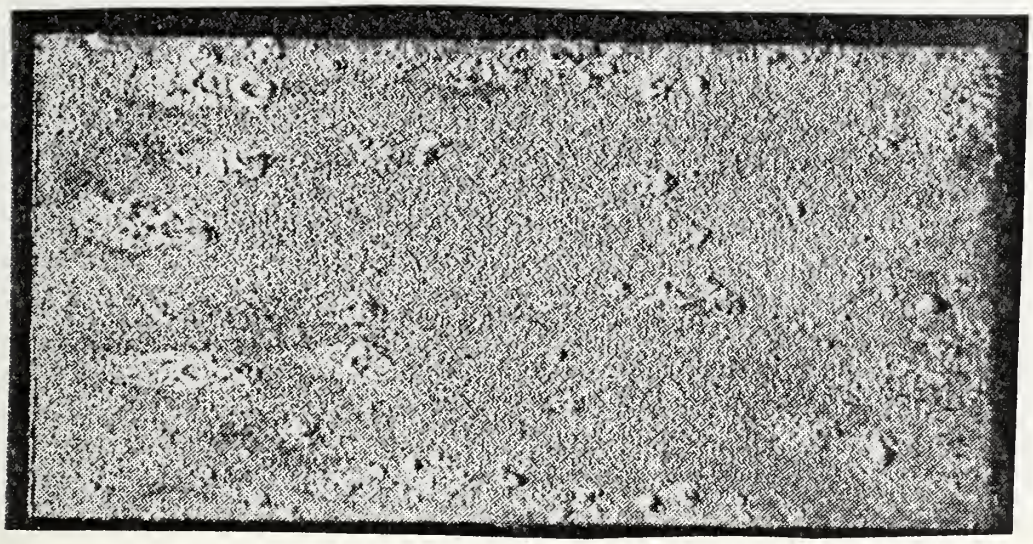

Figure B.32 Al F.S. coating, 56 days PIML

Figure B.33 Al F.S. coating, 70 days PIML

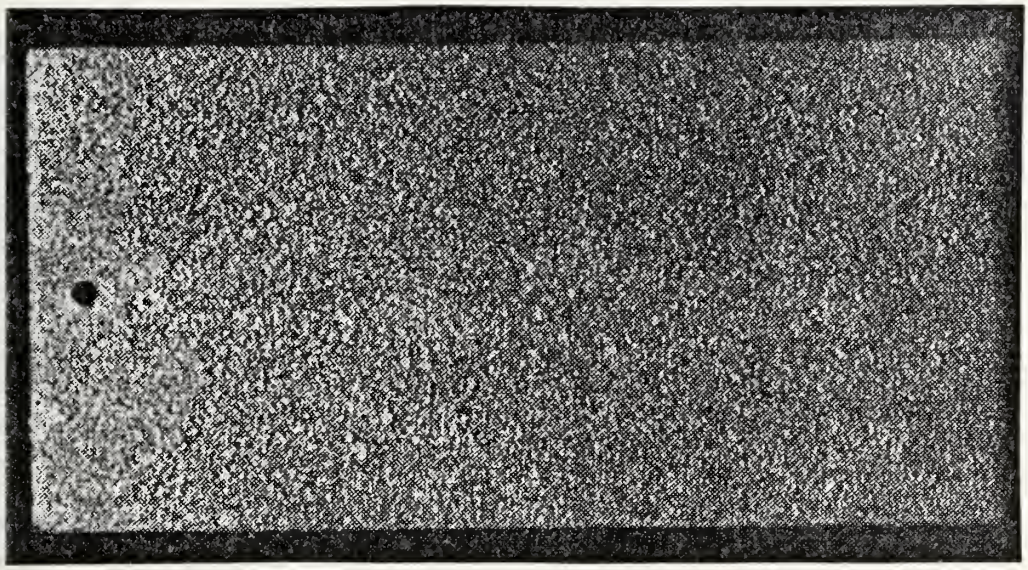

Figure B.34 Al A.S. coating, 21 days CSP

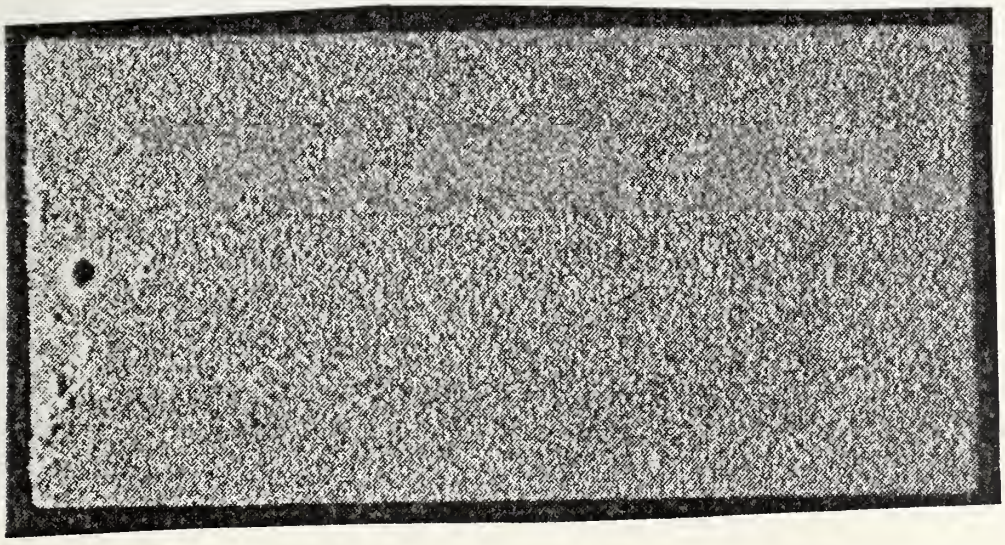

Figure B.35 Al A.S. coating, 42 days CSP

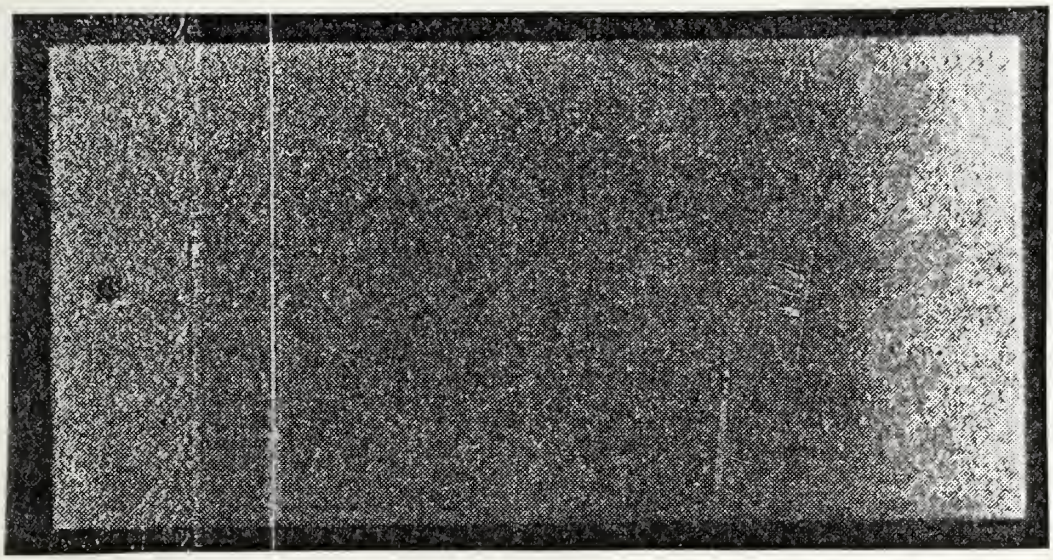

Figure B.36 Al F.S. coating, 21 days CSP

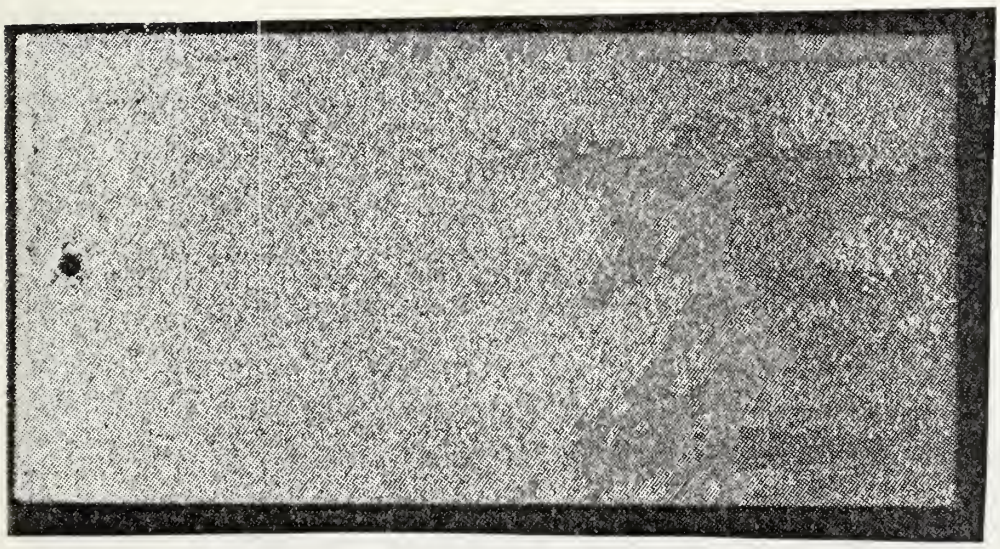

Figure B.37 Al F.S. coating, 42 days CSP

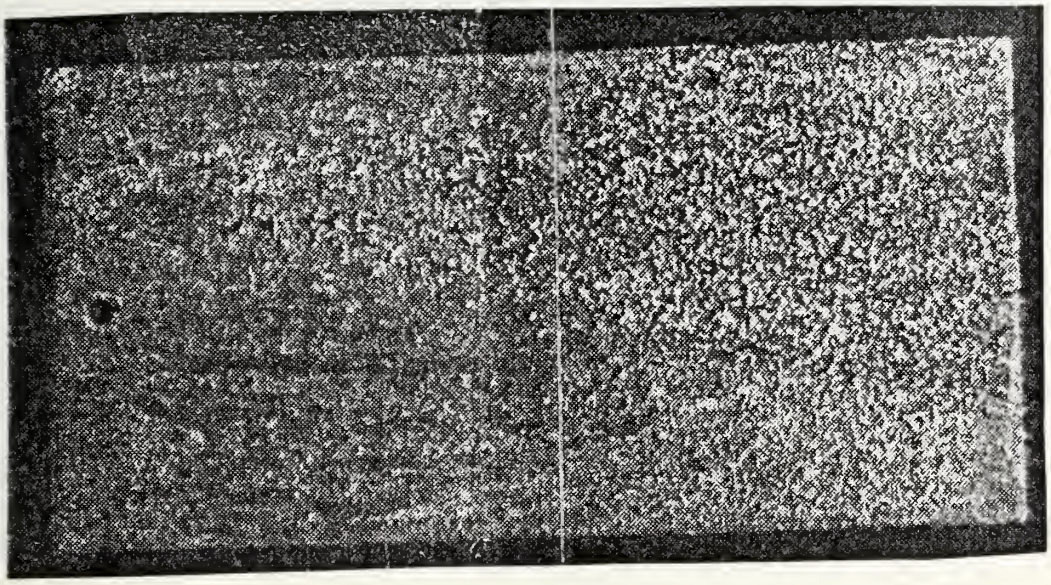

Figure B.38 Zn A.S. coating, 21 days CSP

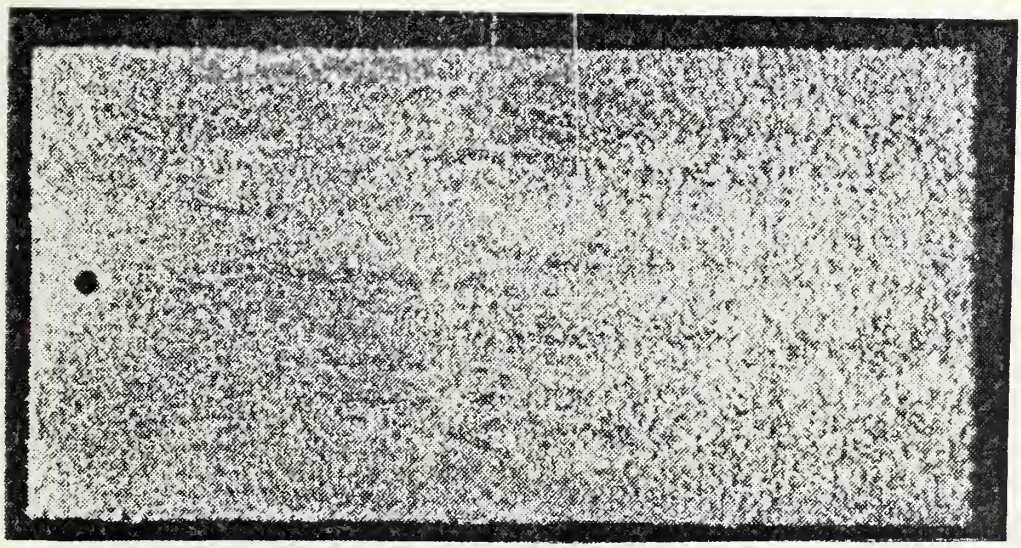

Figure B.39 Zn A.S. coating, 42 days CSP

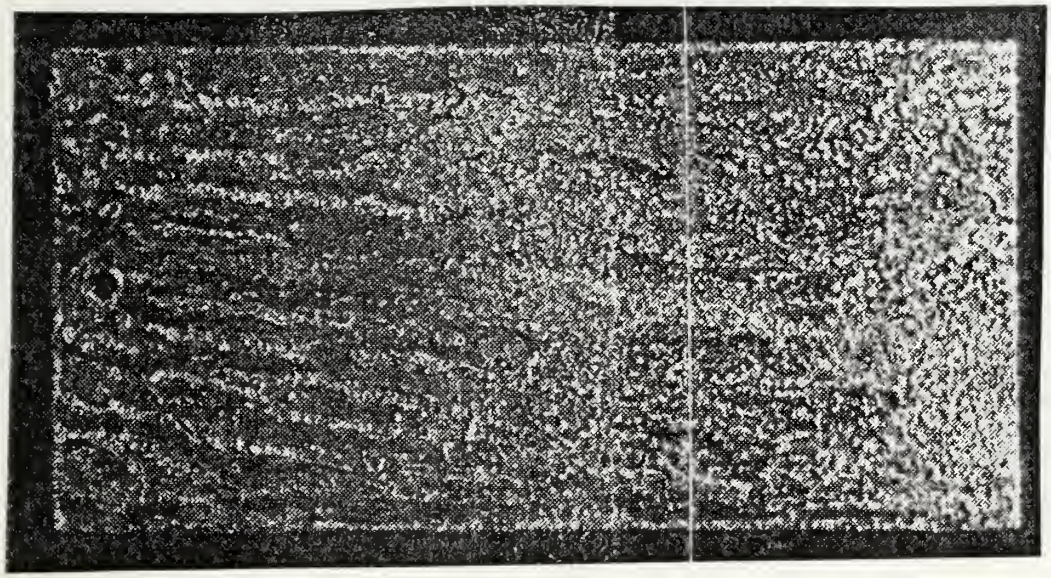

Figure B.40 Zn F.S. coating, 21 days CSP

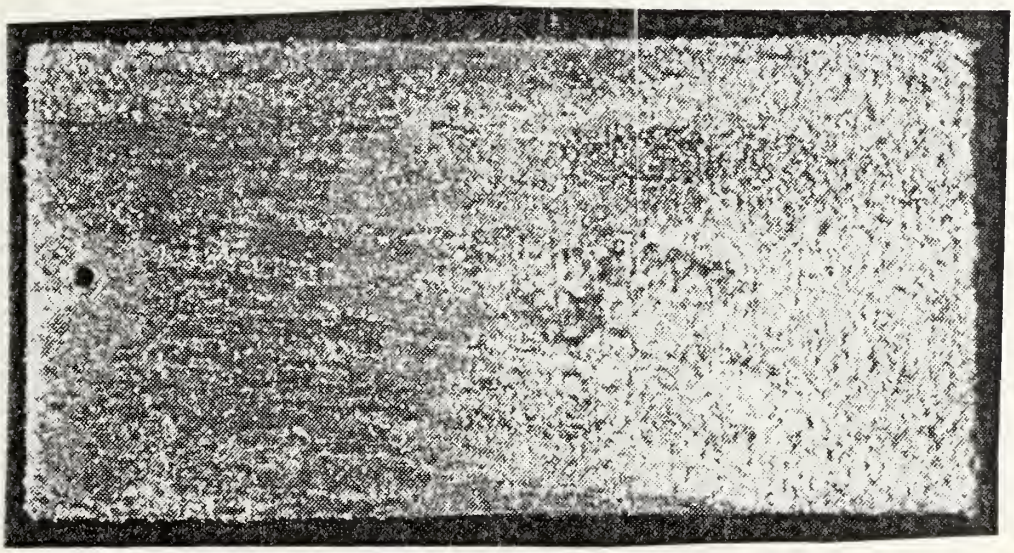

Figure B.41 Zn F.S. coating, 42 days CSP

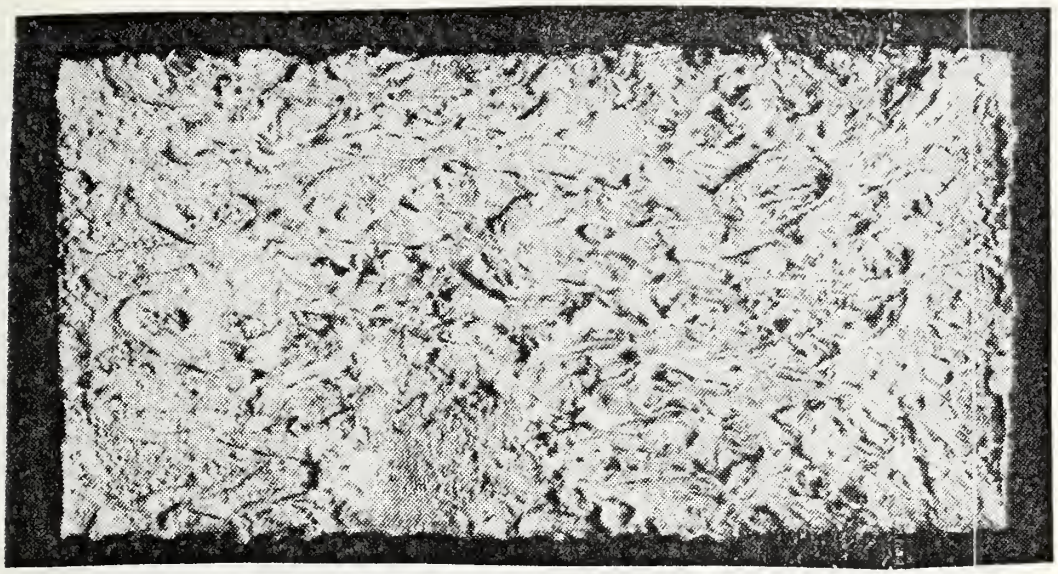

Figure B.42 Zn A.S. coating, 14 days PIML

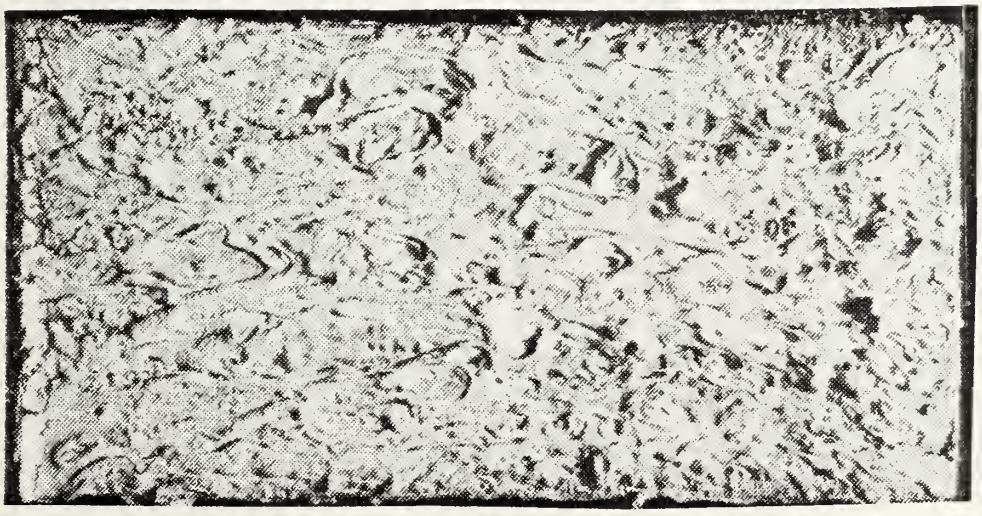

Figure B.43 Zn F.S. coating, 14 days PIML

Figure B.44 Zn A.S. coating, 42 days PIML

Figure B.45 Zn F.S. coating, 56 days PIML

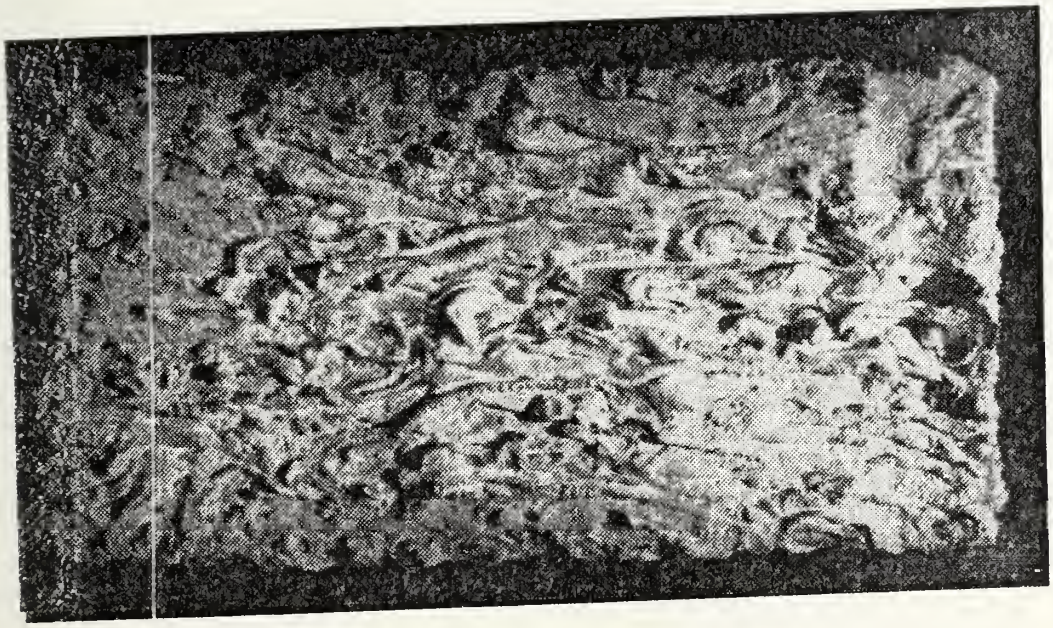

Figure B.46 Zn A.S. coating, 28 days PIML

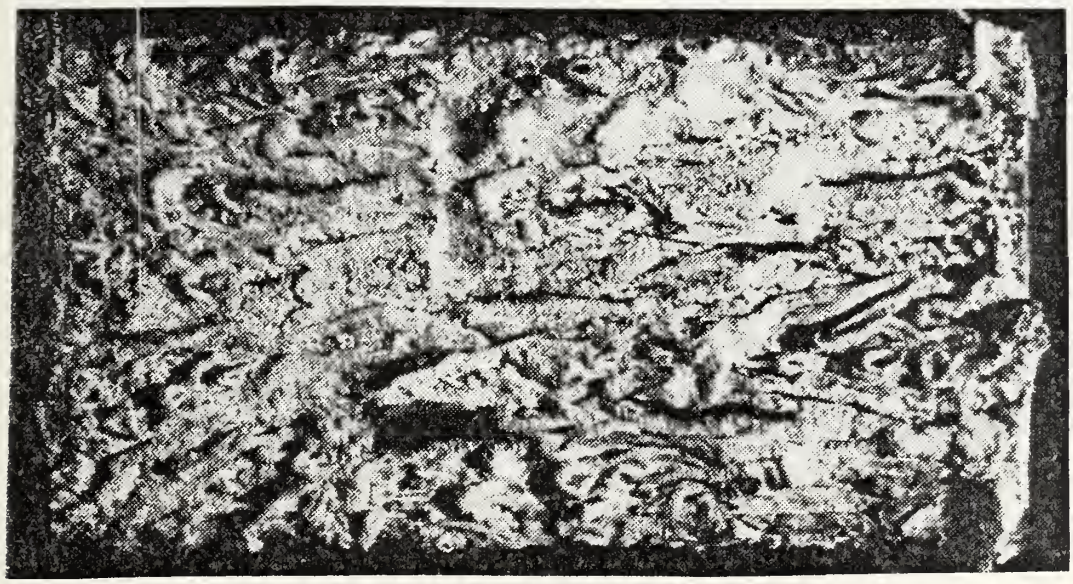

Figure B.47 Zn A.S. coating, 56 days PIML

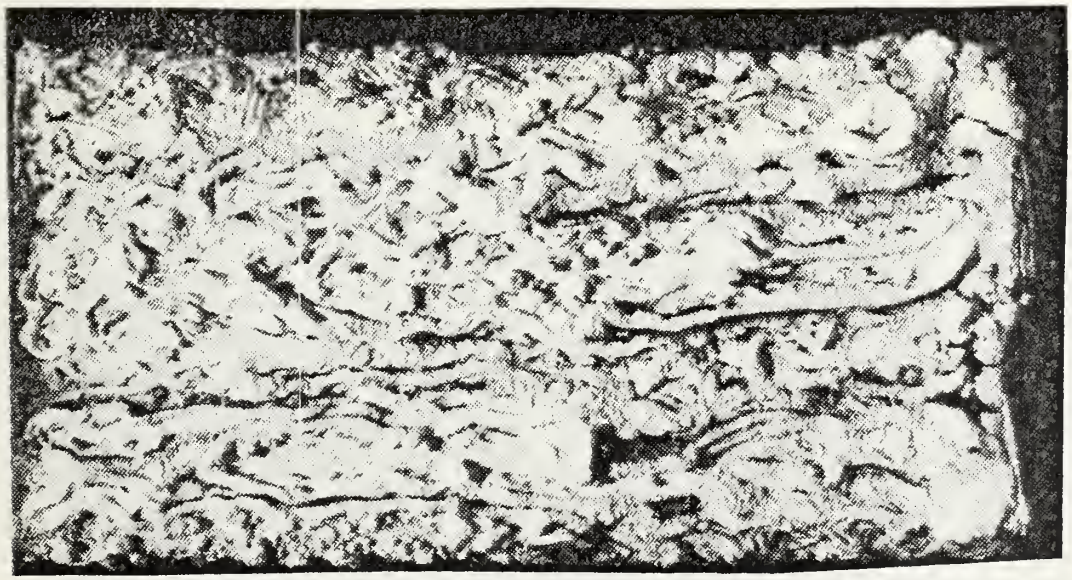

Figure B.48 Zn A.S. coating, 70 days PIML

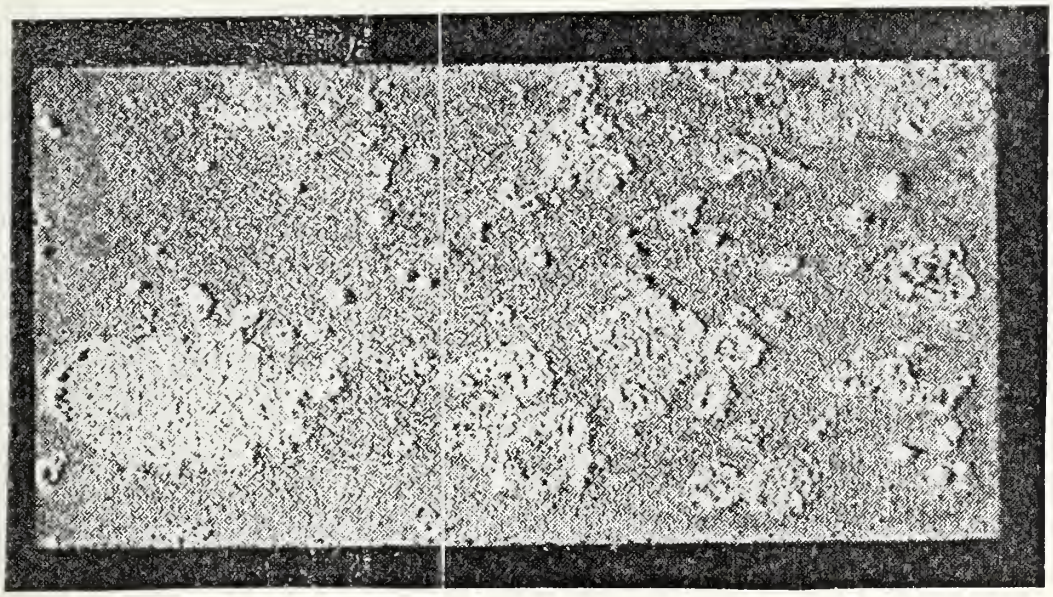

Figure B.49 Alloy F.S. coating, 14 days PIML

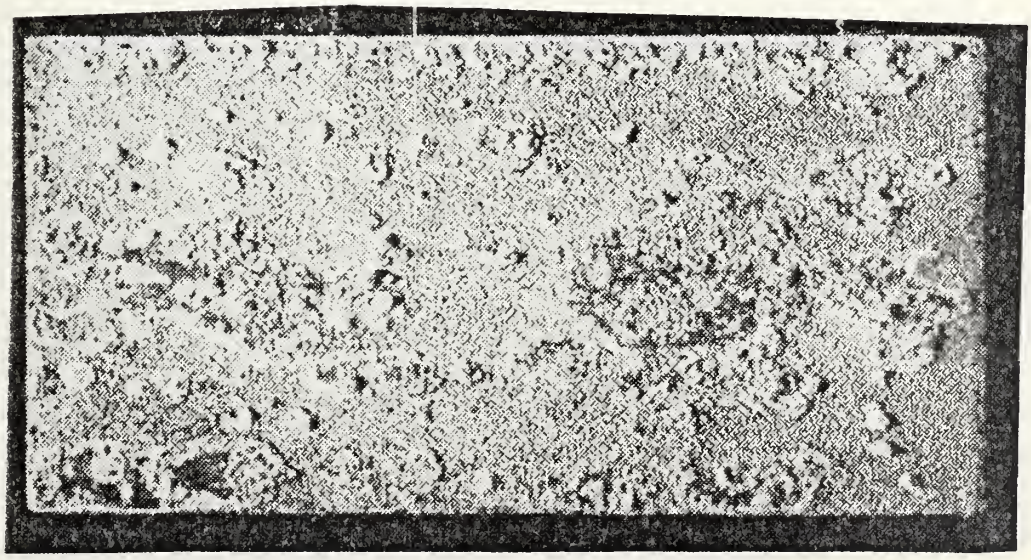

Figure B.50 Alloy F.S. coating, 28 days PIML

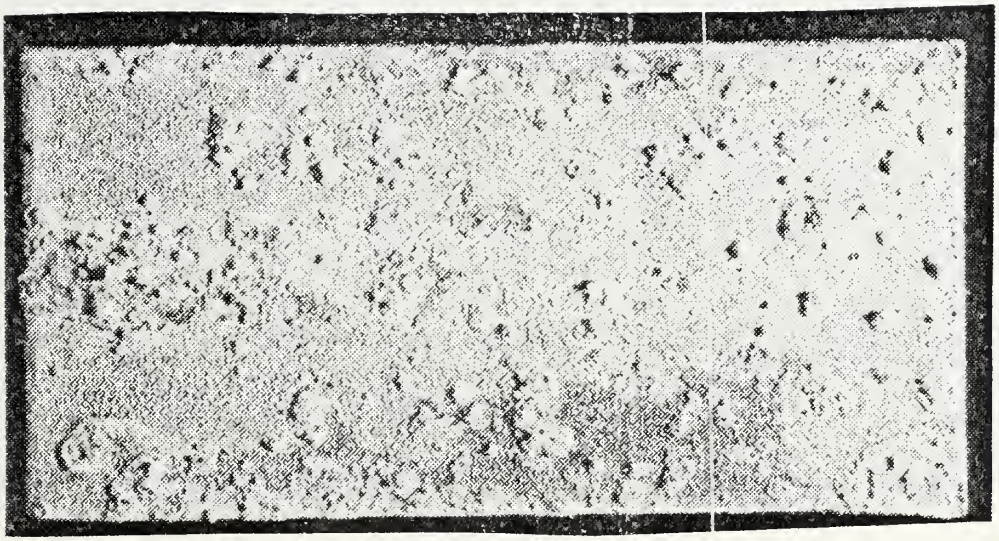

Figure B.51 Alloy F.S. coating, 42 days PIML

Figure B.52 Alloy F.S. coating, 70 days PIML

Figure B.53 Alloy A.S. coating, 14 days PIML

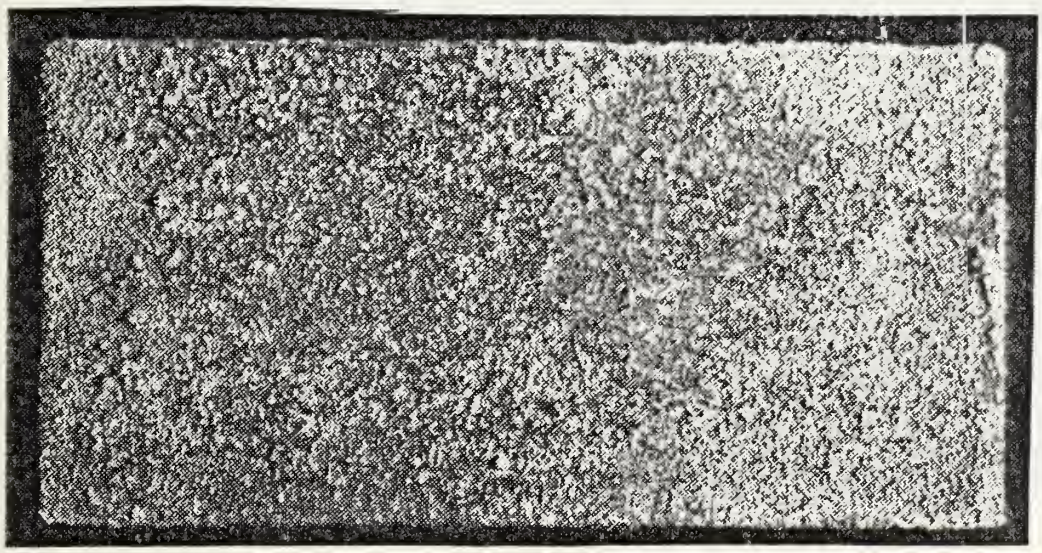

Figure B.54 Alloy A.S. coating, 28 days PIML

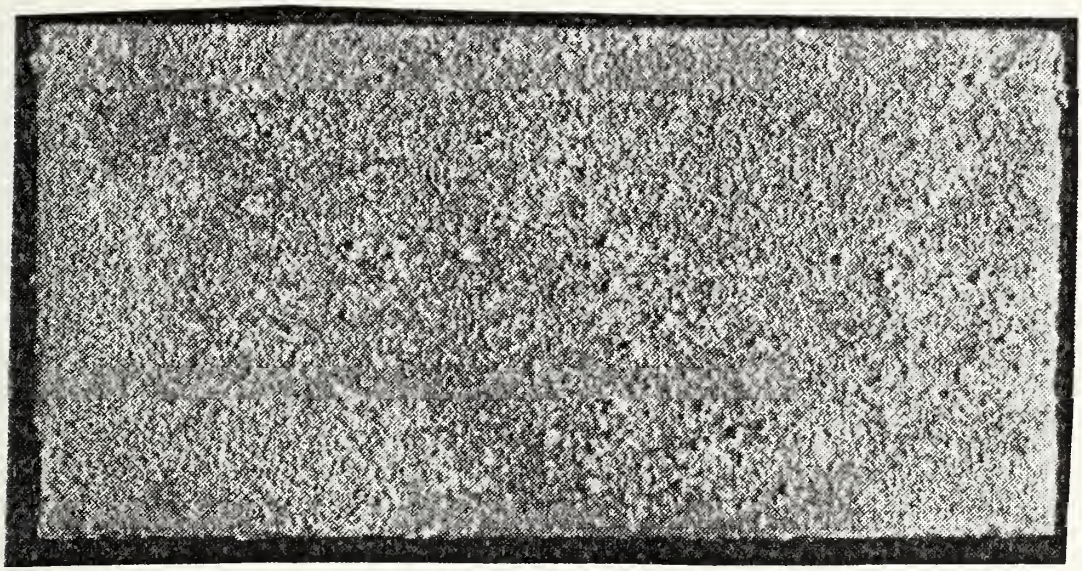

Figure B.55 Alloy A.S. coating, 42 days PIML

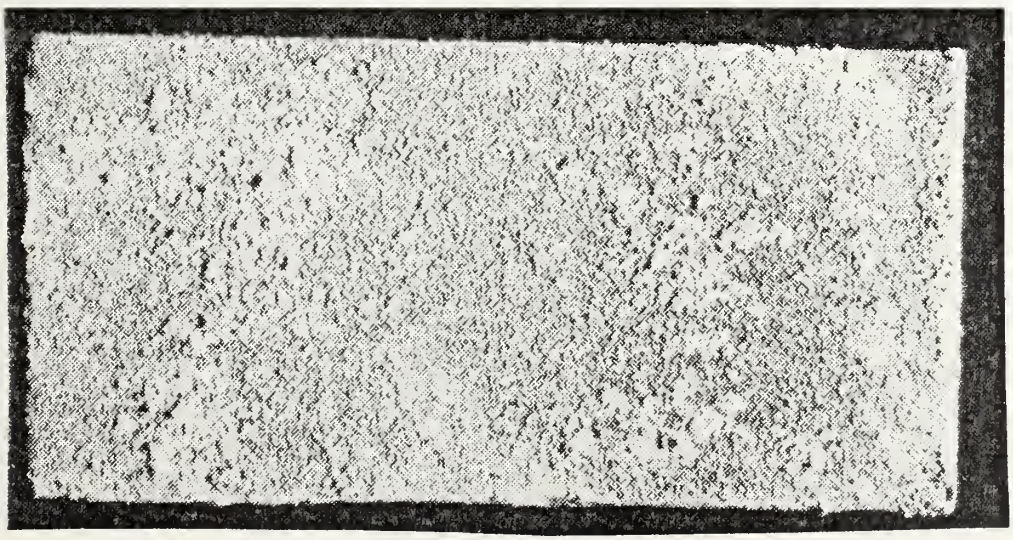

Figure B.56 Alloy A.S. coating, 56 days PIML

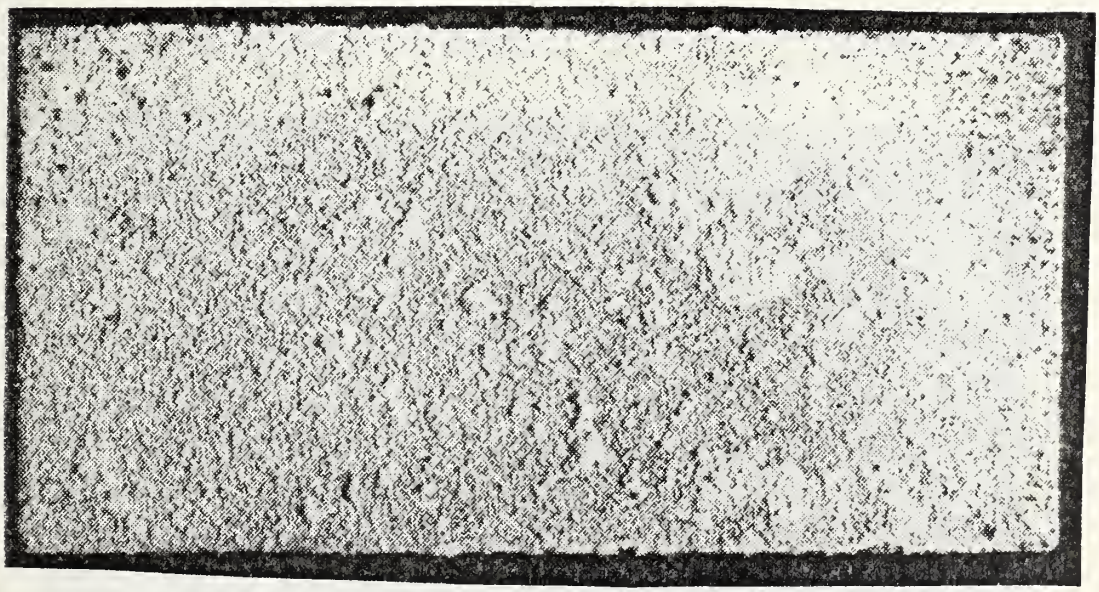

Figure B.57 Alloy A.S. coating, 70 days PIML

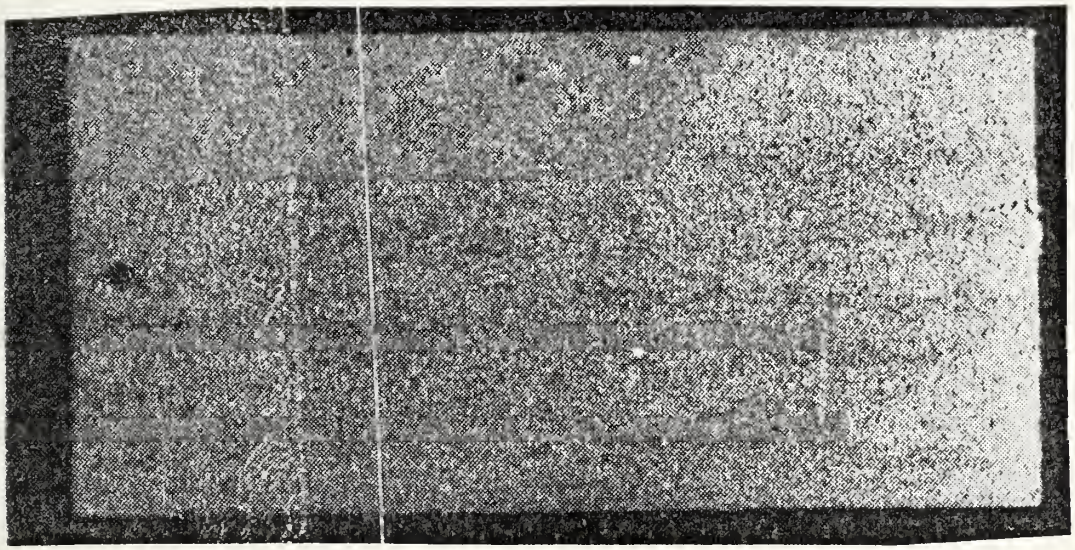

Figure B.58 Alloy F.S. coating, 21 days CSP

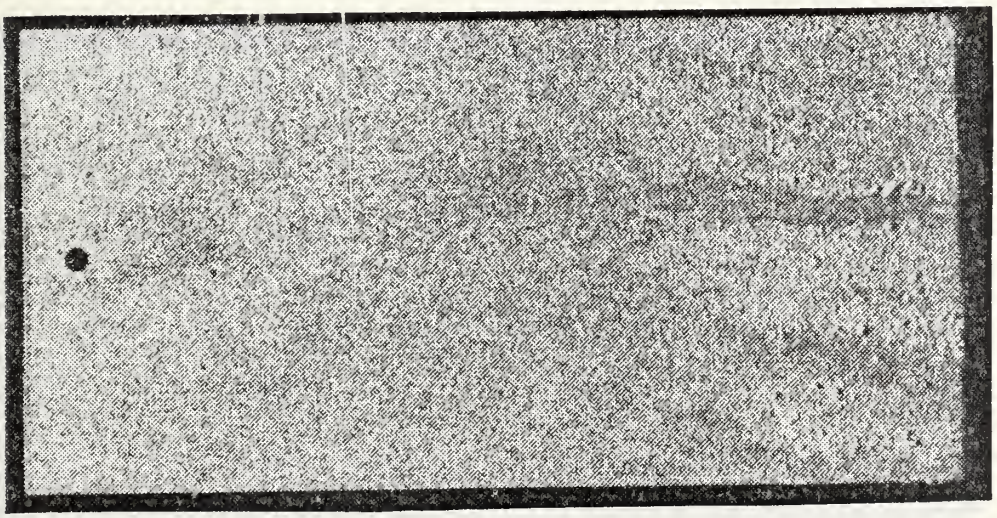

Figure B.59 Alloy F.S. coating, 42 days CSP

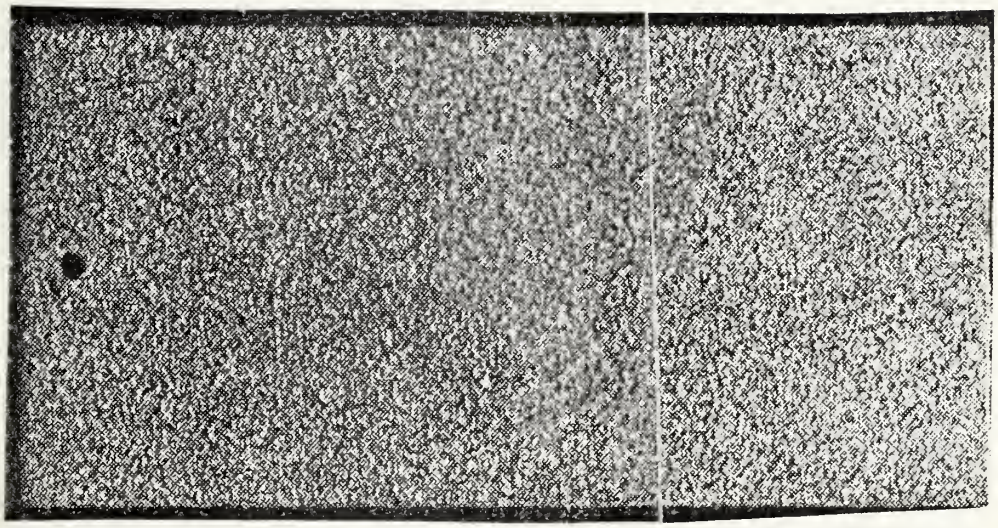

Figure B.60 Alloy A.S. coating, 21 days CSP

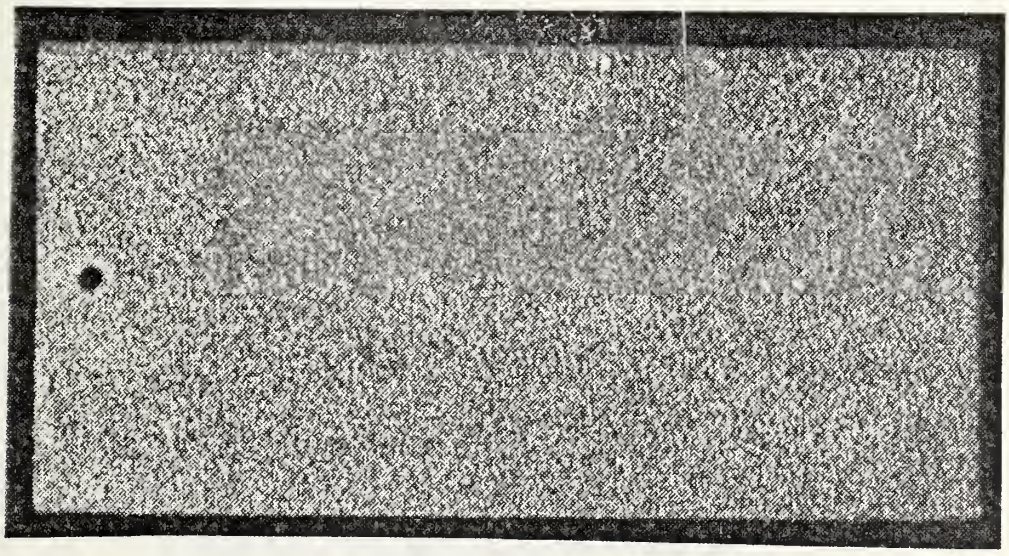

Figure B.61 Alloy A.S. coating, 42 days CSP

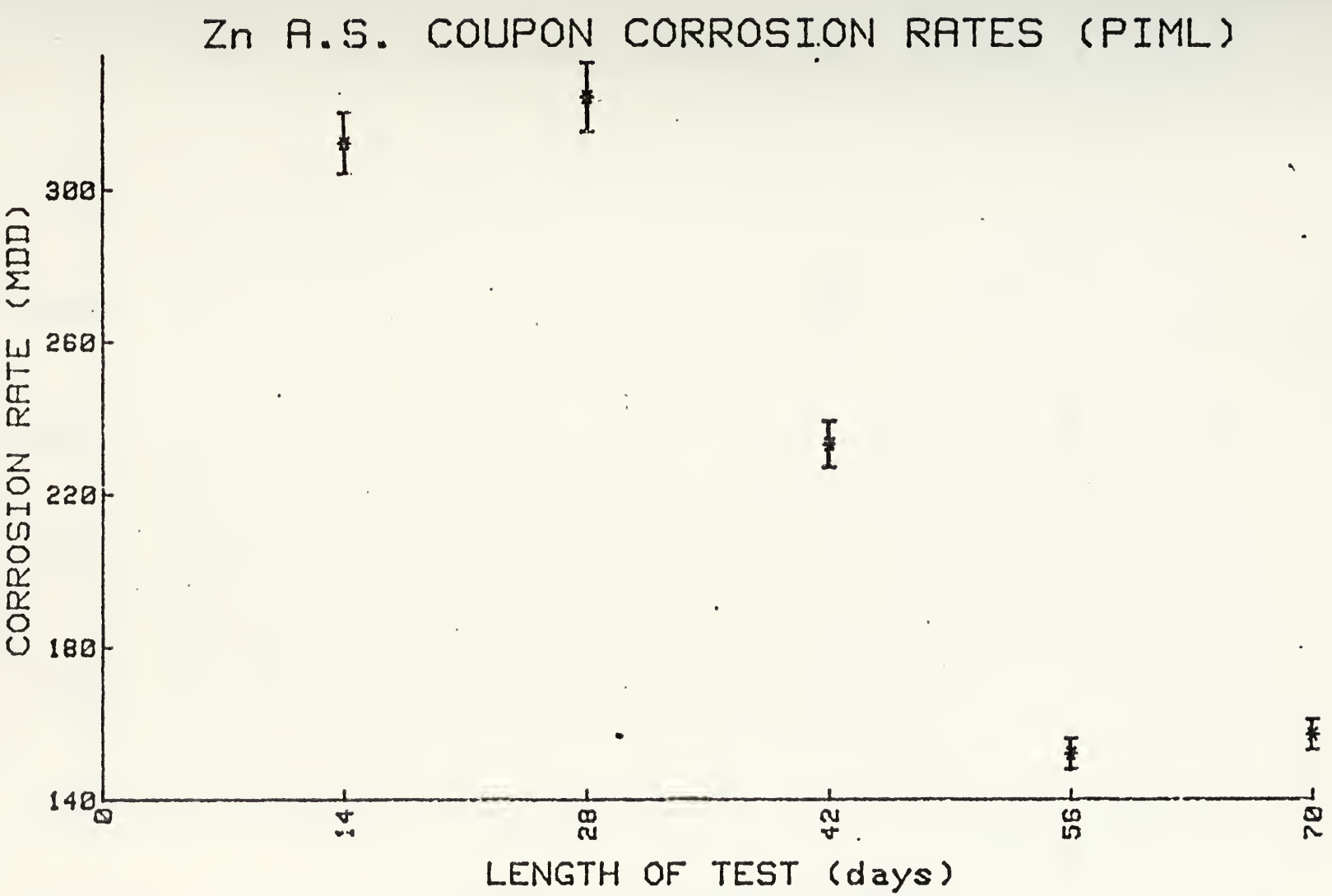


Figure B.62 Plot of Zn A.S. Corrosion Rate

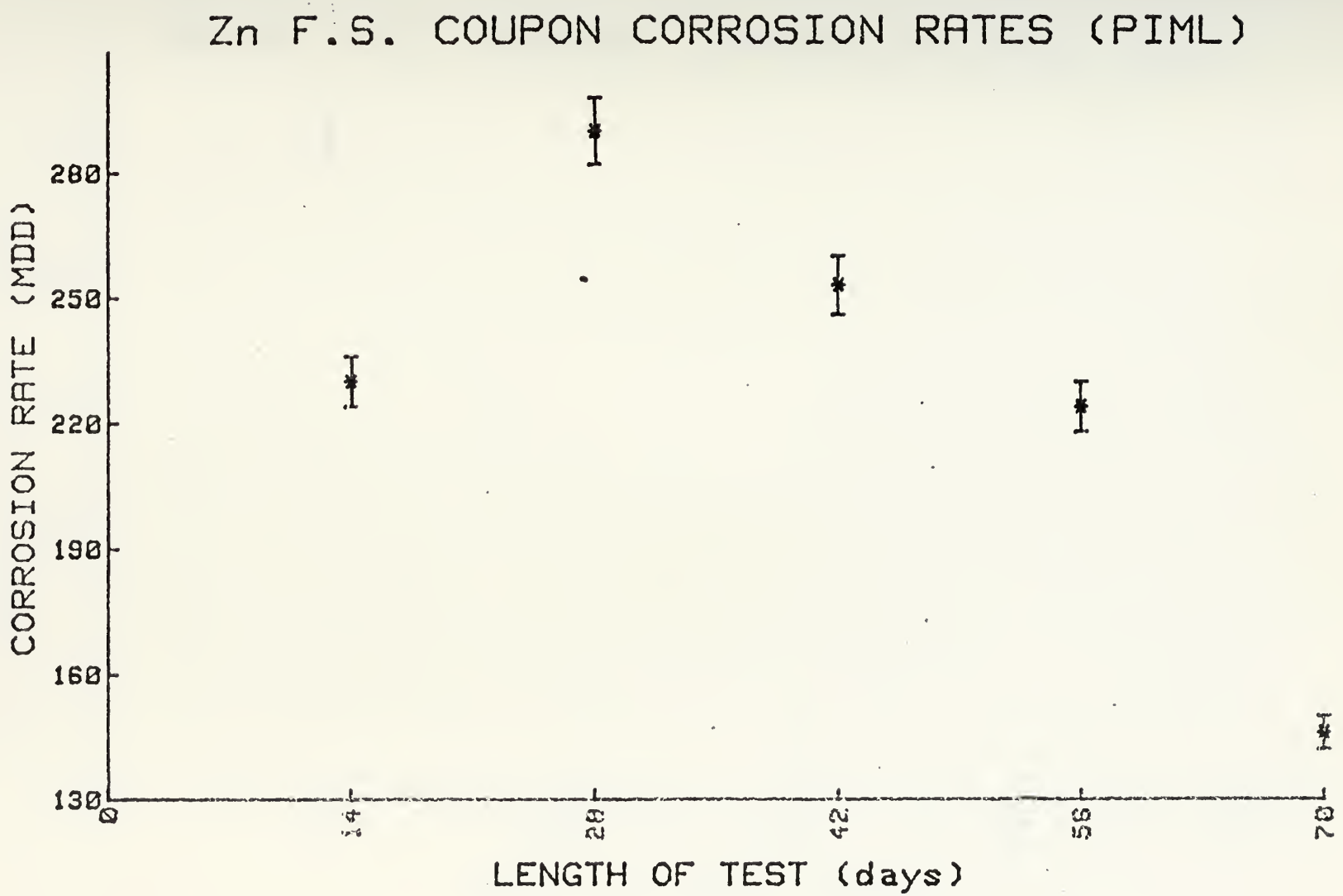


Figure B.63 Plot of Zn F.S. Corrosion Rate

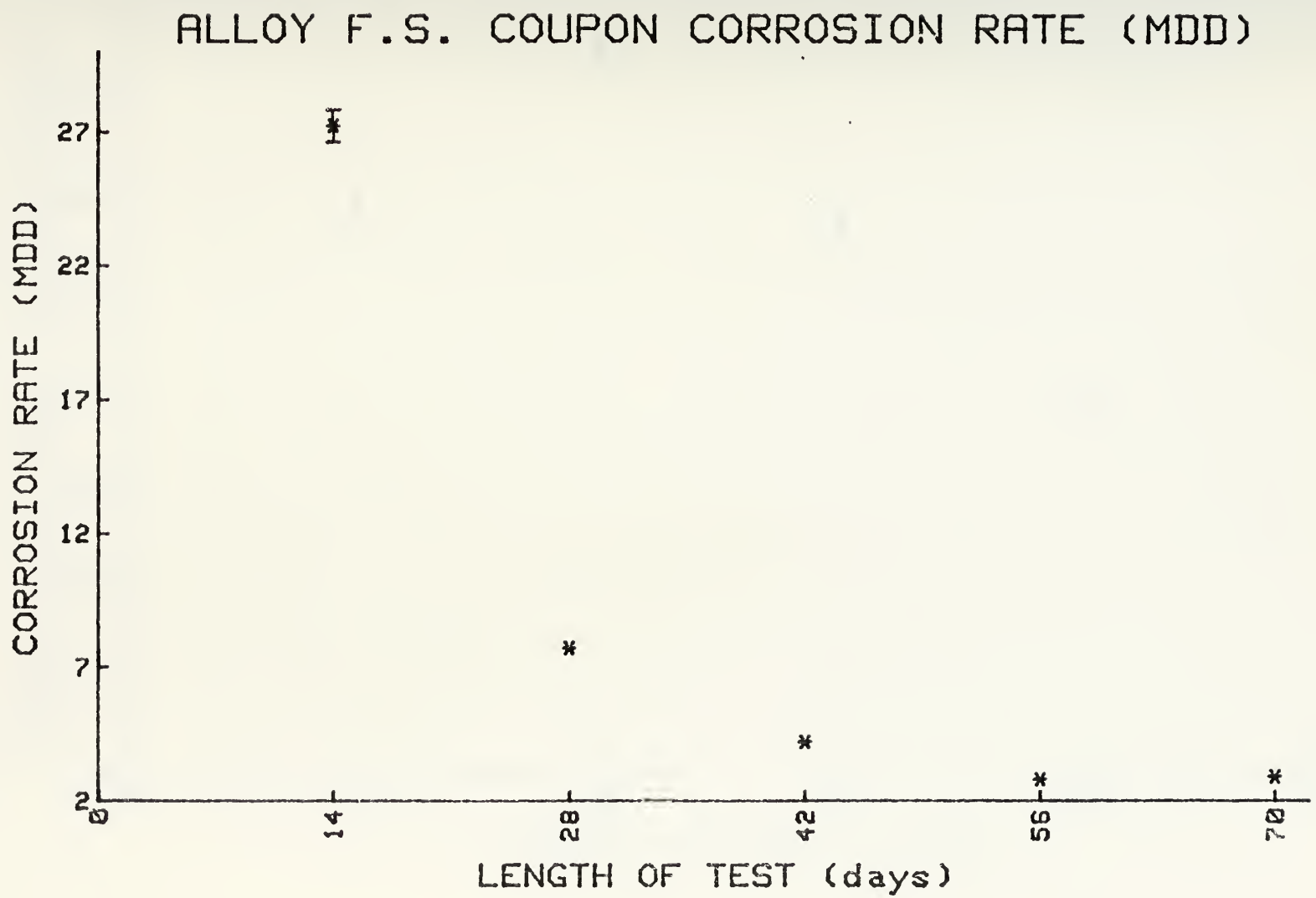


Figure B.64 Plot of Alloy F.S. Corrosion Rate

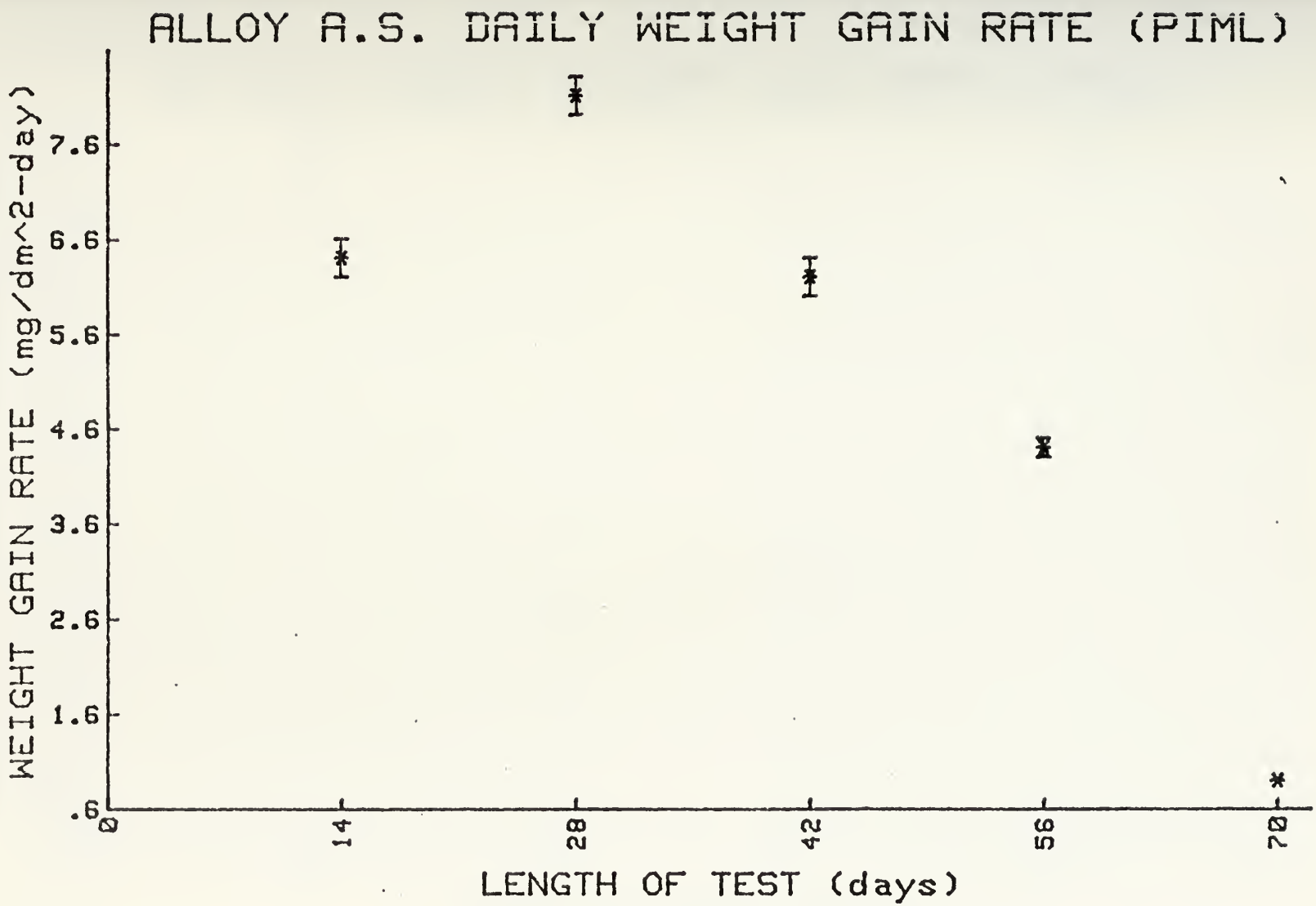


Figure B.65 Plot of Alloy A.S. Daily Weight Gain

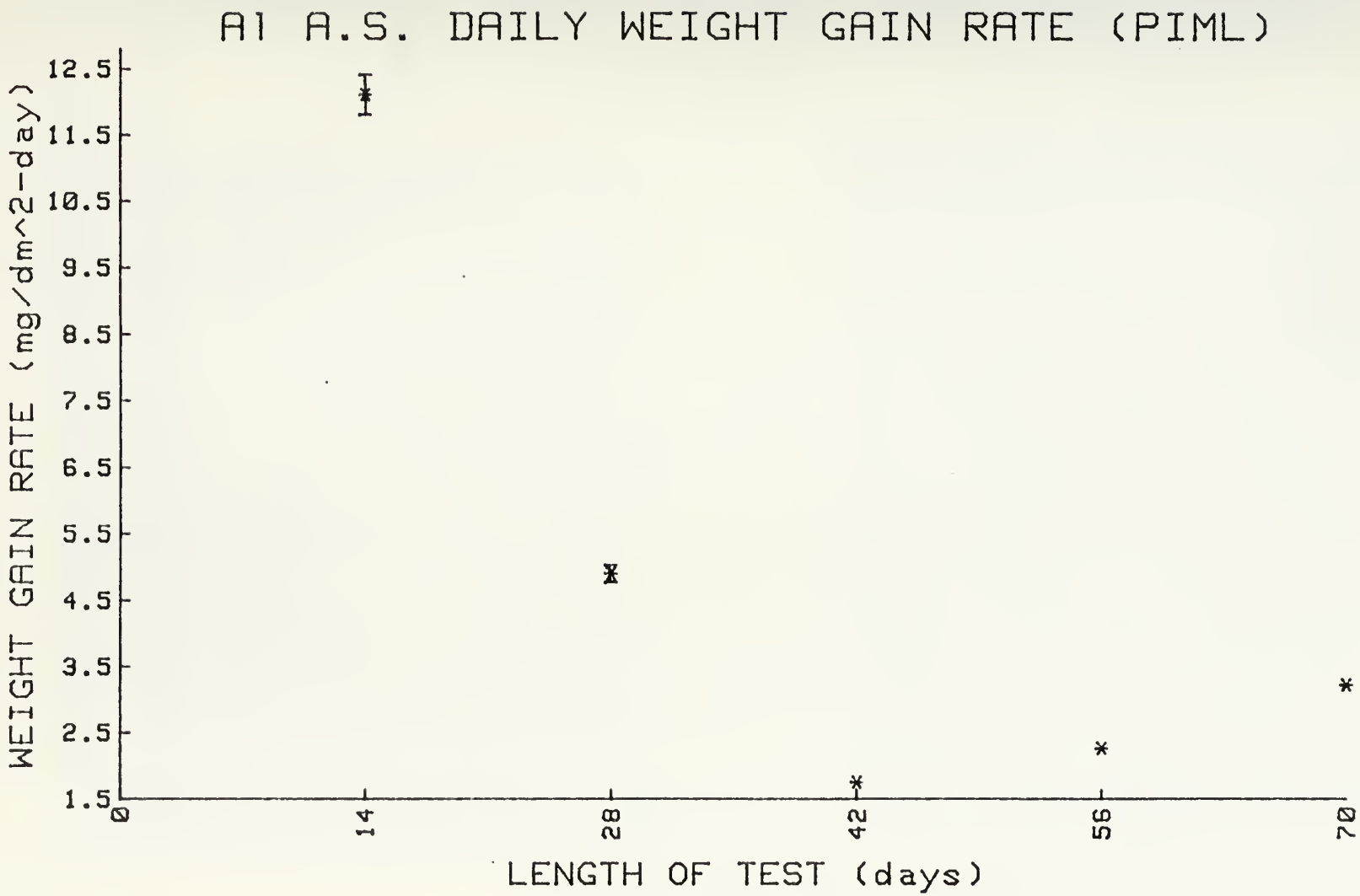


Figure B.66 Plot of A1 A.S. Daily Weight Gain

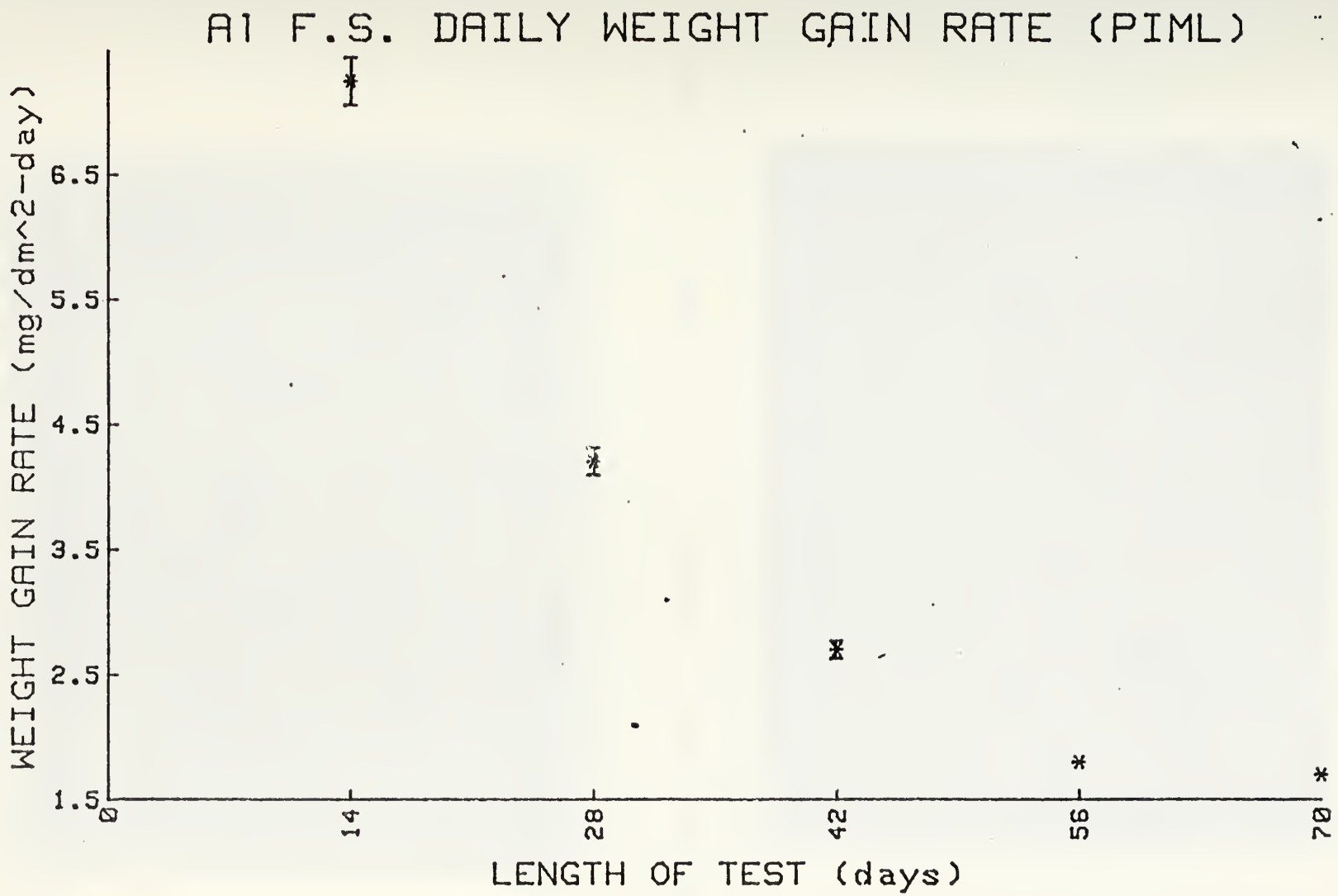


Figure B.67 Plot of A1 F.S. Daily Weight Gain

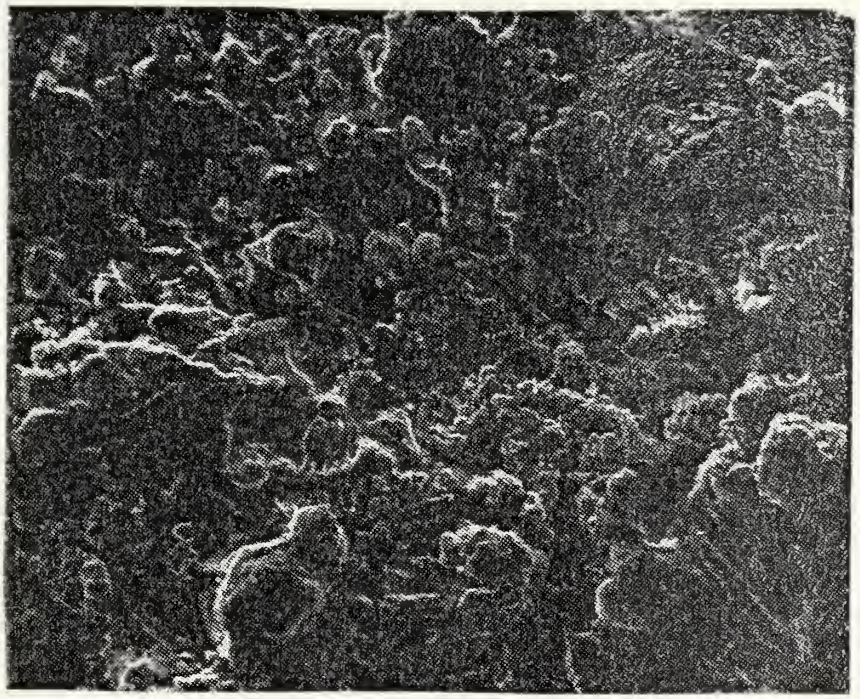

Figure B.68 (X135) Al A.S. coating, 14 days PIML, SEM

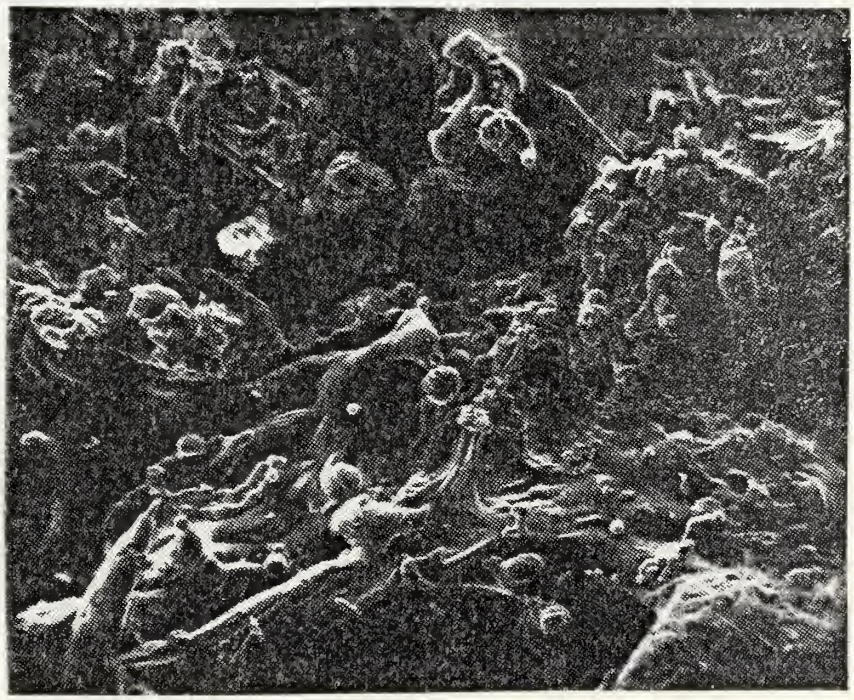

Figure B.69 (X155) Al A.S. coating, new, SEM

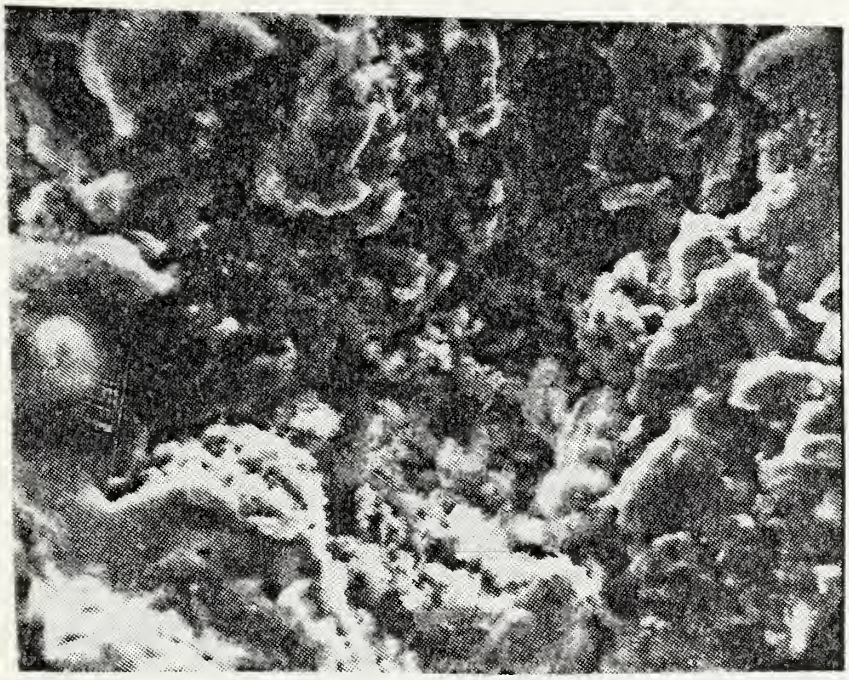

Figure B.70 (X660) Al A.S. coating, 14 days PIML, SEM

Figure B.71 (X130) Al A.S. coating, 28 days PIML, SEM

Figure B.72 (X110) Al A.S. coating, 42 days PIML, SEM

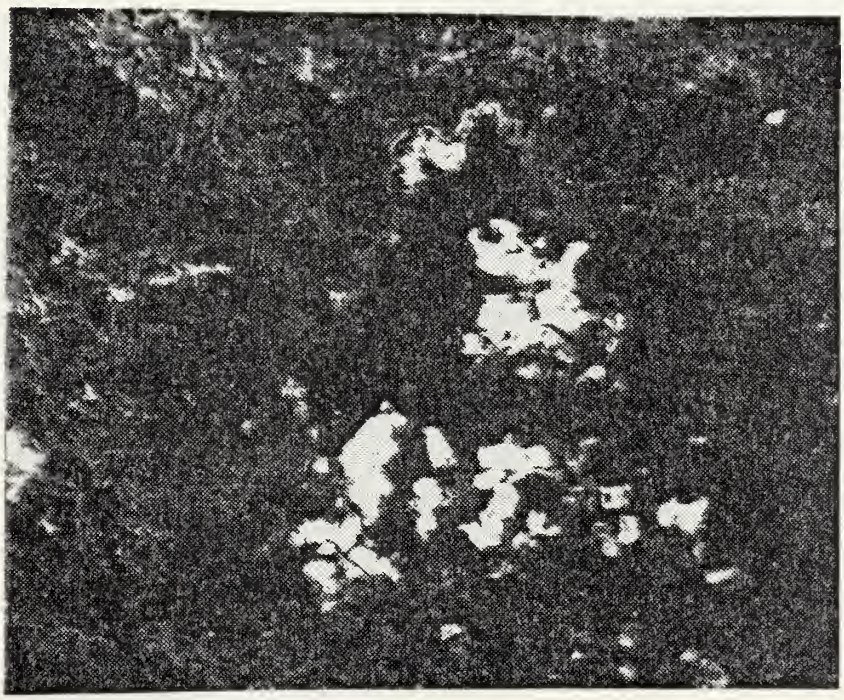

Figure B.73 (X110) Al A.S. coating, 42 days PIML, SEM

Figure B.74 (X110) Al A.S. coating, 56 days PIML, SEM

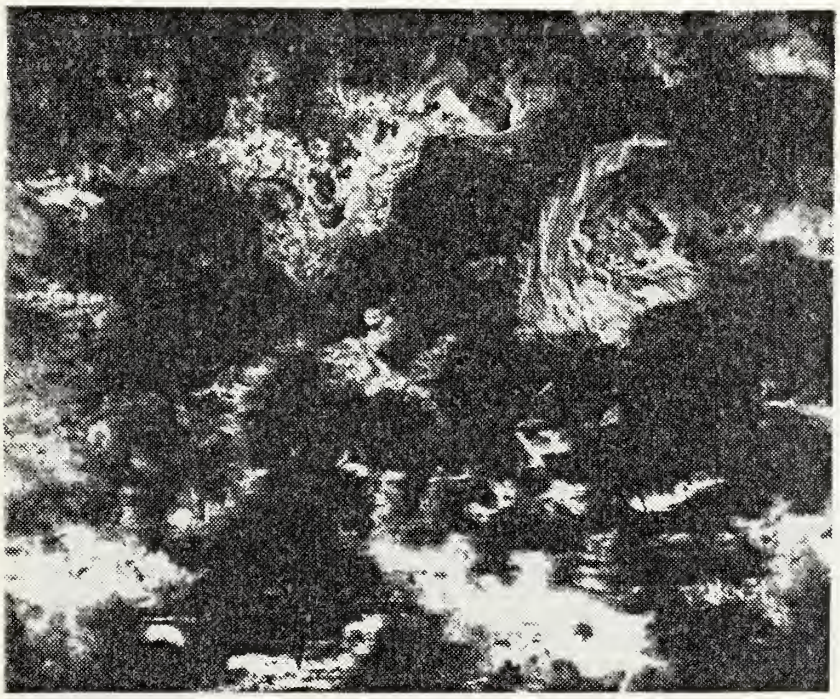

Figure B.75 (X110) Al A.S. coating, 70 days PIML, SEM

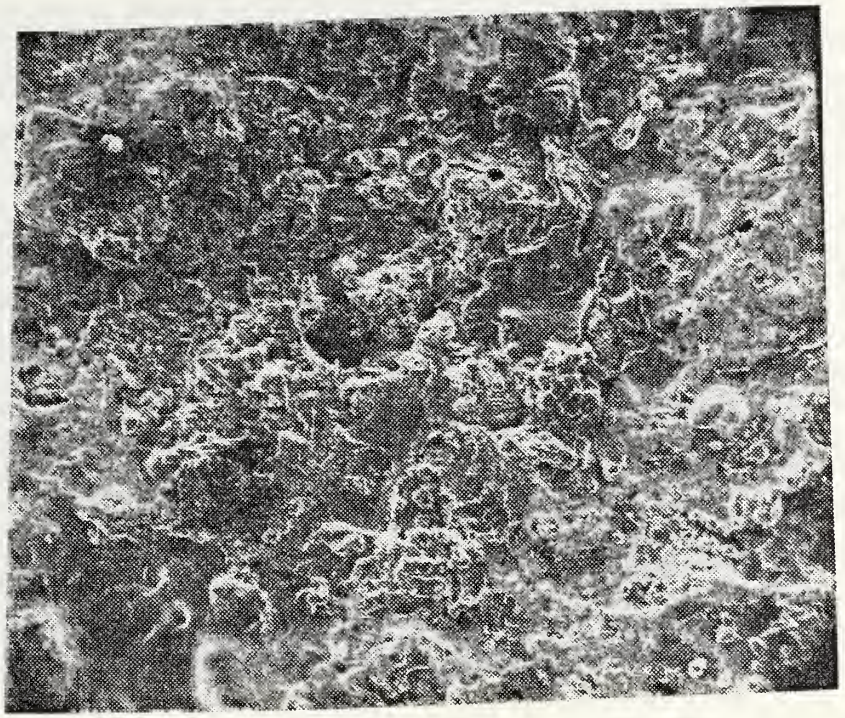

Figure B.76 (X120), Zn F.S. coating, new, SEM

Figure B.77 (X140), Zn F.S. coating, new, cross section, SEM

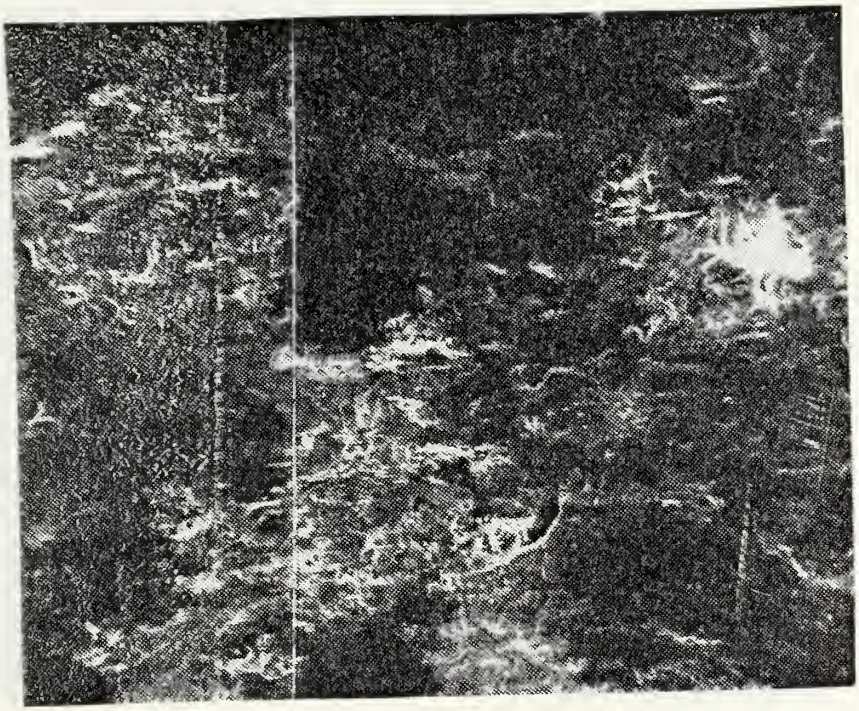

Figure B.78 (X130), Zn F.S. coating, 14 days PIML, SEM

Figure B.79 (X140), Zn F.S. coating, 14 days PIML, cross section, LM

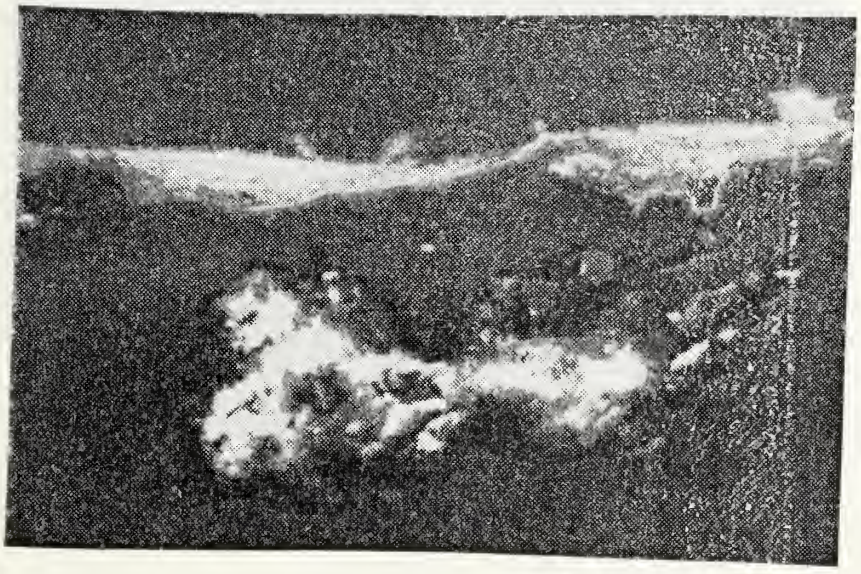

Figure B.80 (X650), Zn F.S. coating, cross section, 28 days PIML, SEM

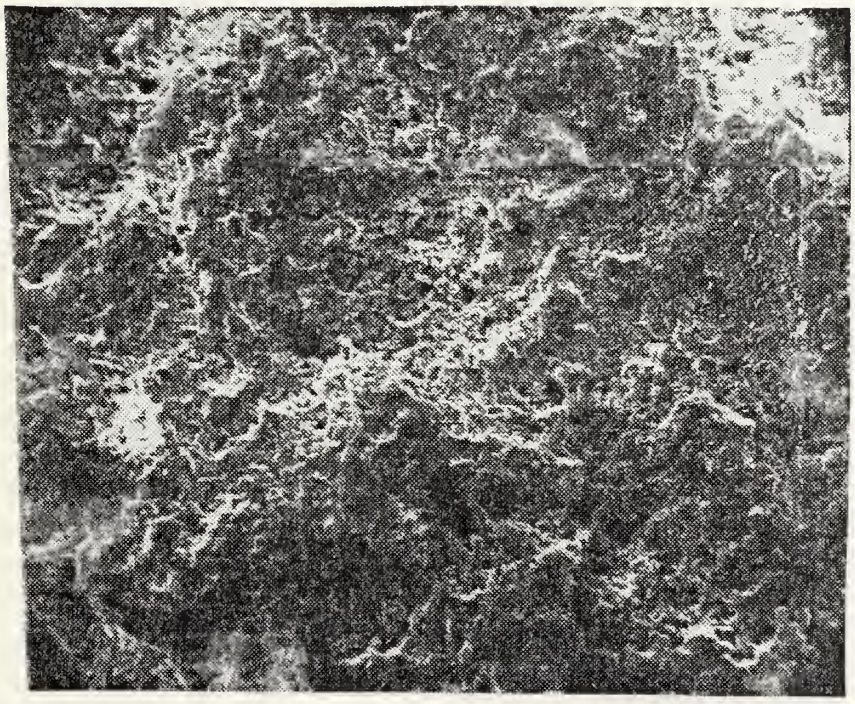

Figure B.81 (X140), Zn F.S. coating, 28 days PIML, SEM

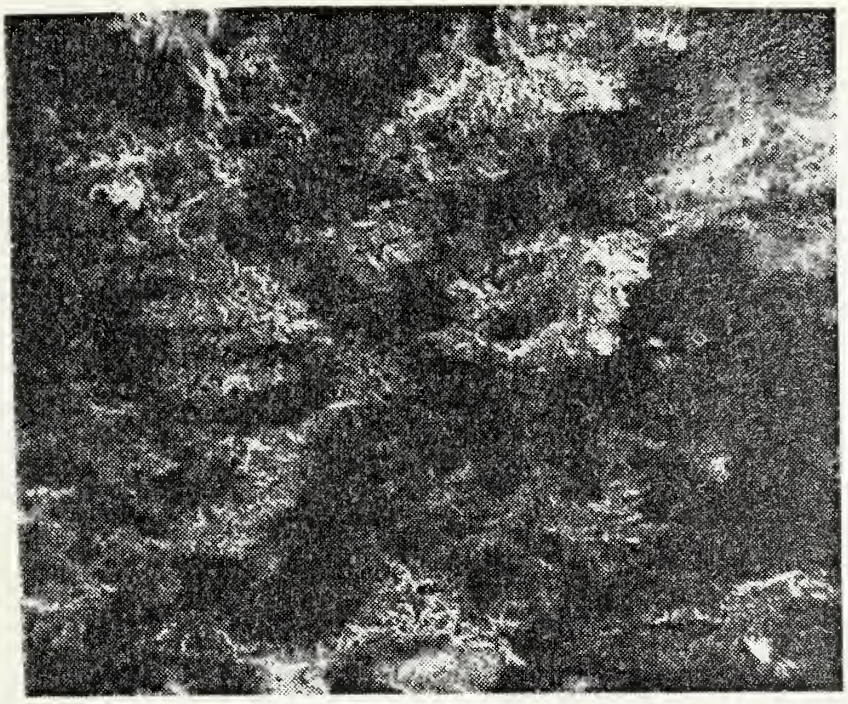

Figure B.82 (X110), Zn F.S. coating, 42 days PIML, SEM

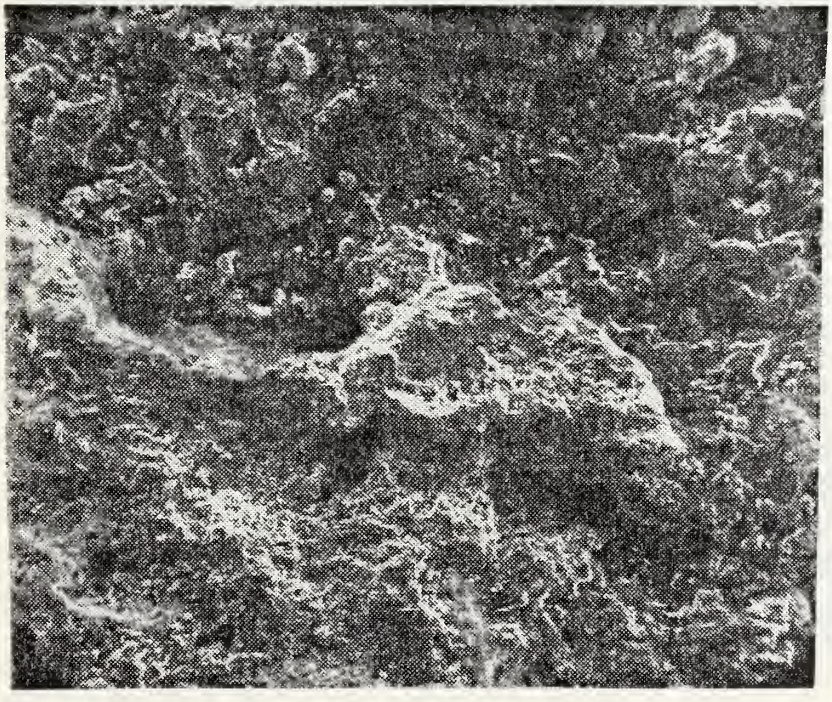

Figure B.83 (X110), Zn F.S. coating, 56 days PIML, SEM

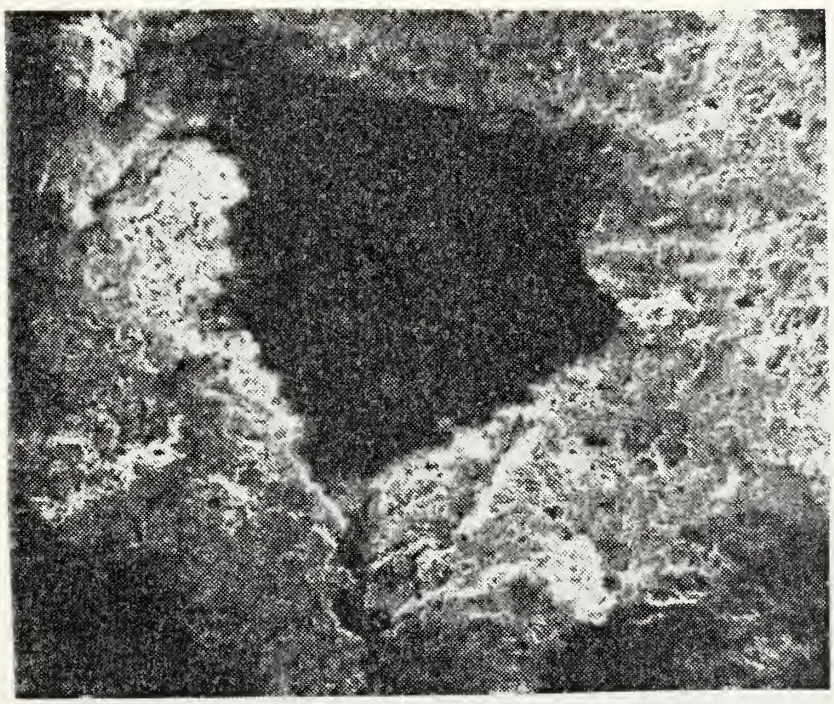

Figure B.84 (X110), Zn F.S. coating, 70 days PIML, SEM

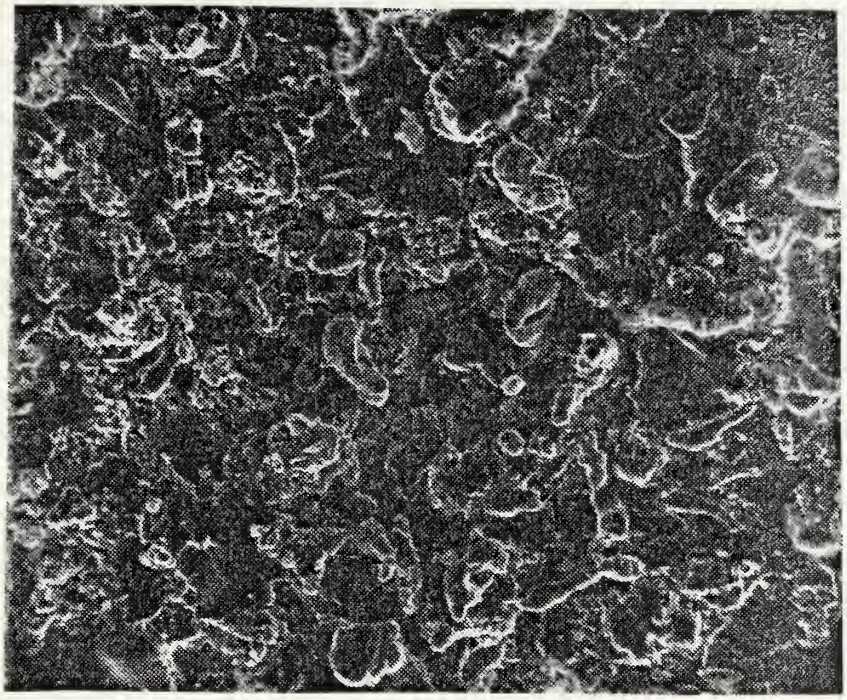

Figure B.85 (X130), Alloy F.S. coating, new, SEM

Figure B.86 (X110), Alloy F.S. coating, 14 days PIML, SEM

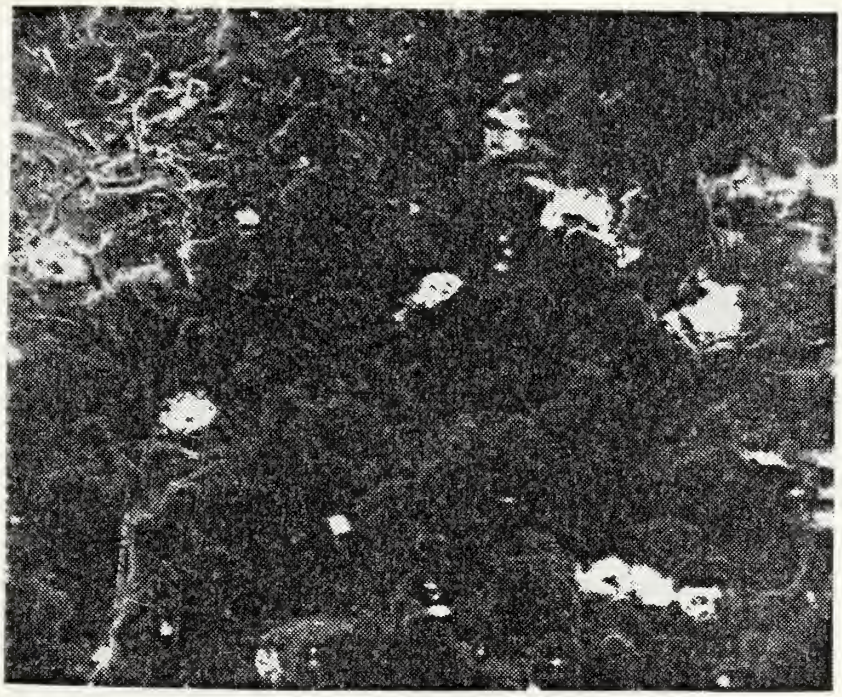

Figure B.87 (X110), Alloy F.S. coating, 28 days PIML, SEM

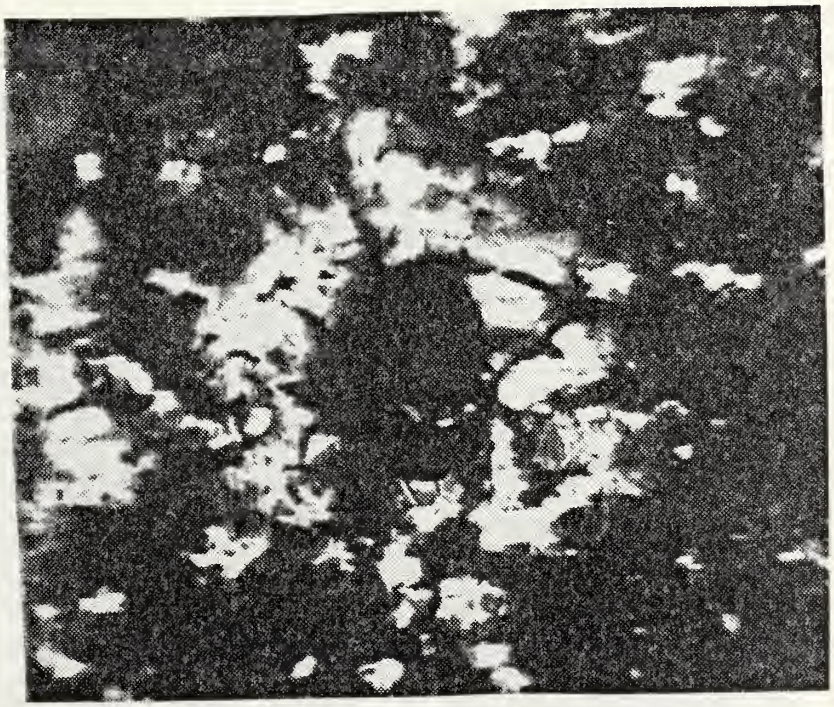

Figure B.88 (X110), Alloy F.S. coating, 42 days PIML, SEM

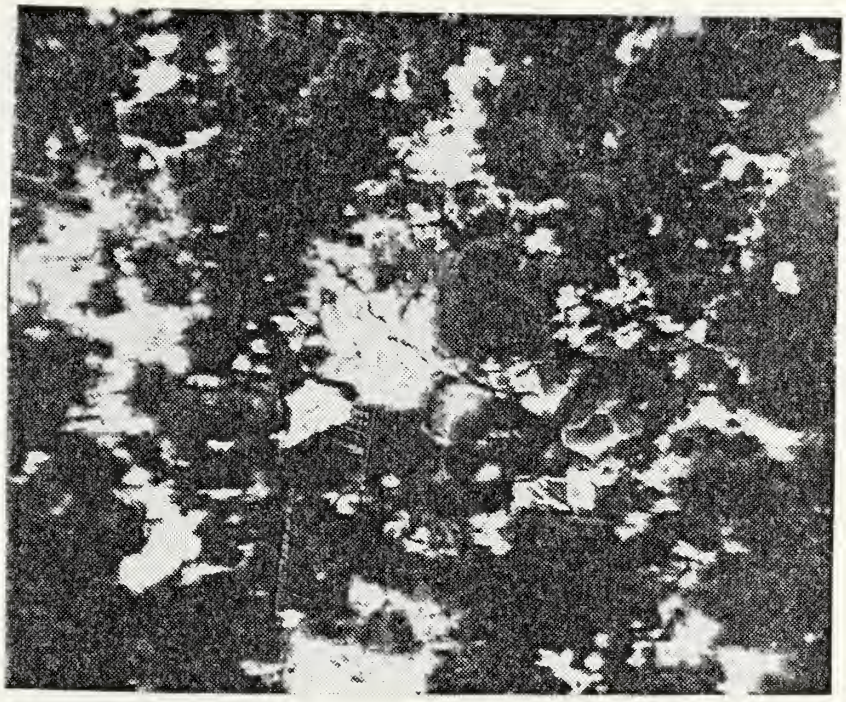

Figure B.89 (X110), Alloy F.S. coating, 56 days PIML, SEM

Figure B.90 (X110), Alloy F.S. coating, 70 days PIML, SEM

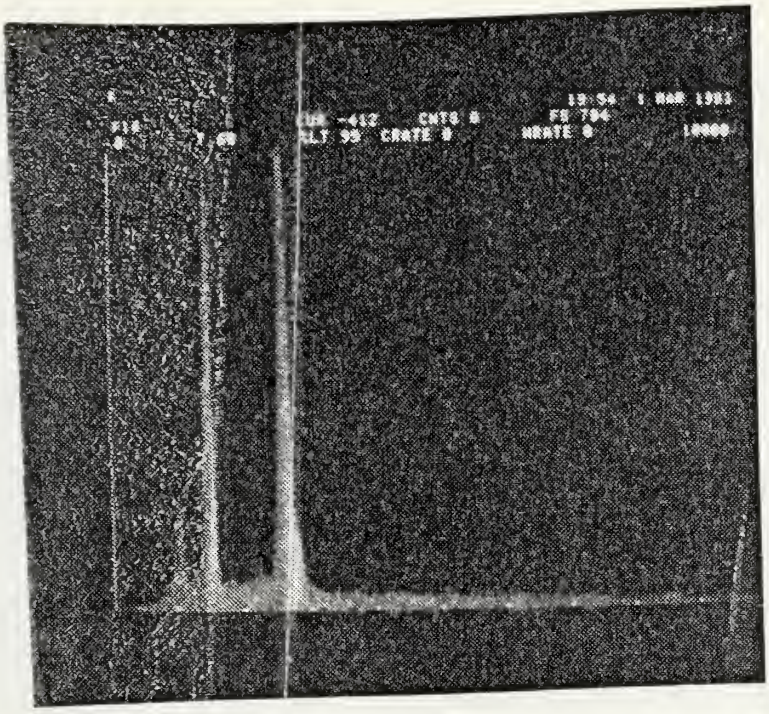

Figure B.91 X-ray spectrum of Alloy A.S. corrosion products, 42 days

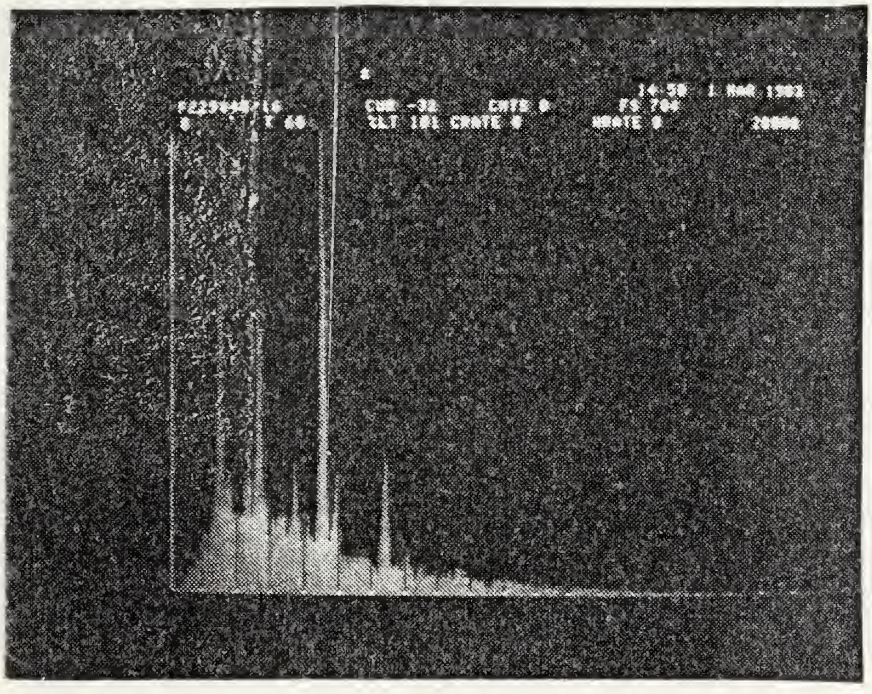

Figure B.92 X-ray spectrum of Alloy A.S. corrosion products, 12 hours

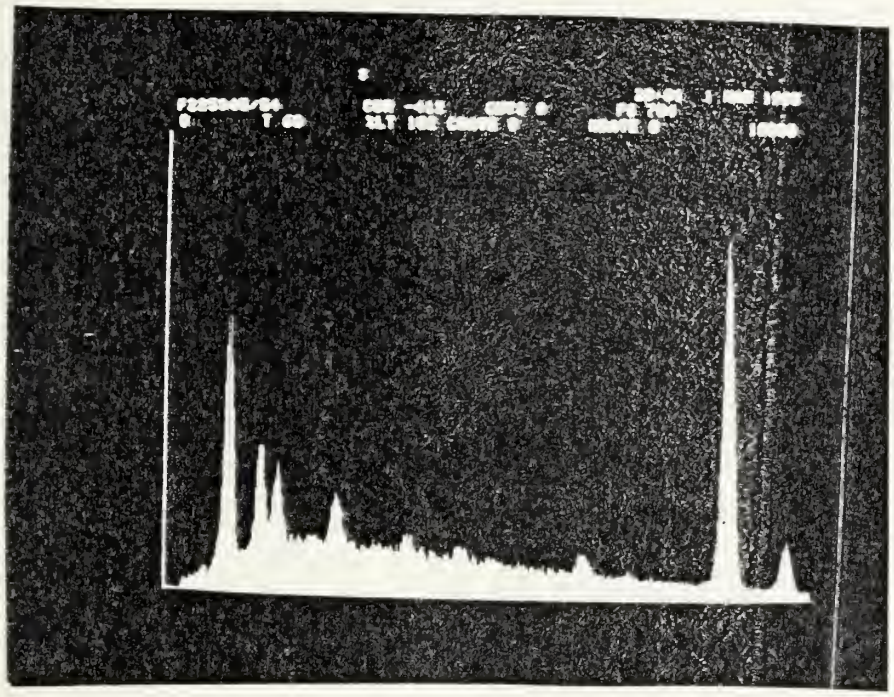

Figure B.93 X-ray spectrum of Zn F.S. corrosion products, 6 hours

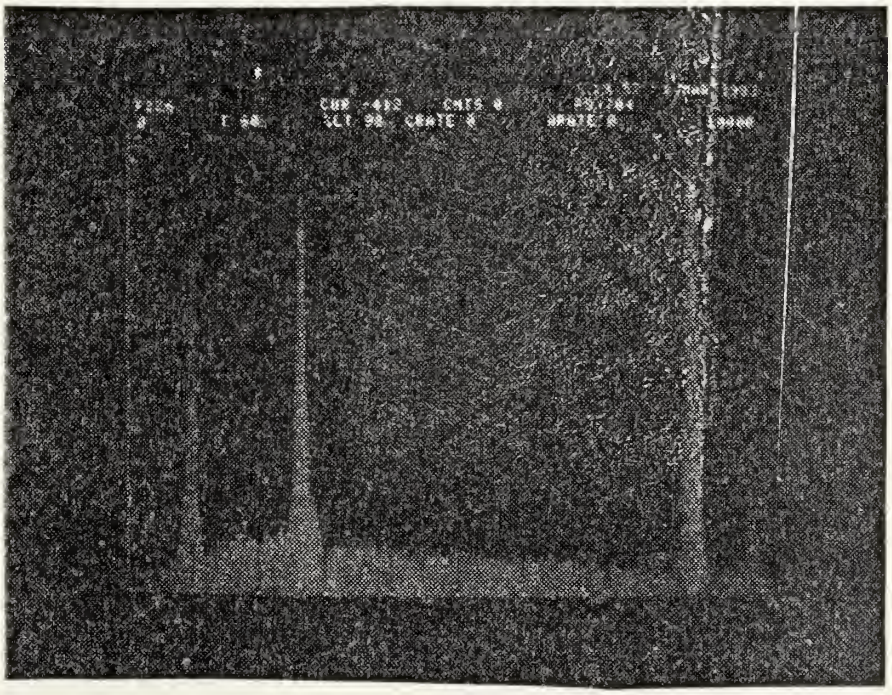

Figure B.94 X-ray spectrum of Zn F.S. corrosion products, 42 days

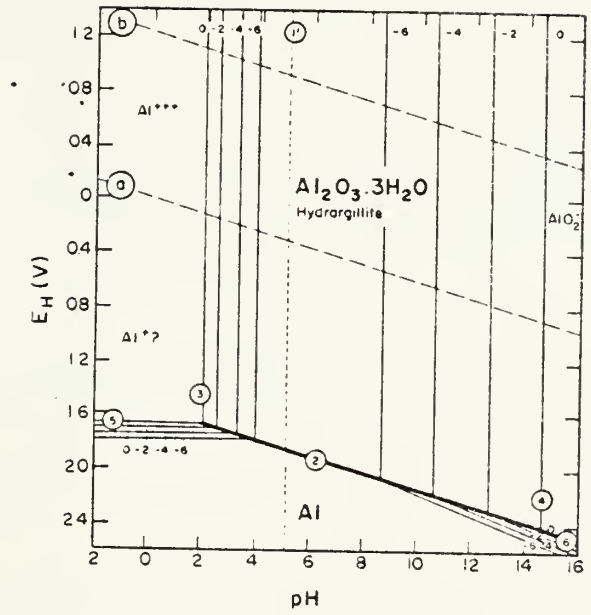


Figure B.95 Pourbaix Diagram for Aluminum

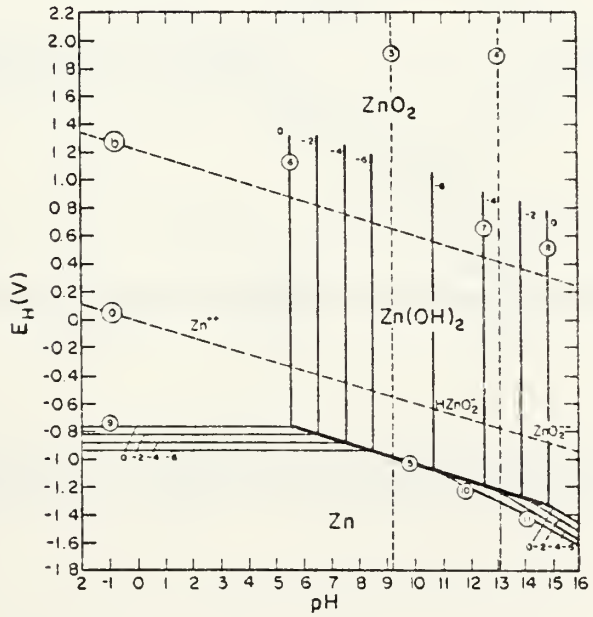


Figure B.96 Pourbaix Diagram for Zinc

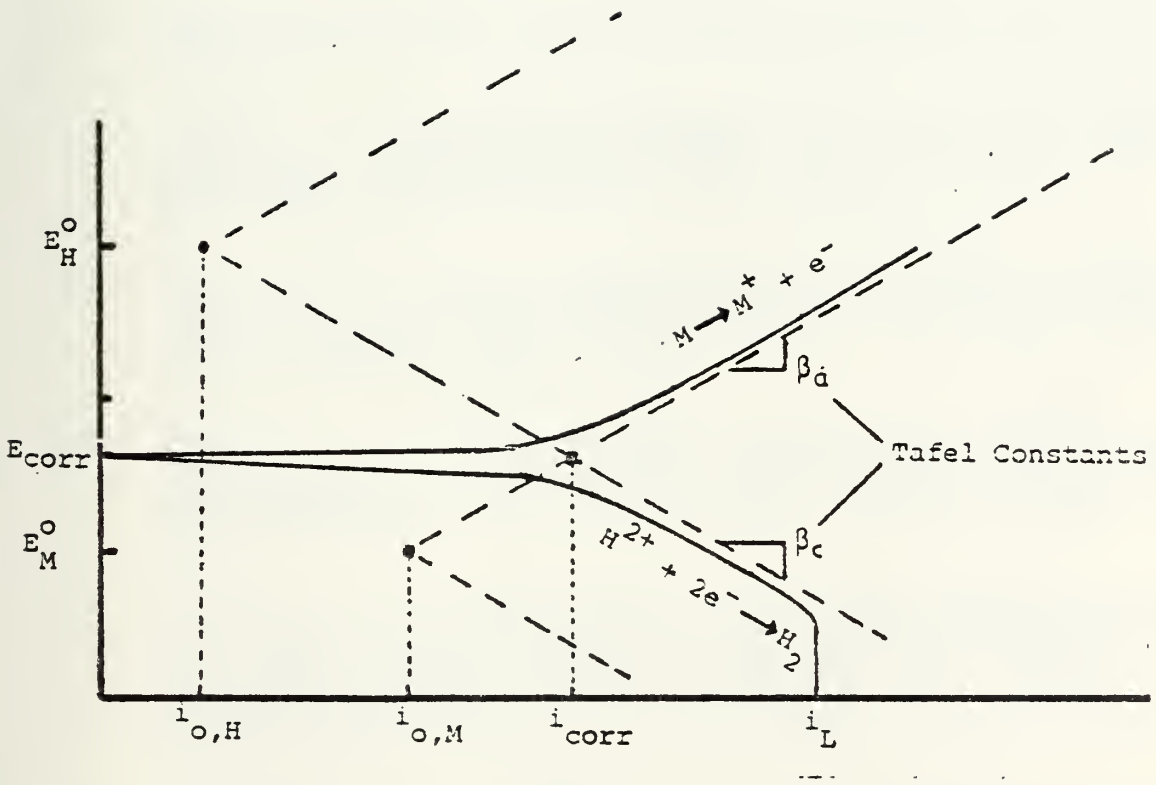


Figure B-1. Schematic Representation of Potentiodynamic Polarization Curve

Figure B.97 Schematic Representation of a PDP Curve

# LIST OF REFERENCES


1. Sulit, R. A., Vanderveldt, H. H., Thermal Spray Technology RDT&E and Service Applications for Hull, Mechanical, and Electrical (HME) Equipment in the U.S. Navy, paper presented at Tri-Service Conference on Corrosion, USAF Academy, 3-7 November 1980.

2. Herman, H., The Response of Coated Steels to Cavitation in Corrosive Environment, Final Report to the Office of Naval Research, Washington, DC, June 1980.

3. Naval Sea Systems Command, A Plasma Spray Handbook, March 1977.

4. Klinge, R., Sprayed Zinc and Aluminum Coatings for the Protection of Structural Steel, in Scandinavia, paper presented International Thermal Spraying Conference, 8th, Miami Beach, Florida, 27 September 1976.

5. Bailey, J. C., U.K. Experiences in Protecting Large Structures by Metal Spraying, paper presented International Thermal Spraying Conference, 8th, Miami Beach, Florida, 27 September 1976.

6. Childs, J. N., Zinc Sprayed Coatings in a Liquid Cargo Tankership, paper presented International Thermal Spraying Conference, 8th, Miami Beach, Florida, October 27, 1976.

7. Sulit, R. A., Vanderveldt, H. J., and Schapper, V.D., Corrosion Control Using Wire Sprayed Aluminum in the U.S. Navy, paper presented International Thermal Spraying Conference, 9th, The Hague, Netherlands, 20 May 1980.

8. Commander Naval Surface Force Pacific Instruction, COMNAVSURFPACINST 9630.1A, Shipboard Preservation with Wire Sprayed Aluminum (WSA), 10 September 1980.

9. David W. Taylor Naval Ship Research and Development Center, SME-78-94, Aluminum Flame Spray Corrosion Control Technology of Machinery Components, U.S.S. WILLIAM H. STANDLY (CG-32), by V.D. Schapper and R.T. Brenna, November 1978.

10. Sulit, R. A., Vanderveldt, H. J. and Schmeller, M. Machine Element Repairs Application and Procedures during U.S.S. ALBERT DAVID (FF-1080) ROH, paper presented at Association of Scientists and Engineers of the Naval Sea Systems Command Technical Symposium, 18th, Washington, DC, March 24, 1981.

11. Leclerq, M., Bensimon, R., Combined Paper: New Zinc-Based Alloy for Metallizing, paper presented International Thermal Spraying Conference, 8th, Miami Beach, Florida, 27 September 1976.

12. Private Communication with F. Rogers, Puget Sound Naval Shipyard, 29 June 1982.

13. Vessely, V., Horky J., Electrochemical and Corrosion Properties of Thermally Sprayed Coatings of Aluminum Alloys, paper presented International Thermal Spraying Conference, 8th, Miami Beach, Florida, 27 September 1976.

14. ASTM specification B117-73, Standard Method of Salt Spray (Fog) Testing, 1982.

15. ASTM Specification G 5-78, Standard Reference Method for Making Potentiostatic and Potentiodynamic Polarization Measurements, 1982.

16. Dean, S. W., Electrochemical Methods for Corrosion Testing, R. Baboian,, Ed., pp. 53-59, NACE, 1969.

17. ASTM Specification G 3, Conventions Applicable to Electrochemical Measurements in Corrosion Testing, 1982.

18. Klug, H. P., Alexander, L. E., X-ray Diffraction Procedures for Polycrystalline and Amorphous Materials, p. 397, Wiley, 1954.

19. Herman, H., The Response of Coated Steels to Cavitation in Corrosive Environment, Final Report to the Office of Naval Research, Washington, DC, p. 6, 1980.

20. Baboian, R., and other, Galvanic and Pitting Corrosion - Field and Laboratory Studies, p. 142, ATSM, 1976.

21. Carter, V. F., Metallic Coatings for Corrosion Control, pp. 108-112, Newnes-Butterworths, 1980.

22. Walters, L. J., "Flame Sprayed Protective Coatings for Iron and Steel," Anti-Corrosion, p. 11, January 1972.

23. Leclerq, M., Bensimon, R., combined Paper: New Zinc-Based Alloy for Metallizing, p. 421, paper presented International Thermal Spraying Conference, 8th, Miami Beach, Florida, 27 September 1976.

24. Pourbaix, M., Lectures on Electrochemical Corrosion, pp. 144-146, Plenum, 1973.

25. Holman, J. P., Experimental Methods for Engineers, pp. 81-83, McGraw-Hill, 1978.

INITIAL DISTRIBUTION LIST

| | | No. Copies |
|---|---|---|
| 1. | Defense Technical Information Center<br>Cameron Station<br>Alexandria, Virginia 22314 | 2 |
| 2. | Library, Code 0142<br>Naval Postgraduate School<br>Monterey, California 93940 | 2 |
| 3. | Professor A. J. Perkins, Code 69Ps<br>Department of Mechanical Engineering<br>Naval Postgraduate School<br>Monterey, California 93940 | 5 |
| 4. | Department Chairman, Code 69<br>Department of Mechanical Engineering<br>Naval Postgraduate School<br>Monterey, California 93940 | 1 |
| 5. | CAPT R. A. Sulit, Code SEA-0721<br>Naval Sea Systems Command<br>Washington, DC 20362 | 1 |
| 6. | Mr. Frank Rogers<br>Commander (Code 180.13)<br>Puget Sound Naval Shipyard<br>Bremerton, Washington 98314 | 1 |
| 7. | Mr. James Boyd<br>Commander (Code 138)<br>Puget Sound Naval Shipyard<br>Bremerton, Washington 98314 | 1 |
| 8. | Mr. Henry Bleile, Code SEA-05M-1<br>Naval Sea Systems Command<br>Washington, DC 20362 | 1 |
| 9. | Gregory Mead<br>6088 Cherry Hill Drive<br>Columbus, Ohio 43213 | 2 |

200462

Thesis
M3994 Mead
c.1

An investigation of the corrosion susceptibility of flame-sprayed and electric-arc sprayed anodic metal coatings of aluminum, zinc, and an aluminum-zinc alloy.